1996

INVESTIGATION OF CHELATING DYE IMPREGNATED RESINS FOR THE SELECTIVE ADSORPTION AND SEPARATION OF TRACE METALS FROM AQUEOUS SOLUTIONS

Sutton, Richard Matthew Charles

INVESTIGATION OF CHELATING DYE IMPREGNATED RESINS FOR THE SELECTIVE ADSORPTION AND SEPARATION OF TRACE METALS FROM AQUEOUS SOLUTIONS.

By

Richard Matthew Charles Sutton BSc (Hons), GRSC.

A thesis submitted to the University of Plymouth in partial fulfilment for the degree of

DOCTOR OF PHILOSOPHY

Department of Environmental Sciences,

Faculty of Science.

December 1996.

ABSTRACT.

INVESTIGATION OF CHELATING DYE IMPREGNATED RESINS FOR THE SELECTIVE ADSORPTION AND SEPARATION OF TRACE METALS FROM AQUEOUS SOLUTIONS.

By Richard Matthew Charles Sutton BSc (Hons), GRSC.

The preparation and characterisation of novel, high efficiency chelating sorbents which were suitable for the preconcentration and separation of trace metals from complex matrices using a single column has been described. Hydrophilic and hydrophobic substrates in the form of cellulose and polystyrene resins were modified with chelating dyes by either covalent bonding or physical adsorption respectively.

Large particle size polystyrene resins were used for preliminary investigations of dye loading and metal retaining capacities. After crushing resins to an intermediate particle size, capacity factors (k' values) and metal retaining capacities of four resins were determined. One resin, MN200, was chosen for further investigations after crushing to a small particle size. A study of analytical separations and selectivities on the small particle size dye impregnated MN200, for a range of dyes, was used to determine the suitability for analytical and preparative applications. The selectivity and separating ability of the unmodified resin was also investigated.

Three specific preparative and analytical applications were chosen which would exploit the metal separating capabilities of the modified or unmodified resins. The first of these studies was applied to the isolation of strontium from calcium, rubidium and barium in gypsum samples. The second involved the separation and determination of trace bismuth in lead and the third described the separation and determination of thorium and uranium from a complex metal containing matrix.

CONTENTS.

CHAPTER 2. Dye Loaded Cellulose Based Substrates

CHAPTER 3. Evaluation of Dye Impregnated Polystyrene Substrates Including Small Particle Size Hypercrosslinked Resins

CHAPTER 5. The Determination of Trace Bismuth in Lead

LIST OF TABLES.

CHAPTER 1.

CHAPTER 2.

CHAPTER 3.

CHAPTER 4.

CHAPTER 5.

CHAPTER 6

LIST OF FIGURES.

CHAPTER 1.

CHAPTER 2.

CHAPTER 3.

CHAPTER 6

ACKNOWLEDGEMENTS.

I would like to thank my supervisors, Dr. Phil Jones and Prof. Steve Hill for their continuous support, encouragement and friendship throughout the past three years. I also wish to thank the University of Plymouth for their financial support.

I should like to thank the European Community ERASMUS scheme for the financial support which provided me with the opportunity to spend three months working at the University of Oviedo, Spain. Thanks also go to Prof. Alfredo Sanz-Medel for his guidance during this period and to the members of his research group for their support.

I would like to thank my friends at the University of Plymouth, Pavel Nesterenko and especially Pete and Cathy for helping in the presentation of this thesis. I also would like to acknowledge my wife Karen for her support throughout and my parents for all their encouragement.

AUTHOR'S DECLARATION

At no time during the registration for the degree of Doctor of Philosophy has the author been registered for any other university award.

This study was financed with the aid of a studentship from the University of Plymouth.

A programme of advanced study was undertaken, which included instruction in High Performance Liquid Chromatography theory and instrument operation and a supervised study in Inductively Coupled Plasma Mass Spectrometry.

Relevant scientific seminars and conferences were regularly attended at which work was often presented, external institutions were visited for consultation purposes and papers prepared for publication.

Publications arising from this project:

"The comparison of cellulose and polystyrene substrates for trace metal studies", R.M.C. Sutton, S.J. Hill and P.Jones, J. Chrom. A, 739, (1996) 81-86.

Presentations and Conferences Attended

Departmental research lecture, University of Plymouth, UK, June 1994

Departmental research lecture, University of Plymouth, UK, March 1995

Poster presentation, R and D Topics in Analytical Chemistry, University of Hull, UK, July 1995

Poster and oral presentation, IONEX '95, Wrexham, UK, July 1995

Oral presentation, IICS '95. Dallas, USA, September 1995

Departmental research lecture, University of Plymouth, UK, November 1995

Poster presentation, IICS '96, University of Reading, Reading, UK, September, 1996

Signed.....

Date....7th March 1997

Presentations and Conferences Attended

Departmental research lecture, University of Plymouth, UK, June 1994

Departmental research lecture, University of Plymouth, UK, March 1995

Poster presentation, R and D Topics in Analytical Chemistry, University of Hull, UK, July 1995

Poster presentation, IONEX '95, Wrexham, UK, July 1995

Oral presentation, IICS '95. Dallas, USA, September 1995

Departmental research lecture, University of Plymouth, UK, November 1995

Poster presentation, IICS '96, University of Reading, Reading, UK, September, 1996

Signed.....

Date.....

Chapter 1 - Introduction

1.1 Introduction

The term 'trace elements' relates historically to a period when minute amounts of elements were found in biological systems but could not be precisely quantified using classical methods of analysis. Although more sensitive and specific analytical techniques have been developed, this terminology has remained in popular usage for concentrations less than 100 mg kg^{-1} and a new term of 'ultratrace' levels is used for concentrations which are less than 10 μg kg^{-1}.

There is considerable interest regarding the movement of 'trace metals' in the environment and the effect of anthropogenic activity on natural geological and biological systems. The introduction of relatively high concentrations of toxic elements into natural waters and soils can have deleterious effects on ecosystems causing devastation in the event of serious pollution incidents. The main sources of trace metal pollution in the environment are from industrial manufacturing and processing plant effluents and to counteract this, current European Union legislations are increasing the pressure on local and national industry to conform to lower levels of trace metal output. Previously, liquid wastes have been simply diluted to adhere to legal output limits, but this method is no longer viable since flow rates are now also regulated. Economical methods to remove potential pollutants from effluents are therefore required since the detection limits of analytical methods used to monitor the

contaminating species are improving all the time, providing good evidence to prosecute offenders.

In recent years, many methods have become available for the detection of trace metals in environmental and industrial samples which provide alternatives to more classical titrimetric and gravimetric techniques. There is a wide range of electroanalytical and spectroanalytical techniques, for example stripping voltammetry and inductively coupled plasma-mass spectrometry (ICP-MS), which provide powerful tools for the determination of trace metals in aqueous media. Liquid chromatography is a separative method which offers a reliable, relatively inexpensive alternative to some of these analytical techniques. It has a wide range of applications and offers versatility, as a range of detection systems may be employed depending on the analytes of interest. For instance, liquid chromatography systems can be very powerful when used as 'hyphenated' techniques, such as LC-ICP-MS [1].

Chromatography is a term which has been adopted to describe a variety of separation methods and has evolved dramatically since its first reported account by Tswett in 1903. Tswett described the separation of green plant pigments in a powdered chalk column, but the technology remained essentially unrealised for over twenty years until reports of the separation of carotenes in carrots and xanthophylls in egg yolk in 1930. Since then, there has been the development of gas chromatography (GC), planar chromatography (PC), thin layer chromatography (TLC) and high performance liquid chromatography (HPLC). However, the major breakthrough in chromatography for the determination of anions and cations is considered to be the development of low

capacity ion exchange columns linked to a suppressed conductivity detection system by Small in 1975 [2]. The term "ion chromatography" was used to describe this system but, owing to the prominence of other techniques, it now embraces any chromatographic method applied to the determination of ions [3].

1.2 Principles of High Performance Liquid Chromatography Separations

In high performance liquid chromatography systems, it is generally accepted that multi-component mixtures are separated from narrow zones which are introduced into the columns. In ideal situations, the differential migration of each component causes them to be isolated at different locations on the column. Figure 1.1 illustrates the introduction of a narrow zone onto the column, comprised of components A, B and C. In an isocratic system, i.e. of constant eluent composition, the components are separated along the column owing to their interactions with the eluent (the mobile phase) and the stationary phase. The fastest component, A, is eluted from the column first and is then followed by the components B and C.

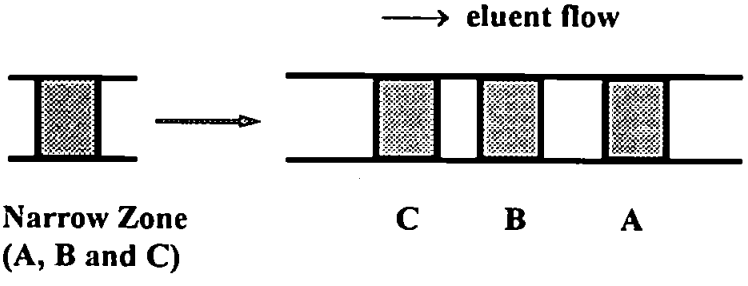

Figure 1.1. The chromatographic separation of a three component system

The level of interaction between the components and the column is given by the distribution coefficient, D, which is defined as:

$$D = \frac{\text{mequiv. metal on resin / g of dry resin}}{\text{mequiv. metal in solution / ml of solution}}$$

Values of D for a range of components may be used to give an indication of the optimum separating conditions. For the maximum separation of two components, their D values must be as far apart as possible. The component with the lowest D value elutes from the column first.

The efficiency of the column may be attributed to both the difference in migration of the components of the mixture and the level of band spreading during migration of the components from the column. An important consideration is that the efficiency of the column will be reliant on the equilibrium constants of the interactions of the components with the mobile and stationary phases. It is generally accepted that the column efficiency is represented by the number of theoretical plates, N, which can be calculated from the retention time of the peak, t_r, and the width at either half peak height, $W_{1/2}$ or the adjusted width at full peak height, W:

$$N = 5.54 (t_r / W_{1/2})^2 \qquad \text{or} \qquad N = 16 (t_r / W)^2$$

The number of effective plates, N_{eff}, of a column of length L (mm), is actually lower than the number of theoretical plates, N, since the dead volume of the system is negated by using the reduced retention time, t'_r, in the calculation (where the reduced retention time, t'_r, is the time of the unretained component, t_0, subtracted from the retention time of the retained component, t_r):

$$N_{eff} = 5.54\ (t'_r / W_{1/2})^2 \qquad \text{or} \qquad N_{eff} = 16\ (t'_r / W)^2$$

Therefore, the height equivalent of a theoretical plate (plate height), H (mm), will in turn be less than the corresponding effective plate height, H_{eff}.

$$H = L / N \qquad \text{is less than} \qquad H_{eff} = L / N_{eff}$$

Figure 1.2 illustrates that the peak width at half height, $W_{1/2}$, is the actual width of the peak, whereas tangent lines are required to determine the peak width at full height. It is for this reason that $W_{1/2}$ calculations are most commonly used.

In practice, it is very unlikely that peaks will assume perfect Gaussian appearances and it is therefore important to quantify the asymmetry of the peaks, A_s. Figure 1.2 illustrates this phenomenon for the second peak. At 10% of the peak height, the distance from the peak front to the centre of the peak, A, and the distance from the peak tail to the centre of the peak, B, are measured and, as a ratio, give the level of asymmetry i.e.,

$$A_s = B / A$$

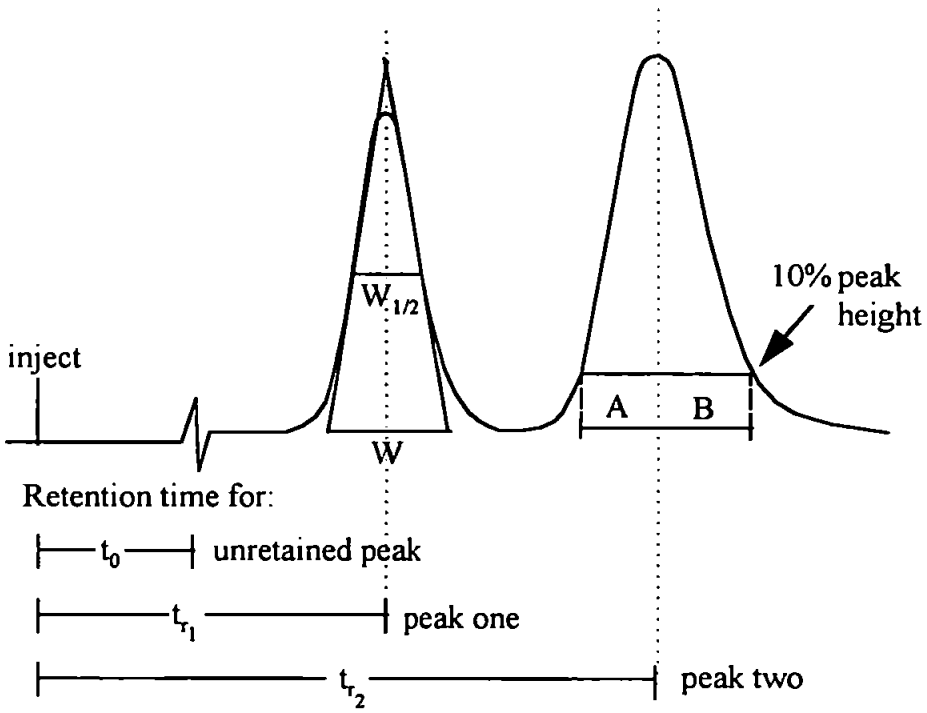

Figure 1.2. A chromatographic separation illustrating parameters used for calculations

The degree of which a sample component is retained on the column relative to an unretained component, is measured in terms of the capacity factor, k'. Using the reduced retention time, t'_r in the calculation, the capacity factor may be represented as

$$k' = t'_r / t_0$$

The capacity factor is a dimensionless constant which gives information on the elution time of a peak relative to an unretained peak and is essentially an indication of the relative speed of separation. For the calculation of the relative separation of two peaks, the selectivity or separation factor, α, is required.

$$\alpha = k'_2 / k'_1$$

The selectivity may be changed by altering either the mobile phase or the stationary phase and can therefore be regarded as the most important part of a chromatographic system. Although in most cases the effectiveness of a column is measured in terms of plate number, N, efficiencies required to give adequate separations without suitable changes in selectivity may be too difficult to obtain. The relationship between the selectivity and the resolving power (or resolution factor), R_s, where $\underline{k}'$ is the average value for the two peaks, is calculated as follows:

$$R_s = (1/4)\,(\alpha-1)\,N^{1/2}\,(\underline{k}' / 1+\underline{k}')$$

This equation emphasises the importance of α for well resolved separations. Since $N^{1/2}$ is used in the calculation, the number of plates must be quadrupled to double the resolution, and improvements in resolution by increasing $\underline{k}$' can dramatically increase run times.

1.2.1 Effect of particle size on separations

In practice, the plate number can be increased by using smaller particle size packing materials, but at the cost of an increase in pressure to maintain a certain liquid flow through the column. In general, this relationship is given by the pressure drop along the column:

$$P = \nu\eta L / K$$

where P is the pressure drop, ν is the mean linear velocity of the mobile phase, η is the viscosity of the mobile phase and K the permeability of the support particles.

Columns with narrow particle size ranges suffer less band broadening by reducing the effects of four principal inefficiencies in the system. These are known as A) eddy diffusion, B) longitudinal diffusion, C) mass transfer of sample between the phases and D) extra-column diffusion. The plate height, H, can be expressed as a sum of these factors

$$H_{TOTAL} = H_{\text{eddy diffusion}} + H_{\text{longitudinal diffusion}} + H_{\text{mass transfer}} + H_{\text{extra-column}}$$

Eddy diffusion relates to uneven flow paths of molecules through the column. Irregular packing in the column may be prevalent in the form of agglomerated particles, low density of packing near the column walls and by mixtures of fine and coarse particles. Longitudinal diffusion can be a particular problem in low mobile phase velocity systems but for most practical purposes in liquid chromatography the diffusion of the sample along the column may be considered negligible. Mass transfer affects solute molecules which diffuse into the stationary phase particles and are subsequently left behind by molecules which bypass the stationary phase. Band broadening is increased as the equilibration of the sample molecules between the stationary and the mobile phase becomes slower and the mobile phase velocity becomes higher. Extra-column dispersion is produced by dead volumes outside of the column i.e., in the injector, tubing or detector. Dead volume in the system should therefore be kept to a minimum by using fine bore tubing and zero dead volume connectors.

The van Deemter plot (Figure 1.3) is used to determine the optimum flow rate where three of the band spreading mechanisms mentioned previously will cause minimum affect on the system (extra column diffusion is taken as negligible). The plate height is the sum of the three factors and is plotted against the flow rate, ν. The eddy diffusion, A is independent of ν (although in practice A tends to increase slightly with increasing ν). With small particle size resins, the values of A, B and C are reduced, which in turn causes a reduction in the minimum plate height. For the same column length, a smaller plate height increases the number of plates and thus the column efficiency is improved.

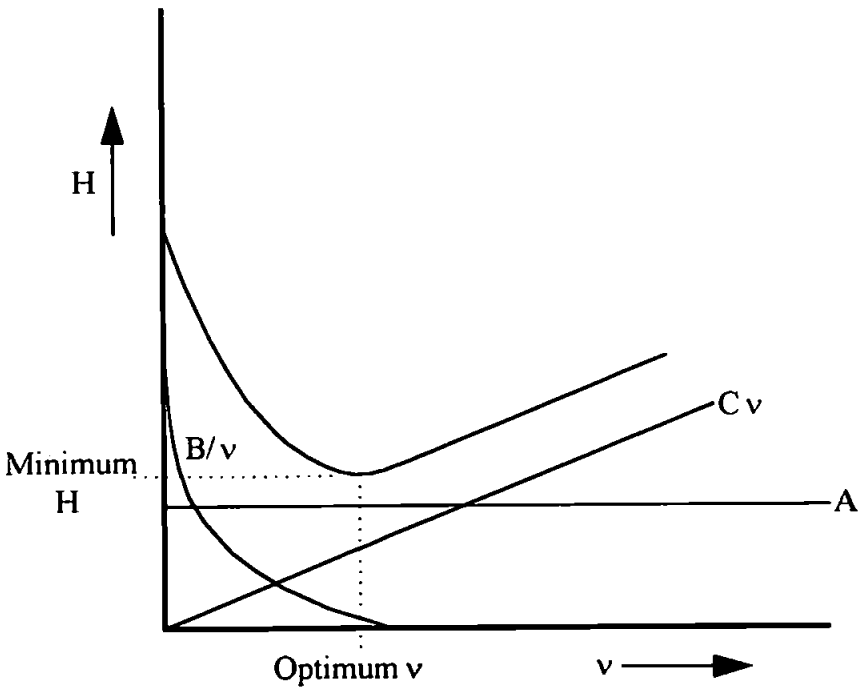

Figure 1.3. The van Deemter plot. The top curve is the total of the three spreading mechanisms.

In summary, the parameters described enable basic evaluation of a liquid chromatographic system which engulfs four main areas - adsorption, partition, ion-exchange and size exclusion. Any of these areas of liquid chromatography which are used for the separation and determination of ions may now be regarded as belonging to the field of 'ion chromatography' and encompasses the work described in this thesis.

1.3 Ion chromatography

Ion chromatography (IC) is an area of HPLC which covers a wide range of methods that are used to achieve the separation and enable the determination of both inorganic and organic anions and cations. The first recognised IC system was developed by Small *et al.* [2] in 1975 and described high performance separations which used simple ion-exchange. It is now accepted that IC embraces any chromatographic system which enables the rapid determination of anions and cations and this system may be classified into three main areas of separation mechanism - ion exchange, ion exclusion and ion pairing (interaction). Of these three mechanisms, ion exchange has been the most widely used and this can again be classified into two areas - simple ion exchange and chelating ion exchange.

1.3.1 Simple ion exchange

Ion exchange is analogous to adsorption chromatography in that the sample interacts with an active surface but in this case, the surface carries a charge. Suggestions for a more precise definition of ion exchange and ion exchangers have been made by Harjula *et al.* [4] and are detailed below:

"**Ion exchange** is the equivalent exchange of ions between two or more ionised species located in different phases, at least one of which is an ion exchanger, without the formation of new types of chemical bonds."

"An **ion exchanger** is a phase containing an osmotically inactive insoluble carrier of the electrical charge (matrix)."

The term 'osmotically inactive' means that the carrier cannot migrate from the phase where it is located to another phase. For example, sulphonic acid groups ($-SO_3H$) cannot migrate from a polystyrene (PS)-divinylbenzene (DVB) framework into the solution phase. Thus PS-DVB-SO_3H is an ion-exchanger, but $BaSO_4$ is not, since SO_4^{2-} can migrate into the solution phase due to dissolution.

Anion exchangers carry either weak or strong positively charged sites and cation ion exchangers carry either weak or strong negatively charged sites. In general, ion exchange resins are insoluble, rigid, three dimensional matrices which may be modified, for instance with either amino or ammonium groups for weak (WAX) or strong (SAX) anion exchangers respectively and, similarly, with either carboxylic or sulphonic acid groups for weak (WCX) or strong (SCX) cation exchangers respectively.

The strong cation exchanger is fully ionised above pH 2 and the strong anion exchanger is fully ionised up to about pH 10, whereas the weak cation and anion exchangers are ionised only over a restricted pH range. Cation exchangers have negatively charged sites of exchange:

$$R^- Y^+ + X^+ \rightarrow R^- X^+ + Y^+$$

(resin) (solution)

The counter ion Y^+ is exchanged for a cation, X^+, from the solution. The opposite is true for anion exchangers i.e.,

$$R^+Y^- + X^- \rightarrow R^+X^- + Y^-$$

(resin) (solution)

For trace analysis of free metal ions, cationic exchangers are used. Metal ions exchange with either the free acid (hydrogen form), or the salt form (often Na^+ or NH_4^+) which are present as the resin counter ions. Metal ions adsorbed onto the column will release an equal concentration of counter ions into solution. The exchange potentials for cation adsorption on to a strongly acid resin are influenced by a number of factors, the most important being molecular size (hydrated radii of cations), valency, and concentration. In dilute solutions exchange potentials increase with increasing valency, as illustrated by the following series, for some simple metal ions in 0.1 M solution of the chlorides at 25°C except where otherwise stated [5].

$$Th^{4+}(NO_3) > Fe^{3+} > Al^{3+} > Ba^{2+} > Tl^+ (SO_4) = Pb^{2+} > Sr^{2+} > Ca^{2+} >$$
$$Co^{2+} > Ni^{2+} = Cu^{2+} > Zn^{2+} = Mg^{2+} > Ag^+ > Cs^+ > Be^{2+}(SO_4) = Rb^+ >$$
$$Cd^{2+} > NH_4^+ = K^+ > Na^+ > H^+ > Li^+ > Hg^{2+}$$

In concentrated solutions, the effect of valency is reversed, the adsorption of univalent rather than multivalent ions being favoured. In general for efficiency in ion exchange, the affinity of the ion to be adsorbed must be substantially greater than that of the ion already in the resin.

The capacity of the resins is the amount of solute ions that may be adsorbed for a measured quantity of resin. Capacities of anion exchangers are smaller than those for cation exchangers, with the weak exchangers having higher capacities than the strong ones. One of the major limitations of ion exchange resins is that the high capacity of the ion exchanger necessitates high concentration eluents in order to elute the analytes in a reasonable time scale. This was one of the driving forces behind the fabrication of suppressed conductivity systems since a high level of background electrolyte would swamp the analyte signal and should therefore be removed. The production of low capacity ion exchangers has therefore led to systems in which low eluent concentration facilitates elution of the analyte ions enabling non-suppressed conductivity detection to be utilised. However, low capacity ion exchangers are prone to "swamping" by high ionic strength samples.

In 1935, Adams and Holmes [5] developed insoluble phenol-formaldehyde resins for ion exchange which were relatively unstable. More modern resins have been prepared which show superior stability in comparison to materials derived from phenol. Polystyrene crosslinked with divinylbenzene is now a widely used support for ion-exchange resins and is displayed in Figure 1.4. Different concentrations of divinylbenzene are used to vary the level of crosslinking, the most common being about 8%. A high degree of crosslinking produces a rigid gel which sustains negligible swelling on contact with solvents. As well as divinylbenzene crosslinked polystyrene support for the ion-exchange groups, low porosity beads with a thin surface layer of ion exchange material (pellicular) or bonded phases on microparticulate silica may also be used.

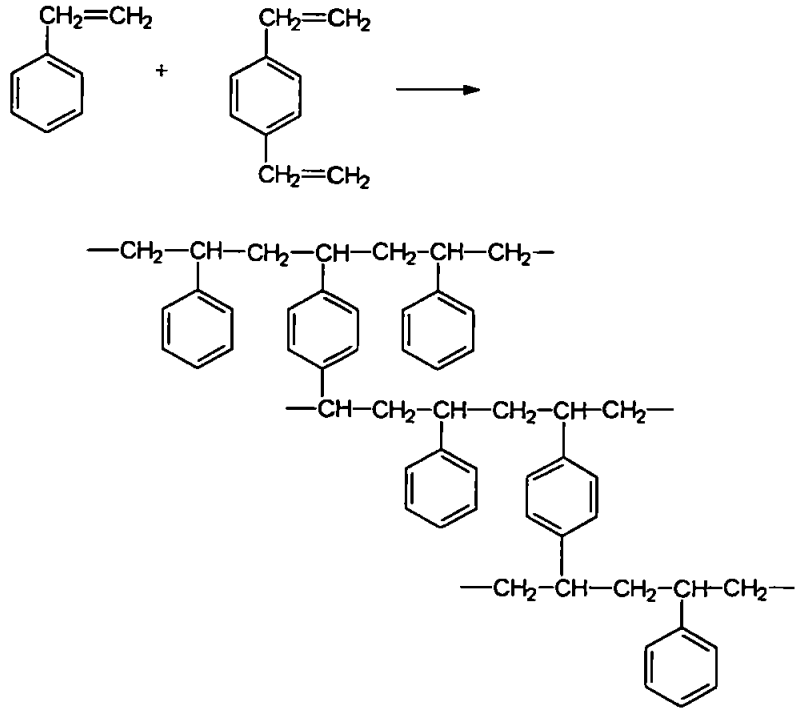

Figure 1.4. Styrene-divinylbenzene resin

1.3.2 Chelating ion exchange

When using samples of high ionic strength, simple ion exchange columns may temporarily experience drastic reductions in capacity, resulting in poor separations of the metal ions of interest. Sample pre-treatment involving the removal of the interfering matrix ions could minimise this problem, but may involve lengthy procedures such as solvent extraction which can then lead to the loss of analyte ions from entrainment effects. An alternative method is to use chelating ion exchange. Chelation is dependent upon conditional stability constants between a metal and the complexing ligand, and offers a far more selective separation mechanism than that available by employing simple ion exchange. Figure 1.5 illustrates the separation of either divalent or trivalent metal ions, M^{n+}, in the presence of a high concentration of monovalent metal ions. With simple ion exchange, the interactions of M^{n+} with the column are strongly influenced by high concentrations of monovalent ions and separations of the analyte ions may not be possible. This may be explained by the relative similarity in capacity factors for metal ions with simple ion exchange resins. Owing to the greater selectivity of the chelating ion exchange, capacity factors for divalent and trivalent metal ions can be many magnitudes greater than for monovalent ions. The chromatography of the analyte ions therefore remains essentially unaffected and separations are generally regarded as being controlled by pH. Competing chelating groups present in the eluent will affect metal ion interactions with the column and generally serve to reduce the capacity factors of selected metal ions. Further, chelating ion exchange offers the ability to separate small traces of metal ions from much larger

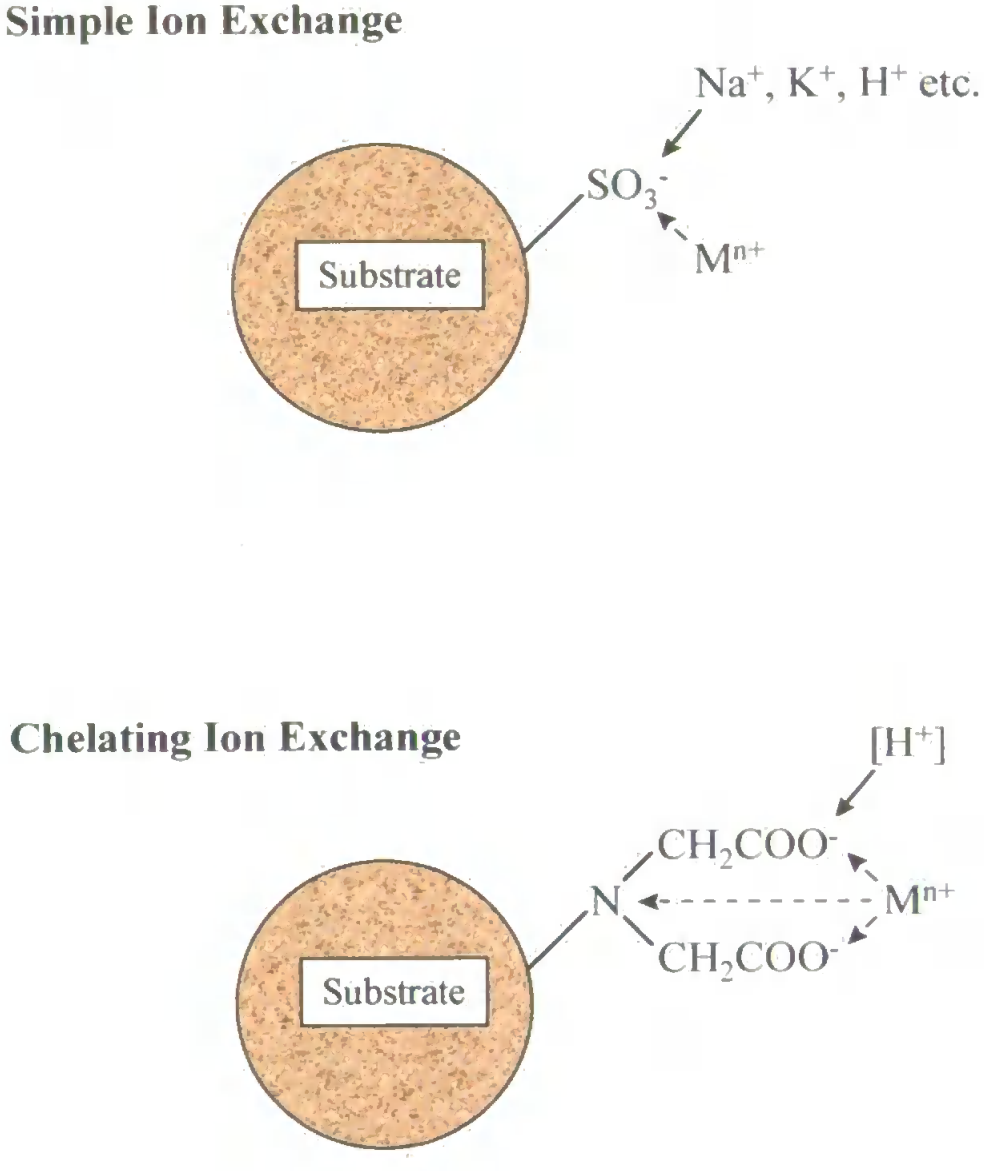

Figure 1.5. Simple ion exchange and chelating ion exchange mechanisms

concentrations of other metal ions provided that their affinities for the chelating columns are sufficiently different.

The selectivity of chelating ion exchange columns is dependent upon the chelating functional groups present. Chelating substrates can therefore be tailored for specific applications by modifying substrates with the desired chelating functionality e.g. O,O' , N,O and N,N' chelators may be used depending on the metal ions of interest. The majority of chelating columns have been prepared using large particle size resins for the preconcentration of metals before detection in spectroanalytical systems, as well as for ion chromatographic applications. Columns for high performance separations require smaller particle sizes and possibly more selective chelating groups when compared to columns which are used for preconcentration alone. There are therefore a large number of possibilities for the preparation of novel chelating substrates that can be developed for preparative as well as analytical applications.

1.4 Theory of Chelation

The Lewis acid approach provides the broadest theory of co-ordination chemistry and is described in terms of acids (electron pair acceptors) and bases (electron pair donors). Metal ions are electron acceptors and are therefore acids. An atom, or

group of atoms, attached to a metal ion by electronic interactions is known as a ligand. Ligands are electron donors and are therefore known as bases. When a ligand, or group of ligands are attached to a metal ion, the resulting combination is regarded as a complex, with the interactions termed 'hard' for ionic interactions and 'soft' for covalent interactions. The term 'hardness' and 'softness' usually refers to the ligating atom:

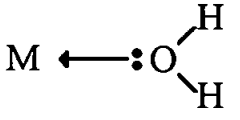

HARD

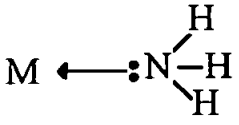

INTERMEDIATE

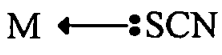

SOFT

Hardness is usually associated with highly charged small anions or cations with low polarisability which are not easily deformed in the presence of another charge. Softness is associated with large anions or cations with high polarisability which are easily deformed and possess a fair degree of covalent character. The general concept is that hard acids form their strongest complexes with hard bases and soft acids form their strongest complexes with soft bases.

Table 1.1 displays a list of metal ions as hard or soft acids and ligands as hard or soft bases. As expected, the triply charged Al^{3+}, with ionic radius 0.51 Å is a hard acid, whereas monovalent Ag^{+} with radius 1.26 Å is a soft acid. Considering other ligands, fluoride is a hard base and iodide is a soft base.

A) Metal Ions as Hard or Soft Acids

Hard

H^+											
Li^+	Be^{2+}										
Na^+	Mg^{2+}	Al^{3+}	Si^{4+}								
K^+	Ca^{2+}	Sc^{3+}	Ti^{3+}	Ti^{4+}	VO^{2+}	Cr^{3+}	Mn^{2+}	Fe^{3+}	Co^{3+}	Ga^{3+}	As^{3+}
Rb^+	Sr^{2+}	Y^{3+}	Zr^{4+}			MoO^{3+}				In^{3+}	
Cs^+	Ba^{2+}	La^{3+}	Hf^{4+}	Th^{4+}							
	Ra^{2+}	U^{4+},	UO_2^{2+}	and the rare earth ions							

Intermediate

Cr^{2+}	Fe^{2+}	Co^{2+}	Ni^{2+}	Cu^{2+}	Zn^{2+}		
	Ru^{2+}	Rh^{3+}				Sn^{2+}	Sb^{3+}
	Os^{2+}	Ir^{3+}				Pb^{2+}	Bi^{3+}

Soft

		Cu^+					
	Pd^{2+}	Ag^+		Cd^{2+}			Te^{4+}
Pt^{2+}	Pt^{4+}	Au^+	Hg^+	Tl^+	Tl^{3+}		

B) Ligands as Hard or Soft Bases

Hard

H_2O	HO^-	RO^-	R_2O	ROH	RCO_2^-	CO_3^{2-}	PO_4^{3-}	NO_3^-	SO_4^{2-}
ClO_4^-	F^-	Cl^-							

Intermediate

NH_3	RNH_2	Aniline	Pyridine		N_2H_4
N_3^-	NO_2^-	ClO_3^-	Br^-	SO_3^{2-}	

Soft

R_2S	RSH	RS^-	SCN^-	$S_2O_3^{2-}$
R_3P	$(RO)_3P$			
I^-	CN^-			

Table 1.1 A) Metal ions as hard or soft acids B) ligands as hard or soft bases [6]

Ligands which have one point of attachment are known as monodentate and those with more than one point of attachment are termed polydentate (or multidentate) ligands. Polydentate ligands form complexes known as chelates (from the Greek meaning 'crabs claw') which are much more stable than those of monodentates. Chelate complexes assume ring type structures called chelate rings when complexed with a metal ion, owing to the attachment of two or more ligands from the same molecule. Five and six membered rings form the most stable arrangements.

$$Ni\,(H_2O_6)^{2+} + 6NH_3 \rightarrow Ni(NH_3)_6^{2+} + 6H_2O \qquad \beta = 10^{8.6} \;\; (\log \beta = 8.6)$$

$$Ni(H_2O)_6^{2+} + 3en \rightarrow Nien_3^{2+} + 6H_2O \qquad \beta = 10^{18.3} \;\; (\log \beta = 18.3)$$

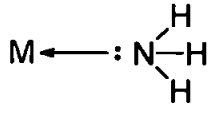

ammonia

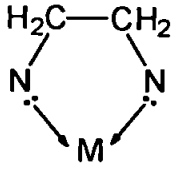

ethylenediamine (en)

The ß term is known as the overall formation constant and gives an indication of the stability of a complex. The increased stability of the ethylenediamine complex over the ammonia complex can be explained by the 'chelate effect'. The chelate effect can be basically described in terms of *entropy*, the degree of disorder of the system. In the ammonia complex, an equal number of water molecules are displaced for ammonia molecules giving no increase in the net number of independent molecules. In the ethylenediamine complex, however, there is a net increase in the number of independent molecules since it only takes 3 en molecules to displace 6 H_2O molecules.

Other somewhat smaller effects can be used to explain trends in the stability of complexes, such as the Irving/Williams series of stability determined from the 'Crystal Field Theory' concerning d-orbital "splitting":

$$Ba^{2+}<Sr^{2+}<Ca^{2+}<Mg^{2+}<Mn^{2+}<Fe^{2+}<Co^{2+}<Ni^{2+}<Cu^{2+}>Zn^{2+}$$

In every case, copper forms the most stable complex. Furthermore, steric factors can cause some ligands to be highly specific for certain metal ions particularly in biological systems e.g. the eniatin B-potassium complex .

1.4.1 Stability of Complexes

To facilitate the determination and use of stability constants, measurements are taken at 'constant ionic strength' (usually 0.1 M) in order to avoid changes in activity. The concentration stability constants of complexes, K_{STAB}, are therefore given for a particular ionic strength (in very dilute solutions, K_{STAB} becomes the same for activity). For a one ligand system, where only soluble mononuclear complexes are formed, the equilibrium relations may be expressed as *stepwise formation constants*:.

$$M + L = ML \qquad K_1 = \frac{[ML]}{[M][L]}$$

$$ML + L = ML_2 \qquad K_2 = \frac{[ML_2]}{[ML][L]}$$

$$ML_2 + L = ML_3 \qquad K_3 = \frac{[ML_3]}{[ML_2][L]}$$

$$\downarrow \qquad\qquad \downarrow$$

$$ML_{N-1} + L = ML_N \qquad K_N = \frac{[ML_N]}{[ML_{N-1}][L]}$$

There are N equilibria, where N represents the maximum co-ordination number of the metal ion M for the ligand L, and in some cases, N may vary from one ligand to another. In the case of Al^{3+}, the chloro complex has four ligands, $AlCl_4^-$, and the fluoro complex has six ligands, AlF_6^{3-}, as the highest complexes.

Equilibrium relationships may also be expressed in terms of the *overall formation constants:*

$$M + L = ML \qquad \beta_1 = \frac{[ML]}{[M][L]}$$

$$M + 2L = ML_2 \qquad \beta_2 = \frac{[ML_2]}{[M][L]^2}$$

$$M + 3L = ML_3 \qquad \beta_3 = \frac{[ML_3]}{[M][L]^3}$$

$$\downarrow \qquad\qquad \downarrow$$

$$M + NL = ML_N \qquad \beta_N = \frac{[ML_N]}{[M][L]^N}$$

The relationship between the stepwise stability constants and the overall formation constants is given by:

$$\beta = K_1K_2K_3 \cdots K_k = \prod_{i=1}^{i=k} K_i$$

Depending upon the situation, either constant may be used for convenience. In general, there is a slowly descending progression in the value of K_i for both charged and uncharged systems, as illustrated by the following Cd complexes:

$$Cd^{2+} + NH_3 = [Cd(NH_3)]^{2+} \qquad K = 10^{2.65}$$

$$[Cd(NH_3)]^{2+} + NH_3 = [Cd(NH_3)_2]^{2+} \qquad K = 10^{2.10}$$

$$[Cd(NH_3)_2]^{2+} + NH_3 = [Cd(NH_3)_3]^{2+} \qquad K = 10^{1.44}$$

$$[Cd(NH_3)_3]^{2+} + NH_3 = [Cd(NH_3)_4]^{2+} \qquad K = 10^{0.93} \qquad (\beta = 10^{7.12})$$

Or in the case of CN^-

$$Cd^{2+} + CN^- = [Cd(CN)]^{+} \qquad K = 10^{5.48}$$

$$[Cd(CN)]^{+} + CN^- = [Cd(CN)_2] \qquad K = 10^{5.12}$$

$$[Cd(CN)_2] + CN^- = [Cd(CN)_3]^{-} \qquad K = 10^{4.63}$$

$$[Cd(CN)_3]^{-} + CN^- = [Cd(CN)_4]^{2-} \qquad K = 10^{3.65} \qquad (\beta = 10^{18.8})$$

The stepwise and overall formation constants assume that the reactants, or products, are in one form, but in practice the amount of metal or ligand available for complexation is determined by the *conditional stability constant*, K_{COND}, which can be represented as

$$K_{COND} = \frac{ML}{\Sigma M \Sigma L}$$

The conditional stability constant can not only give information on how much of the product [ML] is formed, but also the total concentration of uncomplexed metal [M'] and the total concentration of the uncomplexed reagent [L']. Therefore, the conditional stability constant is not a thermodynamic constant, but depends on the experimental conditions, especially upon the concentrations of other species in the solution. Species distribution diagrams may be used to calculate the conditional stability constants under certain conditions. Figure 1.6 shows a species distribution diagram for 0.0010 M Ca (II) and 0.0010 M EDTA at 0.100 M ionic strength and 25°C. It is clear that at pH 2 there is about 100 % of the free metal ion. At pH 4.5 there is approximately 50 % of the free metal, M, 50% of the H_2L species, and therefore about 50 % of the complexed metal, ML. At pH 8 approximately 100 % of the metal is complexed with the EDTA molecule.

Figure 1.7 displays the conditional stability constants, $K_{M'L'(ML')}$, of various metal EDTA complexes as functions of pH. The curves represent maximum values of conditional constants, which are only attained if no side reactions, except those affected by hydrogen and hydroxide ions, occur. In the case of some metal ions, e.g. Al, the complex with EDTA is heavily influenced by hydroxide species.

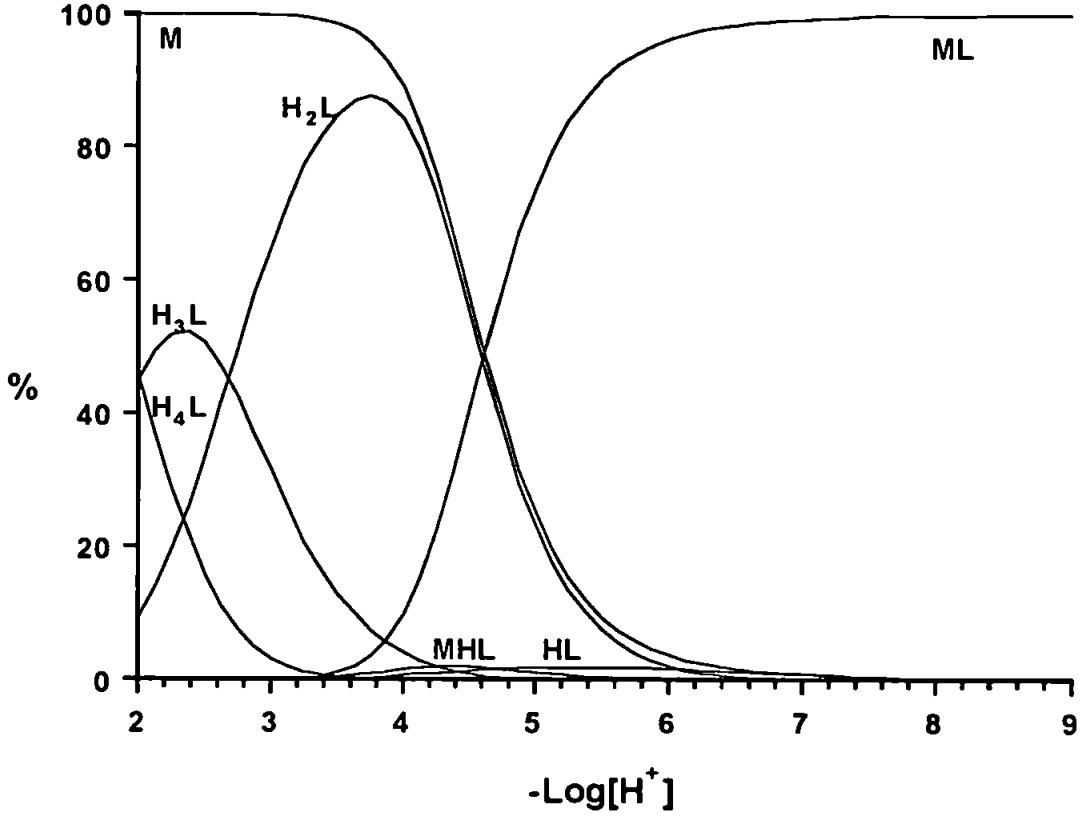

Figure 1.6. A species distribution diagram for 0.0010 M Ca (II) and 0.0010 M EDTA at 0.100 M ionic strength and 25°C.

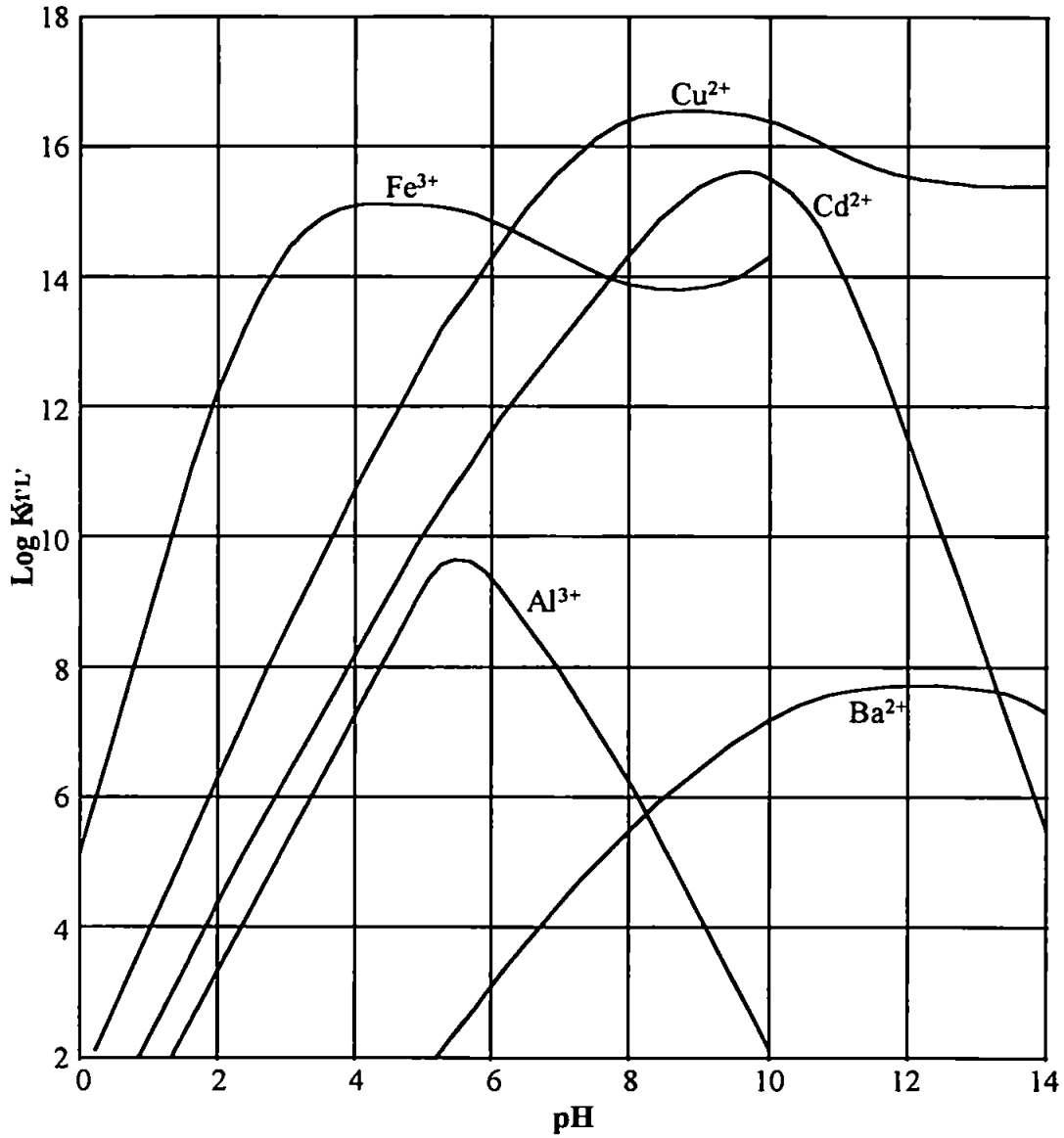

Figure 1.7. Conditional stability constants, $K_{M'L'(ML')}$, of various metal EDTA complexes as functions of pH [7].

1.5 A Review of Chelating Substrates

In general, chelating sorbents are comprised of natural or synthetic substrates which have modified surfaces in order to produce complexing selective adsorption sites for metal ions. From the literature it has been shown that two different types of substrates have become clearly established. The first type are low crosslinked polymer gels such as cellulose based substrates which are suitable for low to medium pressure applications. These lightly crosslinked polymer networks are easily compressed under high pressure and collapse, restricting the flow and reducing the column permeability. The second, rigid macroporous supports such as silica and polystyrene divinylbenzene, can withstand high pressures and have therefore traditionally been the most popular supports for HPLC applications.

There are numerous methods for the preparation of chelating sorbents. In some cases the chelating functional groups are covalently bound to a substrate during or after the preparation of the polymer network. An alternative method is to prepare the chelating sorbent by direct adsorption, or impregnation, of chelating groups onto the surface of a substrate to create a sorbent which is stable under normal working conditions. The latter technique may reduce the preparation time normally associated with complicated organic syntheses and can enable the simple modification of a chosen substrate.

There are a wide number of chelating functionalities which are suitable for the preparation of chelating sorbents and some of these are illustrated in Figure 1.8.

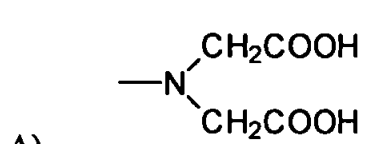

A)

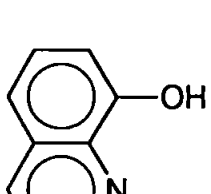

B)

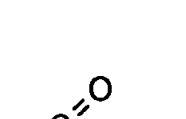

C)

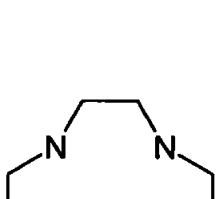

D)

E)

Figure 1.8. Chelating functional groups A) Iminodiacetic acid (IDA), B) 8-Hydroxyquinoline (8-HQ), C) Hydroxamic acid, D) 1,4,8,11-tetraazacyclotetradecane and E) Dithiocarbamate

Although the behaviour of many chelating functional groups in solution is known, it is often difficult to predict their behaviour when they are attached to a solid phase, since there may be strong interactions between the functional groups and the substrates themselves. The co-ordination properties of sorbents may therefore be radically affected, not only by the nature of the chemical groups in the sorbents but by physical characteristics such as the nature of the polymeric matrix, steric factors and sorption conditions [8]. However, in some cases, interactions between chelating functionalities and substrates may be beneficial since they could give rise to unusual selectivities of the sorbent, which may be directed for specific applications.

The majority of publications concerning the preparation and applications of chelating sorbents have mainly described their use for preconcentration purposes and the use of high grade substrates was not essential. Although many different substrates have been utilised, the main emphasis has been on silica and polystyrene based phases and some examples of these are described in the following review. A small volume of work has also been detailed in the literature concerning cellulose based chelating sorbents. These papers will therefore be reviewed in Chapter 2 - 'Dye Loaded Cellulose Based Substrates'.

1.5.1 Silica based sorbents

There is extensive literature on the use of chelating functionalities bonded to silica based stationary phases for the preconcentration of metal ions. One of the most widely used sorbents for trace metal preconcentration has been an 8-hydroxyquinoline (8-HQ)

bonded silica gel column. Hill [9] described the preparation of an 8-HQ silica gel and the application for the removal, concentration and separation of trace amounts of copper and other metal cations from solutions of high ionic strength. Samples of the chelating sorbent were found to possess long term stability in aqueous solutions up to pH 9 and, unlike cellulose based substrates, microbial growth was not readily supported.

The stability constants of 8-HQ are also greater than those of iminodiacetate and the removal of transition metals from solutions should be relatively more effective. Sturgeon *et al.* [10] reported the use of a silica gel with bonded 8-HQ for the preconcentration of Cd (II), Pb(II), Zn(II), Cu(II), Fe(II), Mn(II), Ni(II) and Co(II) from sea water prior to their determination by GFAAS. Good agreement with the accepted values for all of the metals described was found for two near shore and one open ocean sea water sample. Beauchemin and Berman [11] used a miniature column of 8-HQ for the preconcentration of trace metals from sea waters prior to analysis by ICP-MS. The system was successfully applied for the determination of Mn(II), Mo(II), Cd(II) and U(VI) in the reference open ocean water NASS-2 using an isotope dilution technique and the method of standard additions. Mohammad *et al.* [12] reported the use of 8-HQ on controlled pore glass for the on-line preconcentration of Al for determination by AAS. A malonate buffer system was used to prevent hydrolysis of the Al species at pH 8. Good recoveries of Al were found in the presence of interfering ions (F^-, Na^+, Ca(II), Mg(II), Fe(III) and Cu(II)) and a reasonable concentration of Al was determined from an estuarine sea water sample. Chambaz and Haerdi [13] have also described an 8-HQ bonded chelating silica for the

preconcentration of metal ions. Cu and Ni were preconcentrated and eluted using 0.1M potassium cyanide before separation on an ion-pairing C_{18} column. The results were found to be highly reproducible in the concentration range 10^{-8} - 5×10^{-6} M.

Kocjan [14] reported Titan Yellow coated silica gel for the separation and preconcentration of trace metals from alkaline earth or alkali metal salts. The silica gel was treated with a mixture of Aliquat 336 and Titan Yellow to obtain the chelating sorbent. Preconcentration of a range of metals was found to be reproducible for flow rates of up to 4 ml min^{-1}. The preconcentration of Cu(II), Pb(II), Cd(II) and Zn(II) from metal chlorides was also tested with the Titan Yellow sorbent. It was found that the metal ions were completely removed from the solutions after testing the eluates with anodic stripping voltammetry.

Ethylenediamine and dithiocarbamate bonded silica gels have been prepared by Leyden and Luttrell [15]. The extraction of Hg(II), Ag(II), Cr(II), Mn(II) and Cu(II) from relatively high ionic strength solutions was reported, indicating good potential as a preconcentrating agent for X-ray fluorescence and also other analytical methods. Gimpel and Unger [16] described the modification of silica with a range of silanes, but only the silicas with bonded iminodiacetate and ethylenediaminetriacetate groups remained hydrolytically stable.

Chambaz *et al.* [17] reported the preconcentration of divalent trace metals on chelating silicas followed by on-line chromatography. Ethylenediamine triacetate (ED3A) bonded chelating silica was used to preconcentrate Mn(II), Co(II), Ni(II), Cu(II),

Zn(II), Cd(II) and Pb(II). Separation of the ions was achieved using a cation exchange column upon elution from the chelating column. The on-line method was found to be more reproducible when compared to the off-line method. Analysis of a natural river water sample with the system showed that the on-line method was suitable for the determination of Cu(II), Pb(II), Zn(II), Ni(II), Co(II) and Cd(II).

A range of complexing agents on various supports have been described by Terada *et al.* [18]. 2-Mercaptobenzothiazole on silica gel was considered to be the most useful since it could quantitatively adsorb Cu(II) from aqueous solutions at very high flow rates at pH 4.0 (Cu was chosen owing to its high affinity for all of the chelating functional groups). 2-Mercaptobenzimidazole required pH 6.0 to effect the same task. Silica gel was found to be a better support for the chelating ligands than activated carbon and polytrifluorochloroethylene (PTFCE). 2,5-Dimercapto-1,2,3-thiadiazole in silica gel removed copper from highly acidic solutions, but poor adsorption on the silica gel meant that the column capacity was severely restricted.

Glennon and Srijaranai [19] described the use of a biochelation cartridge for the preconcentration of trace metals. Unsubstituted and N-methyl substituted mono-hydroxamate silicas were compared with the biochelator, desferrioxamine (DFA), immobilised onto silica. The DFA was found to display an over-all lower capacity as a function of pH than the other sorbents tested, including carboxymethyl silica, which was used as a reference. A trace metal cartridge, utilising the biochelating silica showed good stability, preconcentration and elution properties for Fe (III), Cu(II), Ni(II), Zn(II), Co(II) and Al(III).

Ryan and Glennon [20] discussed the use of biochelating silicas but with dextran chelating functionalities. Separations of Pb(II), Mn(II), Co(II), Cu(II), Zn(II) and Ni(II) on cation exchange columns were improved after preconcentration on the dextran bonded silica column in comparison to direct injections. Ryan *et al.* [21] also discussed the use of carboxymethyl and hydroxamate dextran-coated silicas which increased the degree of metal ion chelation in comparison to dextran coatings alone. The total percentage metal uptake of the sorbents was similar although, at low pH, the level of complexation of the carboxymethyl dextran coated silica (CMD-Si) was slightly higher owing to an increased number of sites for metal uptake. A chelating cartridge was prepared from the hydroxamic acid dextran coated silica (HAD-Si). A separation of Cu(II), Mn(II), Co(II), Zn(II) and Ni(II) in a river water sample using a CS-5 (Dionex) cation exchange column had increased limits of detection after preconcentration with the cartridge, in comparison with a direct injection. The preconcentration cartridge was also used with AAS detection and showed good correlation with the IC determinations of the trace metal levels in the same river water sample.

1.5.2 Polystyrene based chelating resins

A number of chelating resins prepared from polystyrene divinylbenzene are available commercially. They generally exist as semi-rigid or rigid microporous or macroporous structures which have relatively large particle sizes in comparison to the substrates used for reversed phase chromatography. These chelating resins have been widely used to preconcentrate metal ions from complex matrices such as sea water, before

sample introduction into detection systems such as flame atomic absorption spectrometry (FAAS) and inductively coupled plasma - mass spectrometry (ICP-MS). A number of chelating sorbents for analyte preconcentration with atomic spectrometric detection have been reported in a review by Ebdon *et al.* [22] and more recently by Worsfold *et al.* [23]. In addition, the principle physicochemical and analytical properties of many chelating sorbents have been examined by Myasoedova and Savvin [8]. Applications of chelating sorbents are discussed and practical recommendations for the use of the sorbents and examples of their use in inorganic analysis are given.

A widely used resin with iminodiacetate (IDA) chelating functionalities is commercially available under the name Dowex A-1 and a more purified form is known as Chelex-100. The starting material for the synthesis of this resin is chloromethylated styrene-divinylbenzene which undergoes an amination reaction and is subsequently treated with monochloroacetic acid (Figure 1.9):

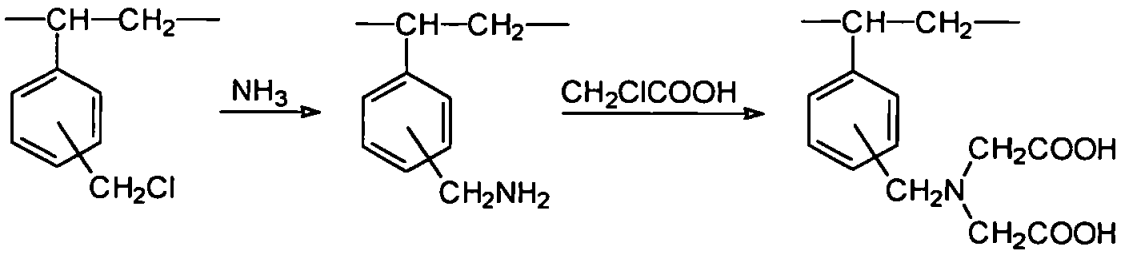

Figure 1.9. The synthesis paths for IDA functionalised styrene divinylbenzene resins

Chelex 100 demonstrates unusually high preference for copper, iron and other heavy metals over alkali and alkaline earth cations, such as sodium and calcium. The IDA

group allows several possibilities for ion adsorption. At very low pH's, in addition to the acetate groups becoming protonated, the nitrogen of the imino group becomes protonated, giving the resin anion exchange properties. Metal ions with very high stability constants may still form chelates under these conditions and the simultaneous chelation and anion exchange mechanisms give the resin a so called 'mixed-mode' performance.

Christell and co-workers [24] made early fundamental studies of the Dowex A-1 resin with regard to the adsorption of trivalent metal ions. Standard solutions of radioactive lanthanum and lutetium were eluted through a column of Dowex A-1 and it was found that the high atomic number lutetium eluted first. Lanthanum should have eluted first, however, if the reaction was chelation controlled. Further fundamental studies of Dowex A-1 were made by Van Willigen *et al.* [25] for the determination of stability constants of the resin with a number of metals. It was found that the selectivity of the resin was not high enough to effect the separation of metals in batchwise operation. Column operations were not possible owing to the large swelling effects of the resin with increasing pH. Luttrel *et al.* [26] reported the effect of pH and ionic strength on the ion exchange and chelating properties of the Dowex A-1 resin. A column procedure was used which showed that alkaline earth metals were adsorbed by simple ion exchange below pH 4 and by chelation above pH 6. Between these values, a mixed-mode exchange was prevalent. The relationship between the elution peak maxima and pH at constant ionic strength, and ionic strength at constant pH, were quantified by empirical equations.

One of the first major analytical applications of IDA based resins was reported by Riley and Taylor [27]. Chelex-100, a purified form of the Dowex A-1 resin, was used in the investigations although it was found that the two resins behaved identically. Chelex-100 was found to adsorb a wide range of trace elements from sea water and gave similar results to another IDA based resin, Permutit S1005. A sample of sea water was stripped of trace metals by elution through columns packed with the chelating resins. Known concentrations of copper, nickel, cobalt and cadmium were added to the clean sea water. The sea water sample, with the added metal ions, was then eluted back through the chelating column at high pH to achieve preconcentration. The metal ions were stripped from the columns and the atomic absorption spectrometric analyses of the eluites indicated good recoveries.

Pai [28] reported the preconcentration of heavy metals using Chelex-100 resin. The efficiency of the resin was investigated by eluting spiked sea water samples through a column containing Chelex-100. The column was divided into small sections and the spiked trace metals were recovered from each section. It was discovered that different pH's were required for the optimum preconcentration of selected metals unless large columns and low flow rates were utilised. If the correct pH is not used during preconcentration then recoveries may be very poor.

The removal of trace metal impurities from phosphoric acid using Chelex-100 has been reported by Murugaiyan *et al.* [29]. A range of trace metal impurities were successfully separated from phosphoric acid and subsequently determined by FAAS and graphite furnace atomic absorption spectrometry (GFAAS). An investigation into

the metal ion adsorption mechanisms was made and it was concluded that a chelation mechanism, through interaction with the IDA group, was responsible and not a precipitation or ion exchange mechanism.

The sorption mechanism of trace amounts of divalent metal ions on Chelex-100 has been discussed by Pesavento *et al.* [30]. The Gibbs-Donnan model was used to predict the extraction coefficients of metal ions and it was found that some metals were adsorbed onto the resin at much lower pH's than anticipated. In addition, it was found that sorption isotherms for some metal ions can be affected by the matrix, e.g. zinc and cadmium sorption may occur at higher pH's in sea water when compared to freshwater samples. Strachan *et al.* [31] discussed the preconcentration of trace transition metals and rare earth elements from highly saline solutions. The results indicated that transition metals and rare earth ions could be preconcentrated with quantitative elution from solutions of both low and high ionic strength.

Although the use of Chelex-100 and Dowex A-1 has been widely reported, there are known deficiencies in the performance of the resins. Owing to the low cross link (gel type) microporous PS-DVB support, the mechanical stability of the resins is poor and substantial changes in the resin volume occur between acidic and basic solutions. Siriraks *et al.* [32] reported a low recovery of metal ions from Chelex-100 which was believed to be caused by the physical degradation of the resin under pressure (>100 psi). It was reported that the performance of a more highly cross-linked macroporous PS-DVB containing the IDA functional group gave better metal recoveries in comparison to Chelex-100. The resin was used to prepare MetPac CC-1 (Dionex)

columns which were not found to physically degrade or become chemically altered when exposed to high pressures owing to a higher degree of physical integrity. The MetPac CC-1 column was used to preconcentrate metals in a complex automated system before separation on a CS-5 cation exchange column. The analysis of Fe(II), Cu(II), Ni(II), Zn(II), Co(II) and Mn(II) in complex environmental and biological samples was achieved with good correlations with certified values.

Blain *et al.* [33] reported the deficiencies of the Chelex-100 chelating resin, and explained that the partial recovery of some transition metal ions was a result of the lack of selectivity of the IDA functional groups. Transition metals are described as soft acids and the alkali and alkaline earth metals as hard acids. The presence of hard acidic sites i.e. oxygen atoms in the resin will reduce the selectivity for transition metals. Therefore, a commercial chelating resin, based on a pentamine ligand (1,4,7,10,13-pentaazatridecane or tetren) and grafted onto an organic polymer, known as Chelamine, was utilised. This resin contains nitrogen atoms and thus soft basic sites, which were shown to have a high selectivity for Cd (II), Cu(II), Mn(II), Ni(II), Pb(II) and Zn(II) in sea water. Groschner *et al.* [34] also used the chelating resin Chelamine in preference to Chelex-100 in a three column system for the speciation and determination of trace metals in natural waters. A Dowex 1-X8 (100-200 mesh) anion exchange resin and a C_{18} phase (Bondelut LRC columns) were also used in the system. The Chelamine was found to retain Cd(II), Cu(II), Zn(II), Pb(II) and Mn(II) in the pH range 5-8 with excellent efficiency for the untreated water samples. A decrease in recovery for the Chelamine column was noted when using standards prepared in distilled water. This was probably caused by the occurence of hydroxide precipitates,

owing to a local increase in pH caused by the strongly basic groups in the resin. The Chelamine was reported to discriminate against the major sea-water cations (Na(I), Ca(II), Mg(II)) better than Chelex-100 and also an 8-hydroxyquinoline column.

A macrocyclic tetramine based chelating resin has been described by Szczepaniak and Kuczynski [35]. Cyclam (1,4,8,11-tetra-azacyclo-tetradecane) forms chelate complexes of varying stability with a number of transition metal cations and forms a selective sorbent when bonded to the matrix of a PS-DVB copolymer (RC resin). The adsorption of a range of transition metals on the RC resin was achieved as well as a separation of Mg(II), Zn(II) and Cu(II) by eluting the metal ions from the column with different eluents.

An N-benzoylphenylhydroxylamine based PS-DVB resin has been prepared by Das and Pobi [36]. The BPHA resin was used to successfully preconcentrate and elute Be(II) from a range of other metal ions, including Al(III) in 100 times excess. One problem with the column was that it was restricted by pH. Above pH 7 the column turned blue and degraded in the alkaline conditions. The preconcentration of Cd(II), Zn(II), Pb(II) and Ni(II) using a thioglycolate chelating resin has been discussed by Howard *et al.* [37]. The resin displayed good stability after being stored dry at room temperature for one year. Full equilibrium of the column with the metal ions was achieved at pH 7 after a period of 90 minutes. The recoveries for all of the metals tested from an acetate buffer were high but only Cd(II) and Pb(II) were suitable for preconcentration from a sea water matrix since the recoveries for Zn(II) and Ni(II) were poor.

The adsorption of Pd(II) and Cu(II) by glycolmethacrylate resins has been reported by Anticó *et al.* [38]. The macroporous hydrophilic glycolmethacrylate resins contained side chains of 8-hydroxyquinoline (Spheron Oxine 1000), thiol (Spheron Thiol 1000) and salicyl groups (Spheron Salicyl 1000). Desorption of Pd (II) was most effective for the Speron Oxine resin and the kinetics of the system were found to be relatively rapid. Separations of aqueous mixtures of Pd (II) and Cu (II) were also discussed.

1.5.3 Impregnated polystyrene based resins

The impregnation of polystyrene resins with chelating functionalities is an effective method of preparing chelating substrates for both analytical and preparative chromatographic methods. Most of the work involving the direct adsorption of chelating groups on the resins has involved the application of organic chelating dyes. Considerable research has focused on these dyes since they can be very selective for certain groups of metals. There are therefore a wide number of commercially available chelating dyes to choose from in order to obtain the selectivity required for the chelating column. The structure of many dyes enables easy adsorption on to polystyrene based resins, owing to π-π interactions between the aromatic groups of the both the dye and the resin. In addition, a form of physical entrapment which prevents the dye from leaving the porous structure of the resin certainly occurs. Steric and physicochemical effects between various chelating dyes and resin substrates can affect the behaviour of the chelating functionalities. This can produce unusual selectivities for metal ions and make the character of some chelating resins, prepared by dye

adsorption, different from the behaviour of the 'free' dye in solution. In addition, by using dye molecules, lengthy synthetic methods for both the preparation of the chelating functionality and attaching the functionality to the resin, may be avoided.

A review by Marina *et al.* [39] lists a number of dyes and other organic ligands impregnated on polystyrene based resins for the preconcentration of trace metals from aqueous solutions. Characteristics and applications for the modified chelating resins were discussed. Lundgren and Schilt [40] reported studies of ferroin type chromogens immobilised on a PS-DVB copolymer. Four chromogens were investigated and 3-(2-pyridyl)-5,6-diphenyl-1,2,4-triazine (PDT) was found to be most effectively adsorbed on the Amberlite XAD-2 resin. The sorbent was found to remove Fe(II), Co(II), Ni(II), Cu(II) and Zn(II) from a synthetic sea water sample. It was also found that the group separations of metal ions was possible, e.g., Mg(II) and Ca(II) could be determined without interference from Fe(II), Cu(II), Co(II), Ni(II) and Zn(II) ions.

Howard and Arbab-Zavar [41] discussed the preconcentration of 'inorganic' and methyl mercury cations on dithizone-coated macroreticular resin beads prior to analysis with AAS. HCl (9 M) was required to remove the Hg(II) from the column. The coated beads gave highly selective and quantitative recoveries of Hg(II) from both fresh and saline samples. However, the dithizone was not stable and the beads would have to be recoated before further use. Brajter *et al.* [42] reported a sulphonated dyestuff, xylenol orange, impregnated on Amberlyst A-26 macroreticular anion exchange resin. Elution curves from the column, determined by AAS showed the

potential of the sorbent by separations of Al-In, Ga-In, Zn-In, and Cu-Mn in various ratios.

Chwastowska and Mozer [43] prepared a chelating sorbent by the immobilisation of 1-(2-pyridylazo)-2-naphthol (PAN) on Amberlite XAD-4. The dye-coated resin was characterised and it was found that optimum sorption of trace metals was at pH 8, since above this level high concentrations of Ca(II) and Mg(II) may interfere. The column was applied to the analysis of trace metals in a river water sample. Selective elution of the trace metals allowed for the determination of Zn(II), Cu(II), Cd(II), Fe(II), Ni(II) and Pb(II) by AAS. Chwastowska and Przygoda [44] described the impregnation of XAD-4 with N-benzoyl-N-phenylhydroxylamine (BPHA). The effective adsorption of metal ions was not fully quantitative for a number of trace metals from aqueous solutions. Preconcentration of trace metals was attained by eluting a 1 litre river water sample through a column of the modified resin at pH 9. After removal from the column using HCl, the determination of Cu(II), Pb(II), Zn(II) and Cd(II) using AAS was achieved. The standard deviations recorded were less than 10% and no value was recorded for Co(II) since it was too low to be determined.

Marina *et al.* [45] reported the impregnation of 2-(*p*-sulfophenylazo)-1,8-dihydroxy-naphthalene-3,6-disulfonic acid (SPADNS) on the anion exchanger Amberlite IRA-400. At pH 6.85 the percentage recovery of Cu(II), Fe(III), and Pb(II) after on column preconcentration was found to be quantitative, but the recoveries obtained for Zn(II) and Mn(II) were very low, indicating that they would not cause much interference in a study of the former three metals in drinking water. There was no

evidence of Pb(II) in the drinking water sample chosen and the preconcentration of Cu(II) and Fe(III) alone was achieved. The determinations made by AAS after preconcentration of the sample were compared with direct GFAAS determinations. Overall, there was good correlation between the results except there were some fluctuations which were believed to be caused by the analyte concentration approaching the detection limits for the GFAAS.

Isshiki *et al.* [46] reported a 7-dodecenyl-8-quinolinol (DDQ) (the active substance of the liquid ion-exchanger Kelex-100) impregnated XAD-4 resin. Although the equilibration times were much longer, the extraction behaviour of the DDQ resin was similar to that of 8-HQ. The quantitative recoveries of Ag(I), Al(III), Bi(III), Cd(II), Co(II), Cr(III), Cu(II), Fe(III), Ga(III), Mn(II), Ni(II), Pb(II) and Ti(IV) were made after preconcentration at pH 8 and determination with GFAAS.

Brajter *et al.* [47] have reported the preconcentration of metal ions using Amberlite XAD-2 impregnated with Pyrocatechol Violet. Graphs obtained from the retention of metal ions as a function of pH on a Pyrocatechol Violet column indicated that only Pb(II) and In(II) could be recovered fully quantitatively. Determinations of Pb(II) from tap water were made after preconcentration using the chelating column and good correlations were made with the results obtained by anodic stripping voltammetry. Singh and Kumar [48] also discussed the preconcentration of trace metals using a Pyrocatechol Violet loaded Amberlite XAD-2 column. The recovery of Zn(II) and Cd(II) was found to be $\geq$ 98 % and 100 times concentration of both metals was found to be possible using the column. The method was applied to the analysis of Zn(II) and

Cd(II) in Yamuna River Water (New Delhi, India) using AAS for the metal concentration determinations. Higher concentrations of Zn and Cd were found in an industrial area compared to a site near a thermal power station and RSD's were less than 5%.

Abollino *et al.* [49] discussed the sorption of 8-HQ on Amberlite XAD-2 and 8-hydroxyquinoline-5-sulfonic acid (8-HQS) on the anion exchange resin Bio-Rad AG MP-1. The resins were used for the uptake and enrichment of Ca(II), Cd(II), Cu(II), Mg(II), Mn(II), Ni(II), Pb(II) and Zn(II). The recoveries of the metal ions and the effect of interferences on recovery was monitored by ICP-AES and the use of 8-HQS impregnated AG MP-1 appeared superior in comparison with the 8-HQS XAD-2 column. Enrichment factors of up to 100 times facilitated the determinations of trace metals in tap water and river water samples.

Handley *et al.* [50,51] reported the use of Xylenol Orange on the anion-exchange resin, Dowex 1-X8. The chelating column was used to preconcentrate alkaline earth metals from saturated brines before determination on a strong cation exchange column. A separation of Mg(II), Ca(II), Sr(II) and Ba(II) at the low ng ml^{-1} level was achieved and the methodology used successfully to on-line monitor feed brines which are used in the Chlor-alkali industry.

Porta *et al.* [52] discussed the on-line enrichment of trace metals with an XAD-2 resin impregnated with 1-(2-thiazolylazo)-2-naphthol (TAN) prior to determination by ICP-AES. A microcolumn prepared from the chelating resin was used to preconcentrate

Cd(II), Cu(II), Fe(II), Mn(II), Ni(II) and Zn(II) from high purity water, river water and sea water matrices with good recoveries. The results obtained from ICP-AES for a river sample after enrichment compared well with determinations made by GFAAS. The concentration efficiency of the column, which combines a preconcentration factor, and analysis time was about 18, which was reported as being one of the highest in the literature.

Naghmush *et al.* [53] have exploited XAD-2 impregnated with PAR, Eriochrome Blue Black R (EBBR) and PCV for the preconcentration of Cu(II) in a flow injection system, prior to determination by AAS. The PCV loaded XAD-2 exhibited higher efficiency compared to the other columns and was used for further investigations. A significant influence on the preconcentration of Cu(II) from a 100 $\mu g\ l^{-1}$ Cu(II) solution was observed in the presence of Ca(II) at a concentration above 50 $mg\ l^{-1}$. The strong interferences observed from Fe(III) could be eliminated by the addition of fluoride to the sample. The results of the determination of Cu(II) by FI-AAS in natural water samples using 20 min preconcentration on a PV loaded XAD-2 column compared well with determinations by GFAAS but the calibration for FI-AAS was only linear up to a Cu(II) concentration of 2 $\mu g\ l^{-1}$.

1.5.4 Summary of chelating sorbents

In essence, the main review discusses the developments and applications of chelating sorbents prepared for low efficiency systems. The utilisation of this technology with smaller particle size substrates, however, increases efficiency and enables chelating sorbents to be used for high performance separations. Both the preconcentration and separation of metal ions is therefore possible using a single column and metal ion determinations from complex matrices can be made in a closed system. Relatively little work has been performed using these high efficiency chelating sorbents. Subsequent chapters will discuss the characterisation and development of novel high efficiency chelating sorbents, developed in this study, along with a review of the relevant literature.

1.6 Spectrophotometric Detection

There are many methods available for the determination of cationic species in IC, and a number of these are discussed in a review by Rocklin [54] e.g. conductimetric, spectrophotometric and fluorescence detection. In this report, spectrophotometric detection was used in all instances.

There are two types of spectrophotometric detection, 'direct' and 'indirect' detection. Direct detection involves measuring an increase in absorbance at the wavelength of the absorbance maxima for the analyte complex. Indirect detection involves measuring a

decrease in absorbance, since the formation of a complex with the analyte ions results in a loss of the species being measured. In this work, direct detection was utilised.

In general, metal ions are 'invisible' to UV/VIS radiation and must be converted to a suitable form to enable UV/ VIS detection in an ion chromatographic system. This may be possible by either pre-column or post column derivatisation of the metal ions. Precolumn derivatisation may be achieved by either modification of the sample (provided that the complex is stable under the conditions used) or by using a complexing agent in the eluent. Toei [55] used the complexing agent xylenol orange and Toei and Baba [56] used phthalein purple in the mobile phase as colour forming reagents for the detection of copper and zinc, and the alkaline earth elements respectively. However, post-column reaction using absorbance detection is by far the most widely reported detection method for metal ions [57].

Post column derivatisation requires a second pumping system and, in some cases, a constant pressure gas flow is used to introduce the post column reagent [58]. The two systems are connected after the column by a zero dead volume t-piece, which is normally followed by long coiled tubing to ensure complete reaction with the complexing species before detection. In order to obtain optimum sensitivity, complexing agents with very high molar extinction coefficients are used. Absorbance in the visible region is often preferred because the background absorbance from the reagents and other eluent components is less of a problem. One advantage of using post column reaction is that detection selectivity can be varied by the selection of chelating reagent or by the use of masking reagents.

In one of the first applications of chelating reagents for the detection of metal ions, Kawazu and Fritz [58] examined 4-(2-pyridylazo) resorcinol (PAR), (Figure 1.10), for the detection of Cd(II), Zn(II), Fe(III), Pb(II), Cu(II), Co(II) and Mn(II) which were eluted from a cation exchange column. Jezorek and Freiser [59] reported that PAR forms water soluble complexes with a larger number of metal ions than any other commonly available indicator. PAR/ZnEDTA (buffered at pH 11 with NH_4^+/NH_3) was used for alkaline earth metals and others which do not react with PAR alone. The detection depends on the displacement of Zn from the ZnEDTA complex and its subsequent co-ordination with PAR. For example:

$$Ca + 2PAR + ZnEDTA \leftrightarrow CaEDTA + Zn(PAR)_2$$

Better baselines were found for acid eluents than for eluents closer to neutral pH. This may have been caused by enhanced mixing of the two eluent streams due to the heat released in neutralisation of the acid by the pH 9 or 11 NH_4^+/ NH_3 PAR solutions.

A post column reagent which has been widely utilised for the detection of rare-earth and actinide elements is arsenazo III [60,61,62]. Arsenazo III is very selective for Th(IV) and U(IV) in solutions of 3.6 M HCl, but may also be used for the detection of other metals at higher pH's. Other post column reagents that have been employed in ion chromatographic systems include Eriochrome Black T [63,64] and Calmagite which are also azo dyes, with α, α' dihydroxy groups (Figure 1.10).

A)

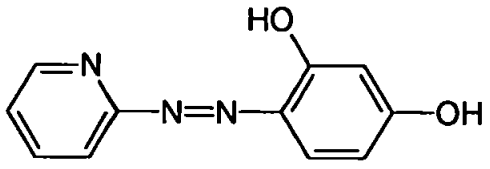

B)

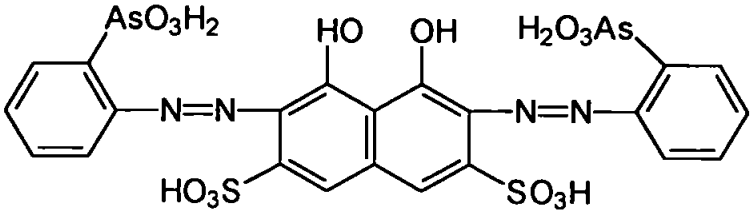

C)

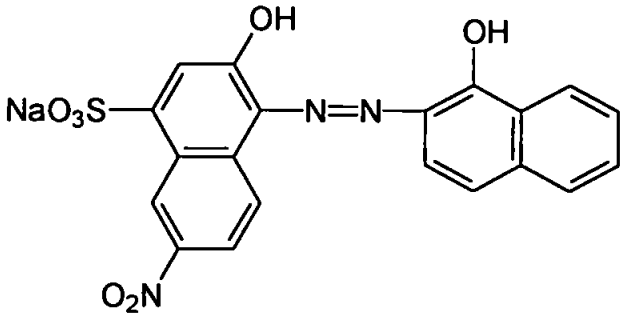

D)

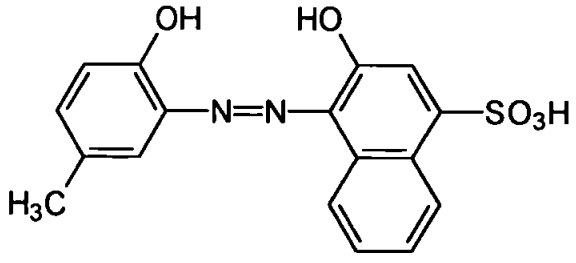

Figure 1.10. Post column reagents A) PAR, B) Arsenazo III, C) Erichrome Black T and D) Calmagite.

1.7 Aims and objectives of this work

The inadequacies of simple ion exchange have been exposed for high ionic strength samples. To overcome this problem, a number of chelating ion exchange sorbents have been developed owing to their greater selectivity for metal ions. Most of the work involving chelating sorbents has, however, concentrated on low efficiency columns which are used for the preconcentration of metal ions prior to determination by ion chromatography or other analytical techniques.

By using small particle size substrates, high efficiency chelating columns may be prepared which are suitable for the preconcentration and separation of trace metals from complex matrices using a single column. Systems exploiting these columns are known as 'High Performance Chelating Ion Chromatography' (HPCIC) systems and little work has been done in this area. Literature concerning these high efficiency substrates will therefore be discussed in subsequent chapters. The main theme of this work is to further expand these studies by developing and characterising novel, high efficiency chelating sorbents.

Chelating sorbents will be selected, according to their selectivities and separation abilities for metal ions, and applied to proposed specific analytical and preparative applications. It is proposed that sorbents will be prepared displaying both hydrophilic and hydrophobic properties. This will be achieved by modifying cellulose substrates for the preparation of hydrophilic chelating sorbents and polystyrene based resins for the hydrophilic sorbents. In both cases, the substrates will be modified with chelating

dyes. The cellulose work will involve covalent bonding of the chelating dye molecules to the substrates and the polystyrene resins will be modified with chelating dyes by direct adsorption. The primary applications for the prepared chelating sorbents involve the separation of small amounts of one metal ion from much greater concentrations of one or more other metal ions in geological and metallurgical samples.

The separation of Sr from Ba, Rb and Ca in gypsum rock samples is necessary so that geological isotopic dating measurements of the rocks can be made. A system is therefore required that is capable of isolating Sr from the sample and will thus enable fractions of pure Sr (as an inorganic salt) to be collected. A chelating column may be used for this purpose and an eluent system is also required which can be easily removed. The Sr will then be of a suitable form for introduction into a high resolution mass spectrometer, allowing the isotopic ratios of Rb and Sr to be found and the age of the rocks to be calculated. The selection of such a chelating column and corresponding eluent system forms a major part of this project.

The determination of trace Bi in pure Pb can be problematic when some techniques are employed. For example, isobaric interferences between Bi and Pb isotopes are commonly identified when using ICP-MS and the Pb matrix must be removed before analysis. The development of an HPCIC system which can determine low Bi concentrations, in the presence of much greater concentrations of Pb, would provide an alternative method with possibly lower limits of detection than other analytical methods currently available, such as graphite furnace atomic absorption spectrometry (GFAAS) and inductively coupled plasma atomic emission spectrometry (ICP-AES).

Another interesting and important application which could be dealt with by high performance chelating sorbents is the separation of Th and U, which are the only actinides present in significant concentrations in the natural environment. Reversed phase systems have already been established that are suitable for the separation of U and Th, but they can be strongly influenced by high concentrations of Fe (III) found in typical environmental samples. A chelating column, suitable for operation in concentrated acid conditions, may possibly be used to separate U and Th effectively in the presence of Fe(III) and investigations attempting this complex separation will be undertaken.

Chapter 2 - Dye Loaded Cellulose Based Substrates

2.1 Introduction

Increasing demands in analytical and biochemistry have led to a requirement for more effective and stable substrates for the preconcentration and separation of trace metals from aqueous media. One area of this research has led to the preparation of chelating sorbents by modification of cellulose based substrates such as cellulose, chitin and chitosan.

Cellulose is the most abundant organic material found in plants forming the principal constituent of their cell walls giving them structural strength [65]. It is composed of glucan units, with free hydroxyl groups suitable for covalent bonding, thus enabling easy modification of the basic structure. Cotton, is a good source of cellulose since its content may reach 96% by mass [66].

Chitin is distributed widely in nature, especially in marine invertebrates, insects, fungi and yeasts [67] and can be easily modified to chitosan by deacetylation. As for cellulose, chitin and chitosan can be obtained in microcrystalline and fibrous forms. Therefore, after modification with chelating functional groups, they are suitable for packing into columns and perform well for low pressure applications.

The structures of the cellulose based compounds may be represented as follows:

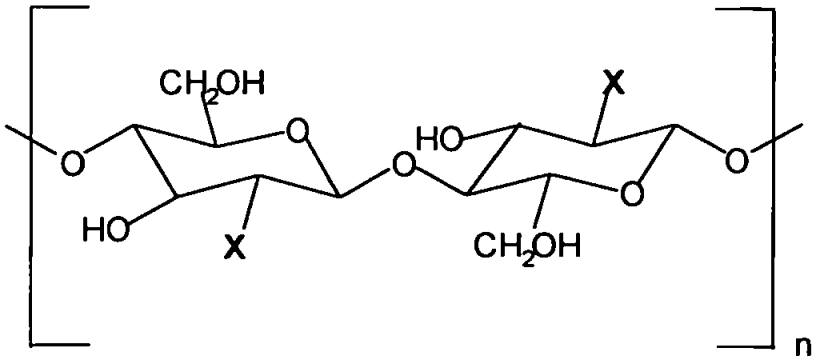

Where X is:

NHAc - chitin
NH_2 - chitosan
OH - cellulose

Cellulose and cellulose derivatives have been developed from different sources yielding mechanical stability and high surface area. Marañón *et al.* [68] reported the removal of trace metals from synthetic solutions and sea water by natural apple waste (30% cellulose/ 19% lignin) and a phosphated apple waste. The phosphated apple waste retained the metals at lower pH's but both substrates were found to be practically quantitative. A study of carboxymethyl cellulose complexes with Cu(II) and Ni(II) has been performed and the results show that the chelation of the metal ions increases with the substitution of carboxymethyl groups per glucopyranose unit [69]. Heinze *et al.* [70] reported the manufacture of carboxymethyl cellulose gel beads. The beads were prepared by interaction of the modified cellulose with Al(III) and a dropping technique was used to create spherical gel beads. On removal of the aluminium, the beads were suitable for adsorbing metal ions with a capacity of approximately 0.3 m mol g^{-1} for selected divalent metal ions.

Further investigations involving carboxymethyl cellulose (Cellex CM) and a phosphonic acid cellulose (Cellex P) have been made by Naghmush *et al.* [71]. The Cellex P was used for elution studies but was found to have a lower efficiency for the lead species than for other sorbents tested, for example, Chelex 100. However, Cellex P provided some possibility for speciation.

A comparison of carboxymethyl cellulose and its cellulose derivative has been made by Deans *et al.* [72]. Both cellulose forms were found to have a much higher capacity for lead than for copper, although the hydroxamic acid derivative was found to be slightly stronger. A study of 8-hydroxyquinoline-cellulose has also been reported as a micro-column for preconcentration coupled to simultaneous ICP-AES [73]. The micro-column was found to successfully preconcentrate and elute a series of metal ions with faster exchange than for a previously tested ethylenediaminetriacetic acid-cellulose column. However, diethylenetriamine tetra-acetate functionalised cellulose filters have displayed very good efficiency for the removal of trace metals from river and sea water samples [74]. Other forms of derivatised cellulose include dithiocarbamate cellulose [75,76], hydroxyethyl cellulose [77] and amidoxime cellulose [78].

There are also many applications for chitin and chitosan which have been extensively studied by Muzzarelli [79]. Chitin and chitosan are reported to be of great value for chromatographic supports and their physical properties can also be improved by modification of their structures, e.g. by forming an epichlorohydrin derivative. Chitin and chitosan alone have been shown to be capable of adsorbing both anionic and cationic species [80] and Millero *et al.* [81] have discussed the properties of chitin for

the sorption of divalent metals in sea water. Dithiocarbamate chitosan has also been reported [82] and displays good recoveries for selected metal ions, but unfortunately had a tendency to gelatinise in acidic media. A more recent paper [83] regarding dithiocarbamate chitin did not describe such a tendency and showed good effective adsorbability for both transition and post-transition metals from an acidic solution. Chitin has also been documented as a separation medium for coloured metal complexes of 1,10-phenanthroline and neocuproine [84], and phospho-molybdenum blue [85].

The main problem with many metal adsorbing materials is that significant complicated organic syntheses may be required in order to achieve the desired functionalities on the main substrate. In the case of cellulose based substrates, time consuming and lengthy syntheses may be unnecessary if the functional groups required for the substrate have a reactive affinity for the hydroxyl groups on the cellulose. An alternative method for the preparation of a metal adsorbing substrate may be to use 'Reactive' metal chelating dyes. 'Reactive dyes' were developed by Rattee and Stephen of ICI in 1954 [66]. Some reactive dyes incorporate metals such as Cu(II), Co(II) and Cr(III) which are adsorbed by chelating groups in the dye and which give them distinct colours. These 'metallated' dyes can be bonded onto cellulose. On removal of these metal ions from the dyes, using acid or complexing chelating agents, the dyed cellulose then behaves as a chelating sorbent. Dyes containing dichlorotriazinyl groups were reacted with the cellulose fibres in alkaline conditions giving dyeings with very high fastness to wet treatments without significant weakening of the fibre. Many dyes with different reactive groups have been developed since that time e.g. acryloylamino and vinyl sulphone, which are used in large quantities in the textile industry.

In this work, reactive dyes were used for the cellulose based substrates which contained mono and dichlorotriazinyl groups. On reaction they formed ethereal linkages with the cellulose chains with an HCl by-product. This is an effective method of forming chemically bonded chelating substrates without any lengthy synthesis e.g. there are five possible products for the reaction of dichlorotriazinyl reactive dyes with cellulose which are illustrated in Figure 2.1 [66].

The heterogeneous reaction of the reactive dichlorotriazinyl group with the fibre is more favourable than the competing hydrolysis reaction and gives high wet-fastness with little bleeding of the dye. Similarly, monochlorotriazinyl reactive dyes give two possible products and the immobilised dyes also form 1:1 complexes with metal ions. Monochlorotriazinyl dyes are more stable in cold alkaline conditions than the dichlorotriazinyl dyes since less dye molecules are lost by hydrolysis. This enables monochlorotriazinyl dyes to be used for printing applications as well as dyeing.

There are several advantages of using chelating dyes as the chelating functions for the substrates, namely there is a very large selection of dyes to choose from, all with different affinities for metals which allow for different elution orders of metals from the columns and they can be very inexpensive. Therefore, investigations into the suitability of dyed cellulose based substrates for metal adsorption for both small and large scale applications was of significant interest and formed the foundation for the following work.

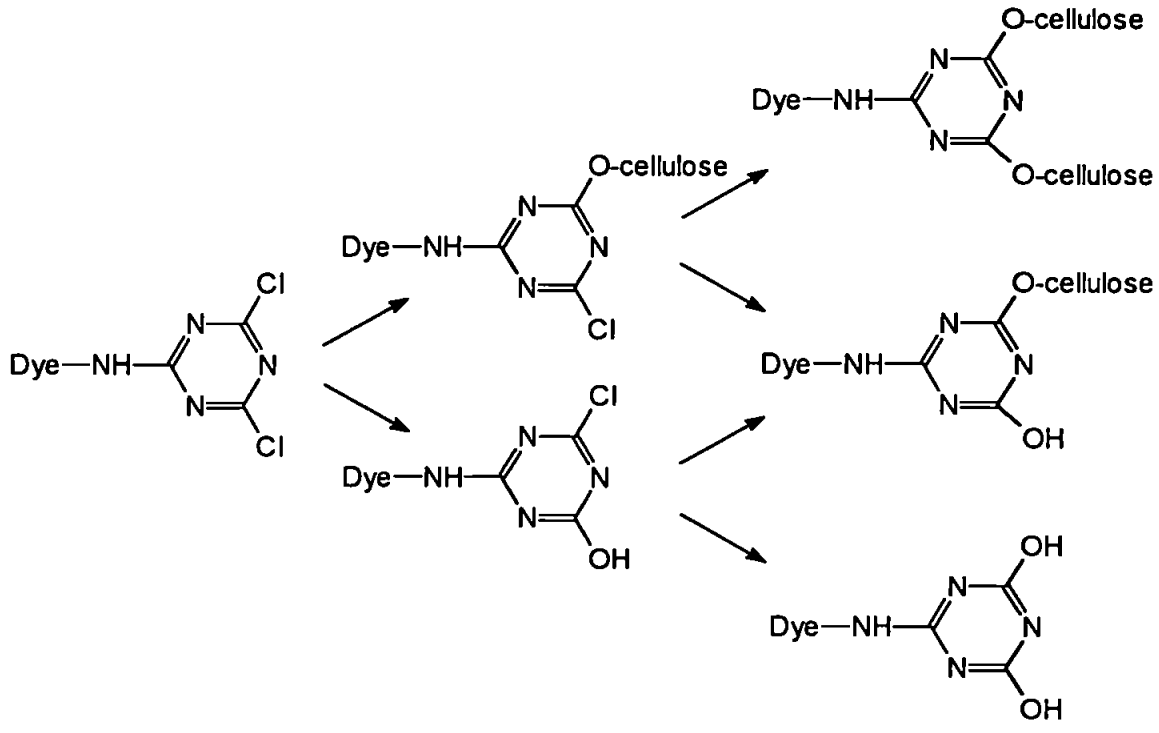

Figure 2.1. Possible reaction products for dichlorotriazinyl dyes with cellulose

2.2 - Experimental

2.2.1 Instrumentation.

The basic instrumentation used for most of the high performance chelation ion chromatography (HPCIC) work is shown in Figure 2.2. A Dionex 4000 series gradient pump (Dionex, Sunnyvale, CA, USA) delivered the eluent and a Dionex 2000 series analytical pump (Dionex) was used to deliver the post column reagent (PCR). Injection of the sample was via a polyether-ether-ketone (PEEK) lined six port injection valve (Rheodyne, Cotati, CA, USA) fitted with a 100 ml PEEK sample loop. The eluent and PCR were mixed at a zero dead volume T-piece followed by a 1.4 m, 0.3 mm internal diameter PTFE reaction coil. Detection was achieved with an SF 770 Spectroflow monitor UV/ VIS spectrophotometer (Kratos, Westwood, NJ, USA). A chart recorder (Labdata, Surrey, UK) and a computer integration system with PE Nelson software (Perkin-Elmer Ltd., Beaconsfield, UK) were used to record the chromatograms.

2.2.2 Reagents

All reagents used were of analytical-reagent grade. The eluent was 0.5 or 1.0 mol dm^{-3} potassium nitrate containing 0.05 mol dm^{-3} lactic acid, adjusted to the appropriate pH using dilute ammonia or nitric acid. Acetic acid and hexamine buffered solutions were also used between pH 4 and pH 8. The post column photometric reagent (PCR) used in these studies was either 1.2×10^{-4} M 4-(2-pyridylazo) resorcinol (PAR) buffered to

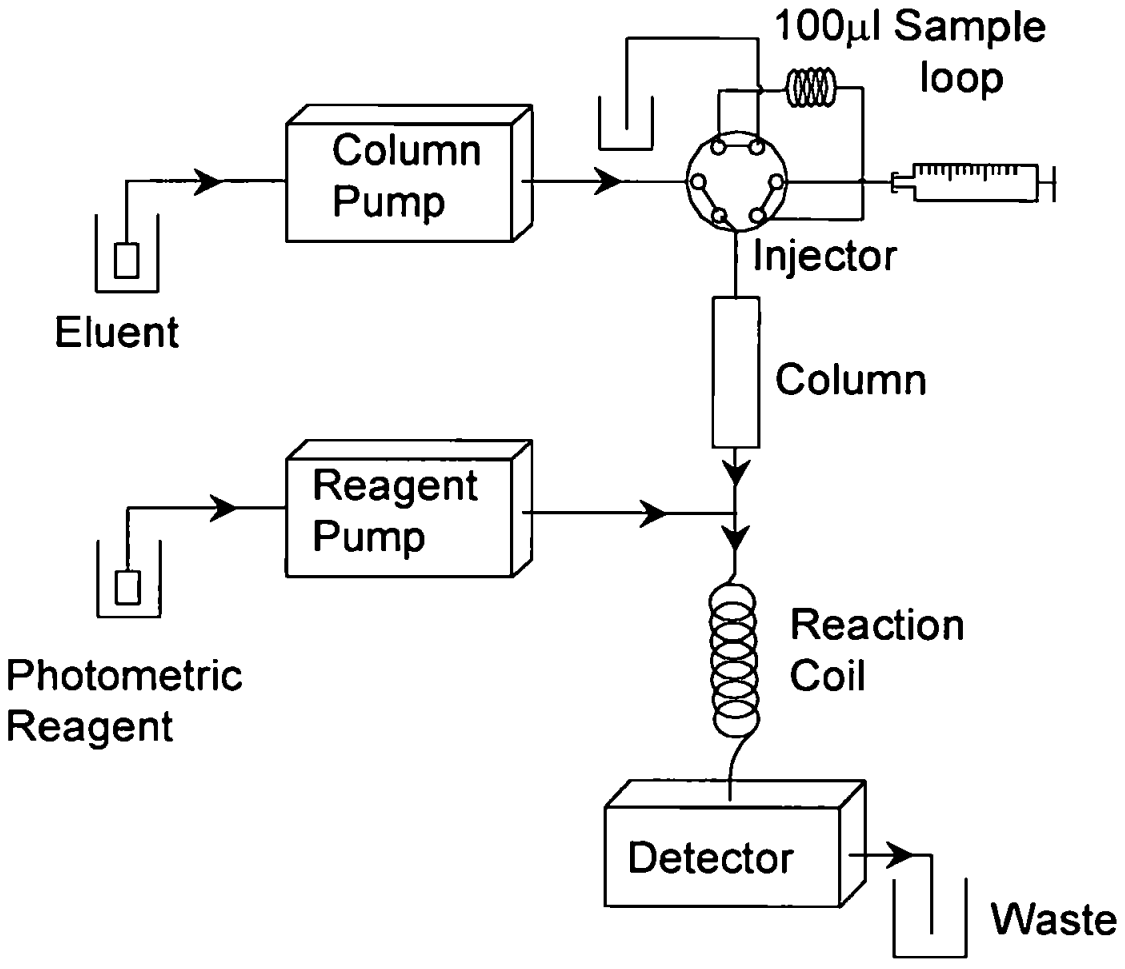

Figure 2.2. A schematic diagram of the HPCIC system employed.

pH 10 using ammonia / ammonium nitrate, or PAR/ zinc-ethylene-diaminetetracetic acid (2×10^{-4} M) (Zn-EDTA, Fluka, Buchs, Switzerland). The eluent and PCR were delivered at 1 ml min^{-1}. Reactive dyes were obtained from Zeneca colours (Zeneca, Huddersfield, UK). Solutions were prepared using distilled, deionised water (DDW) (Milli-Q, Millipore, Milford, MA, USA) and degassed using helium. Metal standards were prepared from commercially available 1000 mg l^{-1} stock solutions.

2.2.3 Mercerisation Process for Cellulose Substrates

A weighed amount (2 g) of the cellulose type sample was shredded (unless already powdered) to ensure maximum surface area was available, and added to a 50 ml solution of 0.1 M sodium hydroxide, 0.1 M sodium hexametaphosphate and 0.1% Teepol® HB7 (ionic surfactant) (Sigma, Poole, Dorset, UK). The mixture was boiled for half an hour. The cellulose type sample was filtered and rinsed with deionised water before boiling in 2 M acetic acid for fifteen minutes. The sample was then rinsed in water, spun dry in the centrifuge and finally dried on a watch glass at 60°C.

2.2.4 Dyeing Procedure for Monochlorotriazinyl Dyes

The mercerised sample was mixed with 200 mg of the dye in DDW (50 ml) at room temperature for ten minutes and was then immersed in a water bath at 80°C. Sodium chloride (3.25 g, 65 g l^{-1}) was divided into four portions (10%, 20%, 30% and 40%) which were added in five minute intervals respectively, whilst stirring with a mechanical stirrer. The mixture was left stirring at 80°C for twenty minutes. Sodium

carbonate (1 g, 20 g l^{-1}) was added uniformly over 15 minutes and the mixture was left stirring at 80°C for a further two hours.

2.2.5 Dyeing Procedure for Dichlorotriazinyl Dyes

The mercerised sample was mixed with 200 mg of the dye in DDW (50 ml) at room temperature for ten minutes and was then immersed in a water bath at 40°C. Sodium chloride (3g, 60g l^{-1}) was divided into four portions (10%, 20%, 30% and 40%) which were added in five minute intervals respectively whilst stirring with a mechanical stirrer. The mixture was left stirring at 80°C for thirty minutes. Sodium carbonate (0.1 g, 5 g l^{-1}) was added uniformly over 5 minutes and the mixture was left stirring at 40°C for a further hour. The sample was rinsed with hot DDW and the washings were collected before boiling in 50 ml of 1 g l^{-1} sodium hexametaphosphate for 15 minutes.

The monochlorotriazinyl and dichlorotriazinyl dyed cellulose type samples were rinsed thoroughly with distilled water and the washings were collected for UV/ VIS analysis using a Lambda-7 spectrophotometer (Perkin-Elmer).

2.2.6 Procedures

The dye loadings on the substrate were calculated using UV/VIS spectrophometry. The absorbance of the dye solutions were determined before and after the dying processes, the difference being directly proportional to the concentration of the dye coated on the substrates. The column capacity was calculated from the midpoint of the

s-shaped breakthrough curve after elution of a buffered zinc or copper solution. The capacity factors for each dye coated substrate was obtained from the retention times of metal ions at various pH values.

2.3 - Results and Discussion

2.3.1 Chitin

Preliminary investigations with chitin powder involved the modification of the structure with dithiocarbamate groups. The method discussed by Hase *et al.* [83] was adhered to and a pale green powdery material was obtained which was packed into a small funnel column. Copper solutions (20 mg l^{-1}) were passed through the column and there were signs of metal retention. However, when the column was washed with very strong hydrochloric acid, it gelatinised and was not practical for further analysis.

2.3.2 Chitosan

Initial interest in chitosan was based upon the manufacture of chitosan fibres which were reported to have high mechanical strength and hydrophilic properties. The company which manufactured the fibres was contacted but production of the fibres had been terminated and replaced by chitopearl beads (chelating chitosan based beads). It was therefore decided that chitosan powder should be investigated. Preliminary investigations with the powder were poor since a gel was formed in weak acetic acid.

The investigation of cellulose was believed to be more suitable for the applications of interest.

2.3.3 Cellulose

There are many different types of cellulose forms to choose from and it was decided that four types of cellulose should be investigated, namely, cellulose fibres, microcrystalline cellulose, cotton wool and calico. As mentioned previously, cotton and calico are natural products with cellulose compositions of up to 96% by weight. The cellulose fibres and the microcrystalline cellulose were in powdered form but the cotton wool and the calico were shredded before any modification. Before dyeing, the cellulose type substrates were mercerised. This process converted the cellulose, in an irreversible process, into a more open structure making it more accesible to dyestuffs.

2.3.3.1 Dye Types Used for Investigations

It was necessary to choose metallated reactive dyes for the experiments since they already contained metal chelating groups in the chromophore attached to the reactive chlorotriazinyl groups. Unfortunately, owing to the manufacturer's restrictions on supplying detailed chemical structures of the particular compounds, the structures of only one of the dyes was available (Figure 2.3), but they were essentially believed to contain azo groups with α-α'- dihydroxy groups for strong metal chelation. Once the dyes were covalently bound to the cellulose, the metal ions adsorbed onto the dye molecules could be released by washing the modified cellulose substrates with fairly

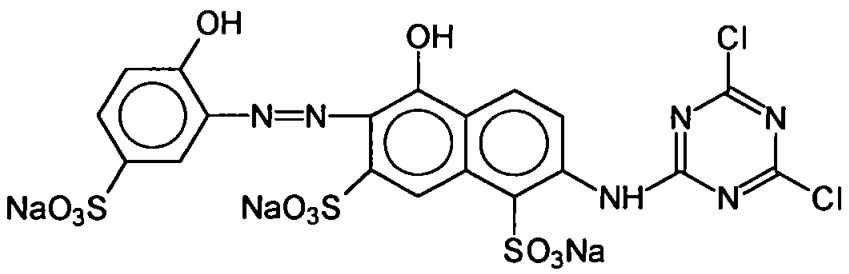

Figure 2.3. The Structure of Procion Rubine MX-B.

strong acid solutions or competing chelating agents. Metal complexing compounds e.g. dipicolinic acid were more favourable since strongly acid solutions could degrade the bonds between the dye and the substrate and also bonds within dye molecules, causing a decrease in the metal adsorbing capacities of the substrates.

Reactive dyes from the Procion Range were chosen for investigation, namely, Violet P-3R, Black P-3N, Rubine MX-B, Blue 5-BR and Brown. These were metallated dyes which contained either Cu(II), Co(II), Cr(III) or a mixture of Cr(III) and Co(II).

2.3.3.2 Dyed Cellulose Investigations

Early dyeing procedures with cotton wool produced fairly intense coloration with some uneven patches. The colour became more uniform after prolonged washing of the cotton to remove the loosely bound dye, thus leaving the covalently bound dye molecules remaining. It was discovered that the dyeing was more uniform and intense for the smaller pieces of cotton wool. Figure 2.4 shows a cotton wool sample dyed with Procion Blue H-ERD.

A range of experiments for the capacity of the dyed cotton wool and the pH of adsorption of certain metals were performed for the five dyes. One initial problem with the Blue H-ERD dye was the removal of the metal ions originally bound to the dye molecule. This was unusual since it was a copper containing dye and any problems encountered were predicted to be with the chromium based dyes, since chromium has a higher valency and is capable of forming much stronger complexes with some chelating

A)

B)

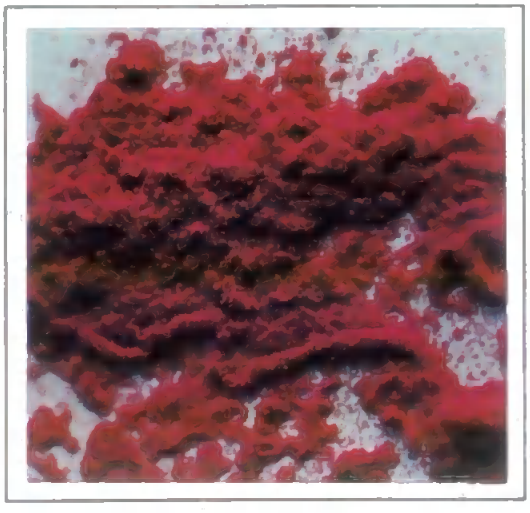

Figure 2.4. A) Procion Blue H-ERD dyed cotton wool and B) Procion Rubine dyed microcrystalline cellulose.

molecules. After the original metal ions were removed from the dyed cotton substrates, selected metal standards were eluted through packed dyed cotton columns and all showed retention for Mg(II), Ni(II), Cu(II), Mn(II), Cd(II), Zn(II) and Pb(II), although some dyes showed more affinity for certain metals than others. Table 2.1 displays some preliminary results for the retention of metal ions as a function of pH in 10 cm PEEK columns packed with dyed cotton wool. A low value of pH corresponds with the formation of a strong complex. The results in Table 2.1 indicate that Cu formed the strongest complex and Mg formed the weakest which was as expected for N,O type chelators.

The Rubine dyed cotton was found to have the highest capacity for metal ions, but this was believed to be caused by the dyeing process. The Zeneca manufacturing dyeing method, supplied with the whole series of dyes was later found to be for dichlorotriazinyl dyes and thus only suitable for the Rubine dye. The rest of the dyes required different dyeing conditions since they contained monochlorotriazinyl reactive groups and a higher reaction temperature was required.

Two dyes were considered for the next series of dyeing investigations with microcrystalline cellulose, based on their metal adsorption capacities found in the previous experiments. These were the dichlorotriazinyl Rubine and the monochloro-triazinyl Violet dyes. The results obtained for the Rubine dye were very different to the ones for the cotton wool substrate, since there was little retention for the metal ion solutions and the capacity was very low. The capacity for the Violet dyed substrate was also less than previously found and so the experiment was repeated using the

	pH required for retention greater than 20 minutes						
Dye	Cd	Cu	Mg	Mn	Ni	Pb	Zn
Blue	6	2	8	8	6	4	6
Violet	>6	2	>6	>6	>6	>6	>6
Brown	8	4	>8	8	8	4	8
Black	8	4	>8	8	8	4	8
Rubine	6	2	8	8	6	4	6

Table 2.1. The pH required to obtain retention times greater than 20 minutes

cellulose fibres. Cellulose fibres were dyed following the same method used for the microcrystalline cellulose with the Rubine dye (Figure 2.4). The same series of metal ions used for the cotton was found to be retained on the column, but again the capacity for metal ion adsorption was negligible.

To complete the series of cellulose substrates tested, a calico sample was dyed with the Procion Rubine dye. The washings from the dyeing procedure were collected and analysed by UV/ VIS spectrophotometry. The results obtained indicated that, from the 200 mg of dye used for the dyeing procedure, only 172 mg were calculated to be present in the washings. This implied that there was 28 mg of dye remaining on the two grams of calico used. However, after packing the calico in a 10 cm PEEK column and determining the capacity using a 20 mg l^{-1} Zn(II) standard, the capacity of the column was found to be negligible. This raised suspicions that the method being used for the capacity checks did not yield accurate results.

An advantage of using dyes is that the different chemical states of the dye can be seen visually. Therefore, a portion of the Procion Rubine dyed calico substrate was packed into a glass column so that the affects of the metal standard solution on the dyed substrate could be investigated. In addition, it was decided that a copper standard should be tested, as an alternative to zinc, since it formed stronger chelates with the reactive dyes. Figure 2.5 illustrates the Procion Rubine dyed substrate in the glass funnel column. Five different stages of colouring were recorded after continuous elution of a 20 mg l^{-1} copper standard solution and these are labelled from A to E. In

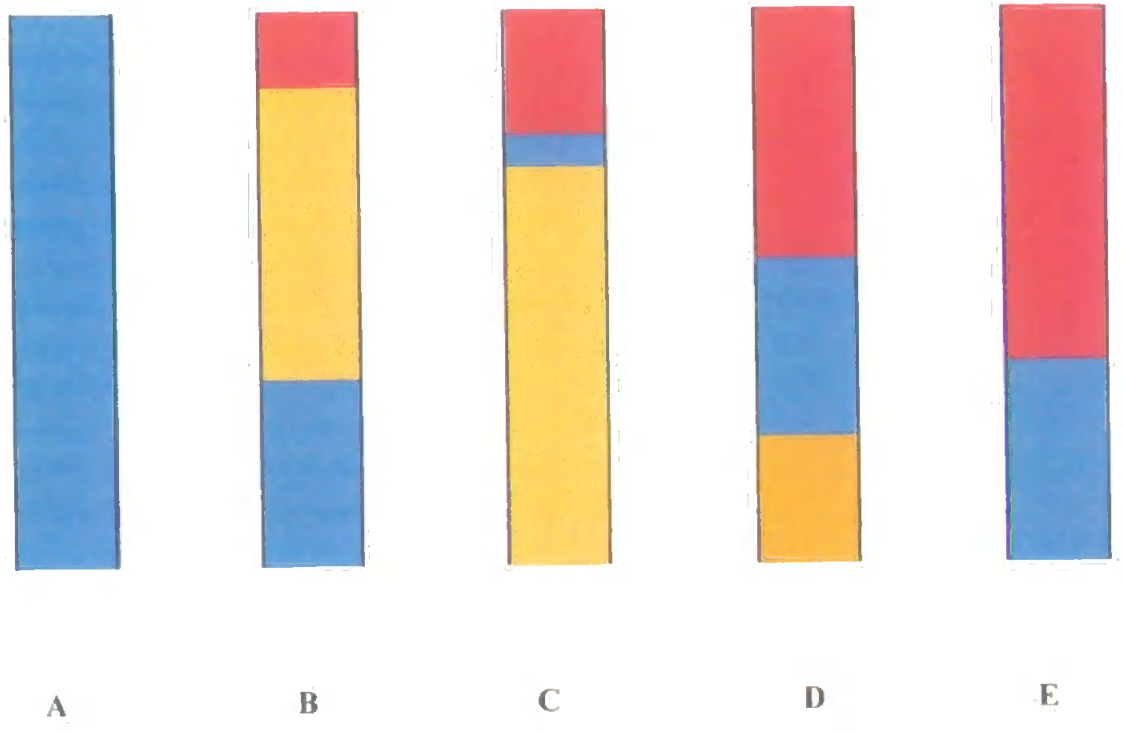

Figure 2.5. Five stages of the Procion Rubine dyed calico column illustrating the colour changes after eluting a 20 mg l^{-1} copper standard through the column.

stage A, a 1 M KNO_3 and 0.05 M lactic acid solution, adjusted to pH 8 with NH_3, was passed through the column until the column effluent measured pH 8. The column appeared bright blue in colour. In step B, the 20 mg l^{-1} copper solution was passed through the column. The top of the column appeared ruby red (as the dye name suggests) indicating that a complex with copper had formed. Below the red was an orange colour which was concurrent with the acid form of the dye. This was probably present owing to a relatively high concentration of protons being displaced from the dye molecules after forming chelates with the metal ions. The bottom of the column was blue since the pH remained essentially unaffected. In step C, the amount of red colouring was greater since more eluent had passed through the column and the number of complexed molecules had increased. A discrete blue area of the substrate appeared below the red since the eluent was overriding the acid and restoring the column back to pH 8 again. The acid plug was eluting from the column and the bottom portion of the column was orange, but no metal ions were yet being detected in the post column reagent. In step D, an even larger portion of the column had become complexed with copper resulting in the top half of the column appearing red. Most of the rest of the column was blue since it had equilibrated with the eluent at pH 8 and now a brown colour was apparent at the base of the column which was believed to be a mixture of the blue and the orange colours. Finally, in step E, most of the column appeared red since a majority of the metal adsorption sites had been filled. Although a fairly large portion of the column was still blue in colour, indicating that there were still more metal adsorption sites available, the post column reagent had changed colour owing to metal ions eluting from the column. Therefore, the capacity of about 10 µmol of copper per gram of substrate was not the true capacity of the column, but was

far greater than the previous results obtained using zinc. This suggested that the acid plug, which was evidently present after elution of the metal standard through the column, was reducing the pH lower than required to retain zinc on the column and zinc was eluting from the column before the metal adsorption sites had been filled, thus yielding a false capacity. Zinc was originally chosen for the capacity tests since it was easier to remove from the column than copper, but copper was removed from the column using hot solutions of 0.1 M EDTA. In order to obtain a realistic capacity for the column using zinc, a heavily buffered standard solution was required.

From the previous investigations, it was concluded that there was no significant difference between the different cellulose substrates in terms of total dye loading and affinity for metals. Cellulose fibres, however, offered the best column packing material and gave uniform dyeing whereas there were possible problems with channelling in the columns packed with the calico and cotton wool. Subsequent investigations were therefore made using the cellulose fibres.

A known quantity of cellulose fibres were dyed with Procion Rubine for a capacity test with a buffered and unbuffered zinc metal standard solution. After preparation, the dyed fibres were packed into a glass column and, after demetallation with an eluent of hot 0.1 M EDTA, the column was adjusted to pH 8. Again, a negligible capacity was obtained for the unbuffered zinc standard solution, but with the buffered solution, a capacity of about 12 μmol of zinc per gram of substrate was obtained. This implied that the previous investigations with the unbuffered zinc standards were invalid.

Further investigations with the cellulose fibres revealed that the monochlorotriazinyl Procion Violet dye was more stable than the dichlorotriazinyl Procion Rubine dye in terms of wetfastness of the dyed substrates, In addition, the Violet dye also had a higher capacity for metal ions of 17.3 μmol of zinc per gram of dry substrate. Therefore, characterisation of a 10 cm PEEK column, packed with the Procion Violet dyed cellulose fibres, was attempted.

2.3.3.3 Evaluation of k' Values

The performance of the dyed substrates can be measured, in terms of capacity and the capacity factor (k') by examining the retention behaviour with various metals in an HPCIC system.

The metal retention performance of the PROCION Violet P-3R cellulose substrate was measured using a zinc standard and a total adsorption of 17.3 μmol of zinc per gram of dry substrate. Relative to the capacities of some dye impregnated polystyrene resins the capacity was low and this was mainly because of the low penetration of the cellulose matrix by the reactive dye molecules. As molecule sizes increase, penetration of the cellulose matrix becomes increasingly difficult and, since the reactive dyes were relatively large molecules, the actual number of dye molecules which could bond with the hydroxyl groups of the cellulose backbone was fairly low, i.e. less than 5 % W/W.

The s-shaped breakthrough curve for the capacity test was very sharp and probably indicates fast kinetics of exchange with metal ions in the column. Thus, the hydrophilic

properties of the substrate may allow the possibility for fast flow-rates through the column with relatively low back pressures.

Figure 2.6 illustrates the variation of capacity factor (of the Procion Violet cellulose substrate) with pH for six metals: Mg(II), Cd(II), Mn(II), Pb(II), Zn(II) and Cu(II). The height of a line on the graph is a measure of the column's affinity for a metal ion. The low lines on the graph indicate a strong affinity e.g. the copper line, and the higher lines indicate a weaker affinity of the column substrate for metal ions e.g. the magnesium line. The selectivity order is broadly as expected for chelating dyes (Cu(II) > Zn(II), Pb(II) > Mn(II), Cd > Mg(II)) with the affinity being particularly strong for copper. The slopes of the lines also indicate a very rapid change in retention time with pH which could assist the isolation of one metal from another, even though the k' values are very similar. The graph may be utilised to determine the optimum pH values for separation of the metal ions.

It was decided that an attempt at a high performance separation using the Procion Violet dyed cellulose fibres column should be made. From the information obtained from the k' values, it appeared that a separation was possible between Mn and Zn. The k' values were sufficiently different to enable a separation, but not too different so that one of the species was retained on the column for a long period of time.

Figure 2.7 illustrates a separation of 2 mg l^{-1} Mn and 10 mg l^{-1} Zn. The eluent was 0.5 M KNO_3, 0.03 M HNO_3, 0.05 M lactic acid and 0.1 M hexamine which was adjusted to pH 5 with NH_3. The post column reagent was buffered PAR with detection at 490

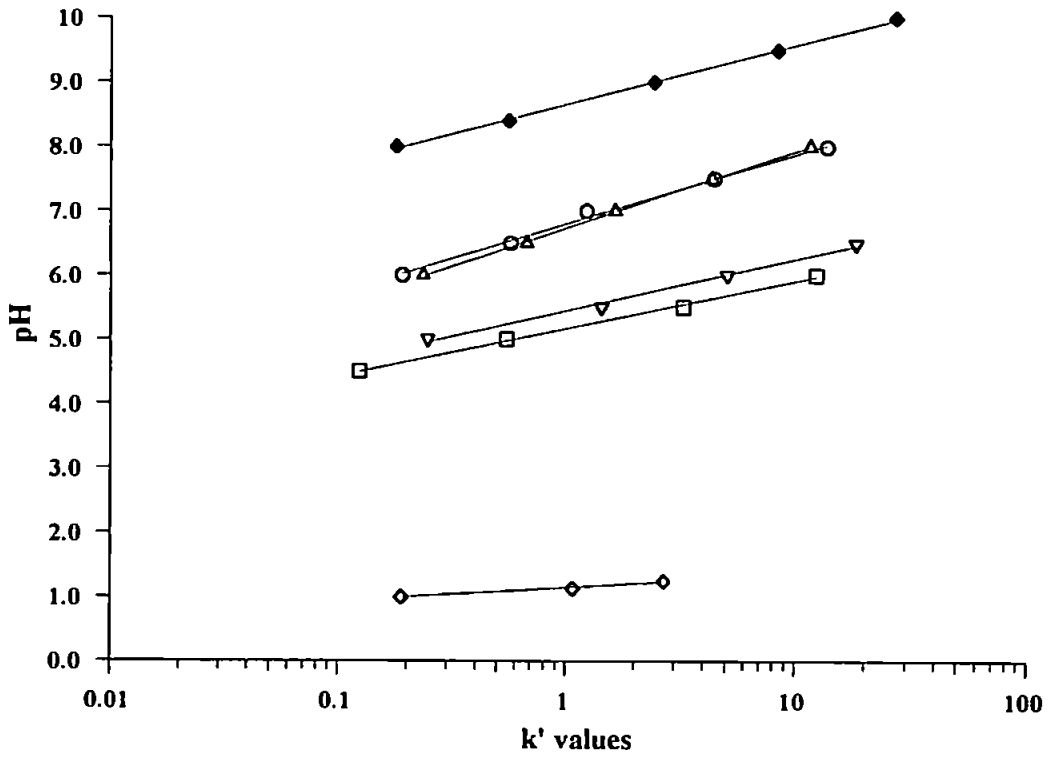

Figure 2.6. The variation of capacity factor with pH for cellulose fibres coated with Procion Violet ◆ = Mg^{2+}; ○ = Cd^{2+}; △ = Mn^{2+}; ▽ = Pb^{2+}; □ = Zn^{2+}; ◇ = Cu^{2+}

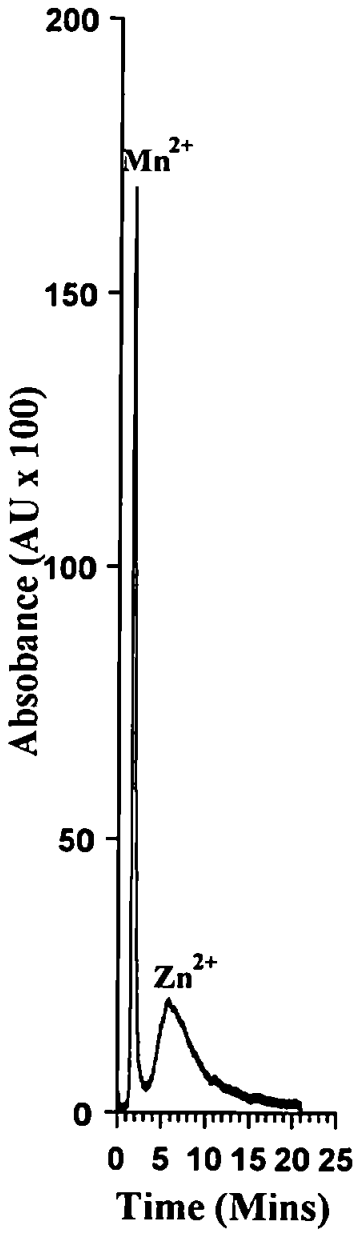

Figure 2.7. A 100 µl injection of 2 mg l^{-1} Mn and 10 mg l^{-1} Zn. The eluent was 0.5 M KNO_3, 0.03 M HNO_3, 0.05 M lactic acid and 0.1 M hexamine which was adjusted to pH 5 with NH_3. The post column reagent was buffered PAR with detection at 490 nm.

nm. The separation was not baseline resolved but displayed clearly that the dyed cellulose could separate two metal ions with relatively similar capacity factors. The shape of the Mn peak was sharp since there was little affinity for the column but the Zn peak shape was broader owing to poor efficiency due to particle size and packing characteristics.

2.4 Summary

In summary, all of the cellulose based substrates behaved similarly when dyed but the cellulose fibres were the most suitable to pack into columns and required less preparation than the cotton wool and calico substrates. There was a high affinity for copper, with all of the dyed substrates being able to assist in its isolation and removal from fairly acid solutions. The overall capacity was quite low, however, and so the substrate may only be suitable for 'polishing" of solutions such as fine chemicals or drinking water. It was evident that the mercerisation process increased the dye loadings by opening up the cellulose structure, yet the dye loadings were still less than 5 % W/W owing to the relatively large sizes of the dyes. Therefore, it is possible that if smaller reactive dyes with chelating functional groups were available, the percentage dye loadings could have been increased, resulting in higher metal adsorption capacities. A high performance separation was achieved but the peak shape of the longer retained peak was poor. Significant reduction and normalisation of the size of the cellulose fibres could possibly increase the performance of future separations since the cellulose dyed substrates appeared to have good kinetics of exchange. Although the cellulose investigations showed potential for some applications, the low capacity and poor

efficiency was not consistent with the aim of this study. For this reason, the remainder of the work in this thesis is concerned with the use of polystyrene based substrates.

CHAPTER 3 - Evaluation of Dye Impregnated Polystyrene Substrates Including Small Particle Size Hypercrosslinked Resins

3.1 Introduction

A number of chelating sorbents have been prepared for general preconcentration purposes for which high grade substrates were not required. The chelating sorbents were prepared by either bonding or adsorbing chelating functionalities to selected substrates and are discussed in Section 1.5. The utilisation of this technology with high grade substrates, however, enables sorbents to be used for high performance separations.

As an alternative to chemical bonding, dye impregnation offers a simple and effective method of modifying substrates with the required functionalities. Many dyes are easily adsorbed on polystyrene based resins by a combination of π-π interactions between the aromatic groups of both the dye and the resin and physical entrapment of the dye in the resin pore structure. The application of dye impregnation to high grade resins has been used to produce both simple ion exchange and chelating ion exchange sorbents.

3.1.1 Dye Impregnated Resins for Simple Ion Exchange

The impregnation of a polystyrene divinylbenzene (PS-DVB) column (PRP-1) with Methyl Green for the high performance separation of inorganic ions has been reported by Golombek and Schwedt [86]. Methyl Green contains quaternary ammonium

groups which behave as anion exchange sites. The separation of eight common anions was achieved with baseline resolution giving a performance comparable to that of a chemically bonded anion exchange column. The column was constantly regenerated by using a small amount of the dyestuff in the eluent. Walker [87] described the separation of anions using Ethyl Violet impregnated resins. The separation of seven anions was effected using both conductivity and indirect visible detection. Linear calibrations from 1 to 1000 mg l^{-1} using a 20 µl sample loop were made, although the system was found to deteriorate as the ionic strength increased.

The separation and indirect visible detection of inorganic and organic analyte cations on Thymol Blue impregnated columns has also been discussed by Walker [88]. Two polystyrene based packings and one silica based packing were impregnated with Thymol Blue and the separation of Mg(II), Ca(II), Sr(II) and Ba(II), and Cu(II), Zn(II), Ni(II), Co(II), Fe(II) and Mn(II) was achieved using the columns. The efficiency of the silica column was greater in comparison with the polystyrene based columns, but the silica based column was unstable and degraded rapidly. Walker [89] also reported the impregnation of Phenol Red on high performance polystyrene resins. The system was affected by increasing ionic strength, even though the dye loading was better, owing to a higher concentration of competing cations. A separation of Ce, Lu, Yb, Tm, Er and Ho (co-eluting), Dy, Tb and Gd (co-eluting), Eu and Sm was achieved using 0.1 mM Phenol Red and 30 mM α-hydroxyisobutyric acid (pH 3.7) in the eluent.

Although dye impregnation of high grade polystyrene resins has been utilised for simple ion exchange with much success, the development of high performance

chelating ion exchange resins using dye impregnation is of greater importance with regard to the work performed in this thesis. High performance chelating columns enable preconcentration, separation and determination of metal ions to be carried out on-line by a single column in a closed system. Separate analytical columns are therefore not required, making the system simpler and also reducing costs. The application of these columns is known as 'High Performance Chelation Ion Chromatography' (HPCIC) and a number of silica and polystyrene based columns have been developed for this purpose.

3.1.2 High Performance Chelation Ion Chromatography

3.1.2.1 High Performance Bonded Silicas

Silica based substrates, modified with chelating functionalities, have been prepared for high performance separations of trace metal ions in aqueous solutions and are reported in a review by Marina *et al.* [90]. An 8-HQ silica gel column has been described by Risner and Jezorek [91] and was an obvious choice of chelating functionality since it reacts with over sixty metals. The 8-HQ gel, with a capacity of 46 μmol g^{-1} (QSG-46), was used for the separation of Cd(II), Pb(II) and Zn(II) using various eluents, of which tartaric acid and phthalic acid appeared to give the best separations. An isocratic separation of Mn(II), Cd(II), Pb(II), Zn(II) and Co(II) was also performed with a tartaric acid eluent. Faltynski and Jezorek [92] reported a range of chelating ligands bonded onto small particle size irregular silica particles. The most promising of the columns appeared to be a diphenylthiocarbazone (dithizone) silica gel upon which a

separation of Pb(II), Zn(II), Ni(II), Co(II), Cd(II) and Mn(II) was achieved. The peaks were not fully resolved but the peak shapes were much improved when compared to other modified silica gels investigated.

The development of crown ethers for metal adsorption has been exploited by Lauth and Gramain [93]. Benzo-18-crown-6-modified silicas were prepared for the chromatographic separations of alkali and alkaline earth metal cations. Although not fully baseline resolved, separations of Li, Na, Rb, Cs and K, and also Mg, Ca, Sr and Ba were achieved. Owing to different retention times of the metal ions with different anions, however, further work was required before application to 'real' samples.

Simonzadeh and Schilt [94] have explored the possibilities of small particle size silica immobilised 2-pyridinecarboxyaldehyde phenylhydrazone (PAPH). A separation of Mn(II), Fe(II), Cd(II), Zn(II), Co(II) and Pb(II) using a perchlorate/perchloric acid eluent was attempted. The resulting chromatogram showed co-elution of Fe and Cd and peak shapes for other metal ions, especially Pb, were poor. Bonn and Rieffenstuhl [95] reported investigations with a silica bonded iminodiacetic acid stationary phase. The retention times of some metal ions on the IDA-silica column were found to decrease with eluents of ethylenediamine, tartaric acid and dipicolinic acid, whereas, with citric acid, the retention times were found to increase. High resolution separations of Mg(II), Ca(II), Sr(II), Ba(II) and also Mg(II), Fe(II), Co(II), Cd(II) and Zn(II) were achieved with the column.

Nesterenko *et al.* [96] investigated the separation of trace metals with silica bonded 2(2'-thiazolylazo) dimethylaminophenol (TAAP) or 2-(2'-thiazolylazo) resorcinol (TAR) compounds. The TAAP silica column was found to be more efficient and a separation of Mn(II), Cd(II), Pb(II), Zn(II), Co(II) and Cu(II) was performed using a citric acid eluent. The resolution of the column was good but, as with most chelating columns, the peak shapes deteriorated rapidly with increasing retention time.

A novel use for 8-HQ bonded silica gel has been reported by Jezorek and Thompson [97]. Injections of samples containing phenols, divalent metal ions and anions were made and detected simultaneously by UV (254 nm), visible (510 nm after post column derivatisation with PAR) and conductance detection respectively, to give three chromatograms for each injection. A separation of Mn(II), Cd(II) and Zn (II) was achieved, although baseline resolution was not obtained for Mn and Cd.

Glennon *et al.* [98] discussed the chromatographic behaviour of silica bonded calix[4]arene tetraesters with alkali and alkaline earth metals and amino acid ester hydrochlorides. Selective retention of Na over the other alkali metals and Ca over Mg ions was found using water as the mobile phase.

A recent paper by Nesterenko and Jones [99] describes the results of a comparative study of chelating silica gels with a chelating dye impregnated polystyrene resin. The IDA-silica and TSK Gel Chelate 5 PW silica gels were found to have higher efficiencies in comparison with a phthalein purple impregnated polystyrene resin, but the polystyrene based sorbent had the best pH stability range.

3.1.2.2 High Performance Bonded Polystyrene Resins

Morris and Fritz [100] described the chromatographic separations of metal ions using PS-DVB resins with carboxylic acid functional groups. One resin had the carboxylic acid functional groups attached to the resin *via* three spacer atoms (e.g. -$COCH_2CH_2CO_2H$) the other resin had its carboxylic acid groups attached directly to the resin (e.g. -CO_2H). Both resins were prepared *via* a Friedel-Crafts mechanism. Various complexing eluents were tested and the rapid separation of several transition metals and alkaline earth metals was achieved in one run.

Although several polystyrene resins, with chemically bonded chelating functionalities have been reported, an increasing number of high performance polystyrene resins impregnated with chelating dyes have been developed since the first investigations in this area by Jones and Schwedt [101].

3.1.2.3 High Performance Dye Impregnated Polystyrene Columns

The preparation, characterisation and metal sorption properties of many chelating dye impregnated resins, suitable for high resolution separations of trace metals, are reported in a review by Marina *et al.* [102]. Jones and Schwedt [101] reported the impregnation of a small particle size polystyrene based resin with Bromophenol Blue for simple ion exchange separations and with Chrome Azurol S, for chelating ion exchange. Chrome Azurol S was chosen from a range of other triphenylmethane and azo dyes since its separation properties were believed to be an interesting comparison

to IDA and 8-HQ bonded substrates. A separation of Cd(II), Co(II) and Mg(II) was achieved with the Bromophenol Blue column. The Chrome Azurol S column was used to effect a separation of Mg(II), Mn(II) and Zn(II). Chelating ion exchange was believed to be the separation mechanism since the ion exchange sites of the column were saturated with at least 0.2 M KNO_3 in the isocratic eluent. The separation was improved by using gradient elution, enabling the separation of Mg(II), Mn(II), Zn(II) and Cu(II). A separation of Al(III), In(III) and Ga(III) was also achieved using the same column with an eluent of 1 M KNO_3 at pH 2.25.

Challenger *et al.* [103] described the performance of two dye impregnated columns with a commercially available Tosoh iminodiacetic acid based column. A Xylenol Orange (XO) impregnated polystyrene based column resin gave a separation of Ba, Sr, Mg and Ca which was approaching the efficiency of the Tosoh column, even though the elution order of the metal ions had changed. Jones *et al.* [104] described further investigations with the XO impregnated polystyrene resin and the isocratic separation of Ba(II), Sr(II), Mg(II) and Ca(II) was achieved at pH 7.6. By using gradient elution, a separation of Ba(II), Sr(II), Mg(II), Ca(II), Mn(II), Cd(II), Zn(II), Ni(II) and Cu(II) was achieved. The preconcentration and separation of Zn(II) and Cu(II) was also achieved from a sea water sample with a single column. Challenger *et al.* [105] reported the separation of Cd(II), Zn(II), Pb(II), Ni(II) and Cu(II) from a spiked sea water sample using an XO impregnated column. In addition, a separation of Al(III), Ga(III), and In(III) using a Chrome Azurol S column displayed a different elution order when compared to a separation performed by Jones *et al.* [101] under similar conditions. This would suggest that there were slightly different influences on the

chelating functionalities from the different polystyrene based substrates, or that the impurities in one of the dyes was affecting the separation.

Paull *et al.* [106] have discussed the HPCIC determination of trace metals in coastal sea-water using an XO impregnated neutral PLRP-S resin (Polymer labs.). The preparation of the column was optimised and the resin was impregnated with the dye and stabilised in less than 3 hours. The XO impregnated column was used to selectively preconcentrate and elute Zn(II), Cd(II), Ni(II) and Cu(II) from three sea water samples, prior to their determination by post column derivatisation with PAR and spectrophotometric detection at 490 nm. The method was validated by the determination of Mn(II), Zn(II) and Cu(II) in a certified standard coastal sea water sample (CASS-2). Good correlations of results with the certified values was achieved. Paull *et al.* [107] have also described the determination of alkaline earth metals in offshore oil-well brines using HPCIC. The column was prepared from Methyl Thymol Blue (MTB) impregnated 8.8 μm PS-DVB resin (Dionex). Ba and Sr were separated from much higher concentrations of Mg and Ca in an oil-well brine sample and the results compared well with ICP-AES determinations of the same samples. The elution order of the metal ions was reversed when compared to simple ion exchange which enabled the Ba and Sr to be determined before the large Mg and Ca peak eluted from the column.

Jones *et al.* [108] reported the separation and determination of Ba and Sr from high calcium containing matrices using high performance chelating columns. An MTB impregnated resin was used for the determination of Ba in mineral waters, and a

Phthalein Purple (PP) column was used to determine Sr in milk powder. The separation between Sr and Ca was better with the PP impregnated resin column, which was required owing to the large concentrations of Ca in the milk samples. All of the determinations for Ba and Sr showed good correlation with ICP-AES determinations.

A comparative study of the metal selective properties of chelating dye impregnated resins for HPCIC determinations of trace metals has been discussed by Paull and Jones [109]. A number of azo and triphenylmethane based dyes were prepared and the pH of the retention of metal ions on the columns was tabulated. Sample separations from some of the columns were given, and the determination of Al(III) in sea water using a CAS impregnated column was used to illustrate the adaptability of HPCIC for the analysis of complex matrices.

A comparative study of HPCIC phases has also been described by Nesterenko and Jones [99]. In this case, a comparison between two commercially available, Diasorb IDA silica and Tosoh TSK Gel Chelate 5 PW columns, and a column packed with PS-DVB impregnated with Phthalein Purple dye was made using maleate, tartrate and oxalate mobile phases. The complexing ability of the ion-exchangers was found to be of the order IDA-silica > TSK Gel Chelate 5 PW > PP impregnated PS-DVB. The selectivities of the IDA and the TSK Gel columns were similar and were both slightly different when compared to the dye impregnated column. Under the conditions used, the IDA silica and the TSK Gel columns were preferred for the isocratic separation of transition metals, but the PP column had the best pH stability range. At low pH's, the

Tosoh column dissolved, which meant that strong complexing agents were required for the removal of strongly held complexes, e.g. Cu(II) and Fe(III).

3.1.3 Types of Polystyrene Resin for Impregnation

Polystyrene resins have been used extensively as substrates for chromatographic analyses in both modified and unmodified forms. They are available as microreticular and macroreticular structures and to increase mechanical strength, they possess a form of crosslinking, typically 8% divinylbenzene. The dye impregnation of standard polystyrene divinylbenzene substrates has already been described for chelating ion exchange separations with much success. However, various forms of 'hypercrosslinked' resins have recently become commercially available. It is therefore of special interest to compare the dye impregnation of hypercrosslinked resins, with the impregnation of a range of standard crosslinked polystyrene resins.

3.1.3.1 Hypercrosslinked Polystyrene Resins

A majority of the research involving polystyrene based resins for liquid chromatography has been based on relatively low crosslinked resins. A range of 'hypercrosslinked' resins have been prepared and are known as 'macronets', owing to the large network of macroreticular pores. The high level of crosslinking in the macronets gives rise to large surface areas. A typical range of surface area may be between 1000 and 1500 $m^2 g^{-1}$ for macronet resins, which is far higher than standard DVB crosslinked resins, such as Amberlite XAD-2, which has a surface area of

approximately 330 $m^2 g^{-1}$ [110]. Davankov and Tsyurupa [111,112,113,114], who are accepted as the pioneers of macronet technology, reported the unusual structure and properties of the isoporous styrene copolymers. A range of crosslinking agents were described which reacted via a condensation (Friedel-Crafts) mechanism with the phenyl rings of the solvent swollen styrene polymer. In the course of this reaction, a bridge was formed between the polystyrene chains, which is two phenyl rings longer than the length of the cross linking agent. It was found that the degree of crosslinking was reduced with increasing DVB concentration.

The use of 'Styrosorb' resins, small particle size hypercrosslinked microporous polystyrene resins, for the adsorption of aromatic amines has been reported by Beth *et al.* [115] and by Tsyurupa *et al.* [116] for the extraction of phenols from water. Purolite have recently produced commercially available macroporous resins under the prefix of 'MN' series resins which are available as neutral or charged hypercrosslinked resins. The resins are easily wettable, and are very rigid, owing to a high degree of cross linking, enabling them to be crushed to smaller sizes with relative ease. The MN series resins are obtained in a wide particle size range of up to 1 mm in diameter as spherical, opaque beads. In terms of cost, the resins are relatively cheap, since they are prepared in cubic metre batches. Figure 3.1 displays MN200 in A) bead form and B) after crushing (the flat patches on the crushed resin illustrate how well the resin packs together and its suitability as a column packing material).

A)

B)

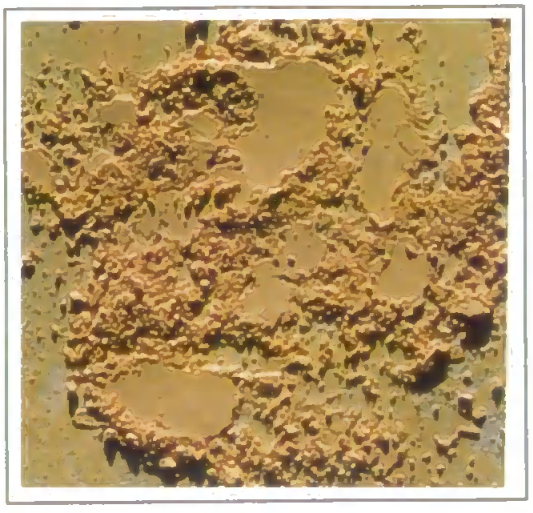

Figure 3.1. MN200 hypercrosslinked resin A) in bead form and B) after crushing.

3.1.4 Aims of this Study

The evaluation of dye impregnated neutral and anion exchange hypercrosslinked resins by comparison with similar dye impregnated standard crosslinked macroreticular resins is of special interest. The ultimate aim is to produce high performance chelating resins with improved characteristics, such as increased capacity and selectivity, over those which have been previously reported.

In order to investigate a wide range of polystyrene resins, preliminary investigations should therefore be performed batchwise on large particle size resins, which will reduce preparation times of the dye impregnated substrates. From these investigations, several resin types could then be chosen for further investigations using an HPCIC system. This would require crushing the resins to an intermediate particle size, suitable for packing in a column, and the batchwise dye impregnation of the resins. The capacity factors (k' values) for selected metal ions could then be determined. Finally, from the results of these investigations, a resin can be selected for small particle size evaluation in an HPCIC system. In this form, the study of analytical separations and selectivities of the resin is possible and its suitability for analytical applications can be determined.

3.2 Experimental

3.2.1 Instrumentation

The HPCIC system used in this study is described in Section 2.2.1 with the exception that a Dionex GP-40 gradient pump (Dionex, Sunnyvale, CA, USA) was used for the eluent, a Constametric model III pump (Laboratory Data Control, Riviera Beach, FL, USA) was used for the post column reagent (PCR) and a spectral array detector (Dionex) was used. The Cu(II) determinations from the batchwise capacity tests were made using an atomic absorption spectrometer (GBC Scientific Equipment, Dandenong, Australia).

3.2.2 Resin Dry Weights

The dry weights of the resins were obtained by simply centrifuging the samples at 2500 rev min^{-1} for 30 minutes and then heating overnight at 105°C. The mass of the resins was taken after each of these experimental steps.

3.2.3 Preparation of Resins

Resins chosen for investigation were MN100 (Purolite, Pontyclun, Wales), MN200 (Purolite), AP250 (Purolite), Amberlite XAD-2 (Aldrich, St. Louis, USA), Amberlite IRA-410 (microreticular) (Aldrich) and Amberlite IRA-904 (Aldrich).

Large particle size resins, as received from the manufacturers, were in bead form. When necessary, the resins were washed in acetone, methanol and DDW solutions to remove any detergents present from the manufacturing process. Intermediate particle size resins were prepared by crushing the resin beads using a pestle and mortar and then sieving to between 125-250 μm. The MN200 resin was crushed to two smaller mean particle size diameter sizes: 20 μm and 10 μm.

In the preparation of 20 μm MN200, the resin beads were crushed (in a small volume of DDW) using a pestle and mortar and were sieved to below 75 μm while retaining the lower fraction. The <75 μm MN200 fraction was then added to a 500 ml measuring cylinder and diluted to 400 ml with DDW. The cylinder was shaken until there was an even distribution of particles and left to settle for approximately three hours. The MN200 particles, suspended in solution, were retained and the process was repeated five to seven times, removing the particles which had settled on the bottom of the cylinder each time (to remove the larger particle sizes). The process was repeated a further five to seven times, but with a settling period of 24 hours. In this instance, the fractions that had settled on the bottom of the cylinder were retained and the suspended particles were discarded (to remove the smaller particle sizes). The particle size of the resin was measured using a Malvern Mastersizer 2.1 (Malvern Instruments, Malvern, Worcs., UK).

For the preparation of 10 μm MN200, the resin beads were crushed, as before, and sieved to a particle size range of 15-38 μm. The samples were centrifuged at 1000 rpm for 5 mins, 3000 rpm for 15 minutes, 1000 rpm for 10 minutes (three times), 1000

rpm for 5 minutes (three times) and then 500 rpm for 5 minutes (the sample was split between eight centrifuge tubes and the same operations were performed on each tube). The pellet at the bottom of the centrifuge tube was collected each time after removing the suspended particles. After the last centrifuge run, the suspended particles were collected and centrifuged at 4000 rpm for 5 minutes. The pellets were kept to be used as the fractions for column packing and the suspended particles were discarded. The particle sizes of both the pellet and the suspended particles were checked using a Malvern Mastersizer 2.1 (Malvern Instruments) between consecutive runs.

3.2.4 Batchwise dye impregnation of polystyrene resins

Large particle size polystyrene resins (1g) were introduced into 100 ml of 2 g l^{-1} dye solutions and adjusted to pH 5 (or pH 7 for PAR). The mixture was left shaking overnight, after which the resins were washed in solutions of 0.1 M ammonia and 0.1M nitric acid respectively until no more dye was present in the wash solutions. The washings were collected for analysis by UV/VIS spectrophotometry to indirectly determine the amount of dye remaining on the resin.

3.2.5 Polystyrene Column Preparations

Intermediate particle size resins (large particle size resins crushed to 125-250 μm) were dyed in a batchwise process as described previously and then slurry packed into metal free columns. Small particle size resins were packed at 2000 psi into PEEK columns using a Shandon column packer (Shandon Southern Products, Runcorn, UK).

The resins were then dynamically impregnated by pumping 5 g l^{-1} dye solutions through the columns at 1 ml min^{-1} overnight. Nitric acid (0.1 M) and ammonia (0.1 M) solutions were then pumped through the column sequentially until the loosely associated dye had been cleared from the column. The dye washings were collected for analysis by UV/VIS spectrophotometry.

3.2.6 Reagents

The reagents and eluents used were as described in Section 2.2.2 except that 2×10^{-4} M Pyrocatechol Violet (PCV) in 0.5 M Hexamine (adjusted to pH 6 with 2 M HNO_3) was used for trivalent metal ions with detection at 580 nm.

3.2.7 Procedures

The dye loadings on the substrate were calculated using UV/VIS spectrophotometry. The absorbance of the dye solutions was determined before and after the dyeing processes, the difference being directly proportional to the concentration of the dye coated on the substrates. The metal retaining capacities of the large particle size resins were performed by adding a Cu(II) standard of known concentration in a 1 M KNO_3 and 0.05 M lactic acid solution. The amount of Cu(II) remaining in solution was found using AAS and the capacity of the resins was indirectly determined. The capacities of the dye impregnated columns were calculated from the midpoint of the s-shaped breakthrough curves after known quantities of buffered zinc or copper solution were

pumped through the columns. The capacity factors for each dye coated substrate were obtained from the retention times of the metal ions at various pH values.

3.3 Results and Discussion

3.3.1 Preliminary Investigations using Dye Impregnated Large Particle Size Resins

For the preliminary investigations, the polystyrene based resins were used in bead form, as obtained from the manufacturer. There was therefore a wide variation in the particle size of the resin beads and, in the case of the macronets, the particle size maximum diameter was 1 mm. Although the ultimate aim is to achieve high efficiency separations, these large particle size resins served to compare important properties such as capacity and coating stability.

Two hypercrosslinked resins, MN200 (neutral) and MN100 (weak anion exchanger) were obtained for dye impregnation and compared with a range of standard crosslinked resins: AP250 (neutral), XAD-2 (neutral), IRA-904 (strongly basic anion exchanger) and IRA-410 (strongly basic anion exchanger). Two dyes were chosen for preliminary studies which are commercially identified as Chrome Azurol S (CAS) and Brilliant Blue R (Figure 3.2). Chrome Azurol S is a triphenylmethane based dye and was selected for use as it had been previously described for the successful impregnation of polystyrene resins by Jones and Schwedt [101]. The resins were impregnated with the dyes by a batch process, described in Section 3.2.4. After equilibration of the dye on

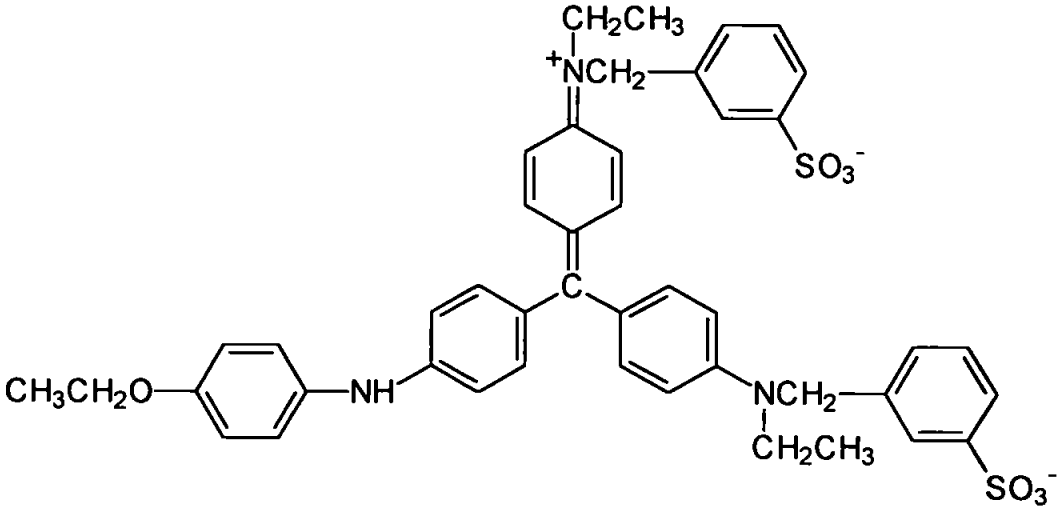

A)

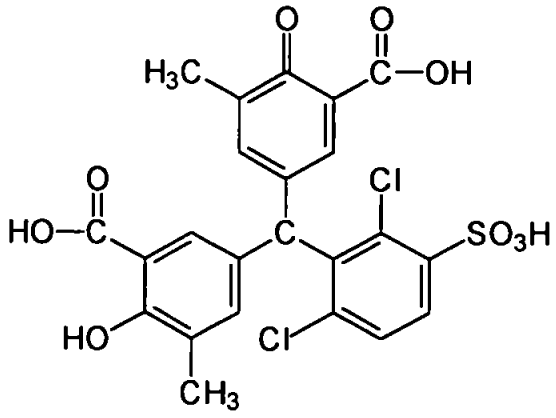

B)

Figure 3.2. Structures of A) Brilliant Blue R and B) Chrome Azurol S.

the resin, the concentration of the excess dye was determined by UV/VIS spectrophotometry and the concentration of dye remaining on the resins was indirectly determined. For the entire resin series, dye loadings were found to be higher in the presence of 10% methanol. After a series of experiments with the Brilliant Blue dye, it was established that the AP250 polystyrene resin had by far the lowest dye loadings. In the case of the CAS dyed polystyrene resins, the AP250 resin also had the lowest dye loading. It was decided that further investigations to calculate maximum dye loading capacities should be made using the four resins with the highest dye loadings, i.e., MN100, MN200, XAD-2 and IRA-904.

The dry weights of the four resins were calculated so that accurate measurements of the dye loadings could be made. The resins were initially centrifuged to remove surface moisture, and were then heated in an oven at 105°C (until a stable mass was obtained) to remove interstitial moisture. The results are displayed in Table 3.1 and it can be seen that, in all resins, relatively high proportions of water were present. The moisture content value supplied with the macronet resins was a nominal 60% and this was comparable to the values calculated in the table.

Three more dyes were chosen to evaluate the dye impregnation of the four chosen resins. These were 4-(2-pyridylazo)resorcinol (PAR), Calmagite and Xylenol Orange and their structures are displayed in Figure 3.3. Calmagite and PAR are azo dyes and Xylenol Orange is another triphenylmethane based dye. The dye impregnation of the resins revealed a lack of stability in the IRA-904 loaded resin. Although the IRA-904 initially had a high level of impregnated dye, instability was observed when the dye

Resin	Initial mass g.	Mass after centrifuging g.	†Mass after drying g.	Moisture %
MN100	1.1454	1.1081	0.4652	58.0
MN200	1.0001	0.9689	0.3926	59.5
IRA-904	1.1249	1.0761	0.4686	56.5
XAD-2	1.1182	1.0888	0.6641	39.0

† Dried at 105°C until a stable mass was obtained.

Table 3.1. Dry weights of polystyrene based resins

A)

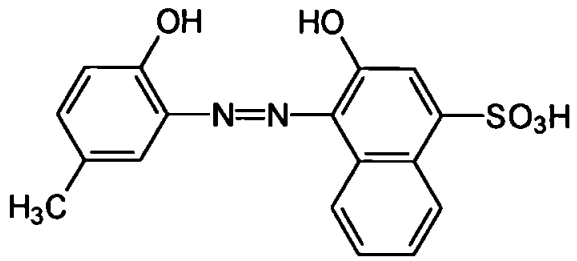

B)

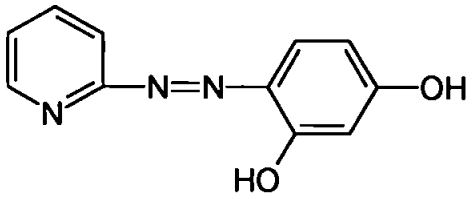

C)

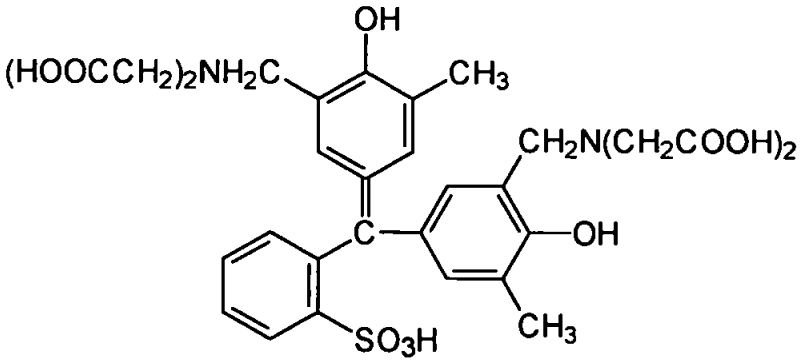

Figure 3.3. Structures of A) Calmagite, B) PAR and C) Xylenol Orange.

came into contact with alkaline solutions after being in its acid form. This resulted in heavy 'bleeding' of the dye from the resin. This 'bleeding' was first apparent when metal solutions were added to the resin and a precipitate of the dye was found to cloud the solution, thus rendering metal capacity investigations invalid. Table 3.2 therefore illustrates the dye loadings for the three remaining polystyrene resins, MN200, MN100 and XAD-2 which were calculated using UV/VIS spectrophotometry. After the impregnated resins had been carefully washed and equilibrated using 0.1 M NH_3, 0.1 M HNO_3 and DDW, they were placed in respective solutions of copper nitrate with 1 M KNO_3 and adjusted to pH 6. Lactic acid (0.05 M) was also added to prevent hydrolysis of Cu(II) ions. The level of copper remaining in solution was found using atomic absorption spectrometry and thus the amount of copper adsorbed onto the dye impregnated resins could be calculated.

The first column in Table 3.2, displaying the amount of dye impregnated in the resins, illustrates that MN100 had the highest dye loadings. MN200 was found to have a lower dye loading capacity, but in most cases had a higher proportion of dye available for chelation with the copper ions. Chrome Azurol S gave relatively high dye loadings, but the original dye was impure and was considered unsuitable for further investigations since effects from other isomers and compounds, present in the dyestuff, could yield erroneous results. The Xylenol Orange loading on the MN200 and XAD-2 was low in comparison to the loadings obtained for the Chrome Azurol S. This was unexpected since Xylenol Orange and Chrome Azurol S are both triphenylmethane based dyes and are similar in structure, indicating that the dye loadings should not differ significantly. In terms of metal retaining capacities, the PAR impregnated

Dye	Resin	Mass of dye per g of resin (mg)	m moles of dye per g of resin	m moles of Cu^{2+} per g of resin	(%) available sites for chelation
CHROME AZUROL S	MN100	149.2	0.246	0.146	59.4
	MN200	101.3	0.167	0.109	64.9
	XAD-2	46.5	0.077	0.039	51.2
CALMAGITE	MN100	73.8	0.145	0.078	75.7
	MN200	54.5	0.107	0.060	79.7
	XAD-2	34.8	0.069	0.017	34.9
XYLENOL ORANGE	MN100	47.25	7.02×10^{-2}	0.072	103
	MN200	9.2	1.37×10^{-2}	0.010	70.1
	XAD-2	8.3	1.23×10^{-2}	0.010	83.1
PAR	MN100	73.4	0.341	0.205	60.0
	MN200	63.5	0.295	0.211	71.5
	XAD-2	43.1	0.200	0.063	31.5

Table 3.2. Comparison of dye impregnated polystyrene resins

MN200 resin had the highest metal retaining capacity and both PAR impregnated MN100 and MN200 had metal retaining capacities of at least three times that of the highest value recorded for the standard crosslinked XAD-2 resin.

3.3.2 Investigations using Dye Impregnated Intermediate Particle Size Resins

For the determination of dye loadings and metal retaining capacities, batch investigations were suitable and the particle size of the resins was not considered critical. For the determination of capacity factors (k' values), however, investigations using a HPCIC system were required which meant that columns, containing the dye impregnated resins, had to be prepared. The columns were 10 cm in length (4.6 mm i.d.) and the large particle size resin beads did not produce suitable packing density for the columns. To overcome this problem, the resins were crushed and sieved so that the resultant particle size distribution was in the range 125-250 μm and an approximately uniformly sized packing material for the columns was achieved.

Owing to the high metal retaining capacities of the PAR impregnated large particle size resins, PAR was again chosen for further impregnation studies using intermediate sized crushed resins packed in columns. Table 3.3 displays the results for the dye loadings for four resins. IRA-904 was selected for use in further work after extensive washing procedures and no apparent bleed was observed from acid to alkaline solutions as in the previous experiments.

Dye	Resin	m moles of dye per g of resin	m moles of Cu(II) per g of resin	(%) available sites for chelation
	MN100	0.159	0.147	95.3
PAR	MN200	0.202	0.140	72.4
	IRA-904	0.069	0.003	4.4
	XAD-2	0.382	0.028	7.9

Table 3.3. A comparison of polystyrene resins impregnated with PAR

The results in Table 3.2 and Table 3.3 for the dye loadings and metal retaining capacities of the PAR impregnated resins are summarised in Table 3.4. It can be seen that the intermediate particle size crushed resins have lower dye loadings and metal retaining capacities in comparison to the large particle size resins, with the exception of XAD-2. The dye loading of XAD-2 was found to be much higher in comparison to the hypercrosslinked resins, but the percentage of dye molecules available for chelation was low. This implies that either the UV/VIS results for the XAD-2 were erroneous or that there was stacking of dye molecules in the resin resulting in little dye being available to the metal ions. After the IRA-904 had been extensively washed, the amount of dye loaded on the resin was lower than that of the other resins and the level of metal ions retained was almost fifty times less than that of the macronet resins.

Capacity factors (k'values) give a good indication of the selectivity and chelating strengths of the dye impregnated resins. They were determined using the relative retention times of Zn(II) and Mg(II) ions at different pH's and it was from these results that a resin was chosen for further investigations. Figure 3.4 illustrates the variation of the capacity factors for the four dye coated resins. The height of a line on the graph is a measure of the column's affinity for metal ions; higher lines indicate a weaker affinity. The capacity factors for IRA-904 are therefore much weaker than those of the other three resins for both Mg(II) and Zn(II). It was also noted that there was a difference in slope between the different resins with a general trend of increasing gradient from the low to the higher lines. No significant differences were apparent when the three other resins were compared for both the Zn(II) and Mg(II) sets of data.

	Resin	Large Particle Size Resins	Intermediate Particle Size Resins
m moles of PAR per g of resin	MN100	0.341	0.159
	MN200	0.295	0.202
	XAD-2	0.200	0.382
m moles of Cu(II) per g resin	MN100	0.205	0.147
	MN200	0.211	0.140
	XAD-2	0.063	0.028

Table 3.4 A comparison of the dye loadings and the metal retaining capacities of the large and the intermediate particle size PAR impregnated resins.

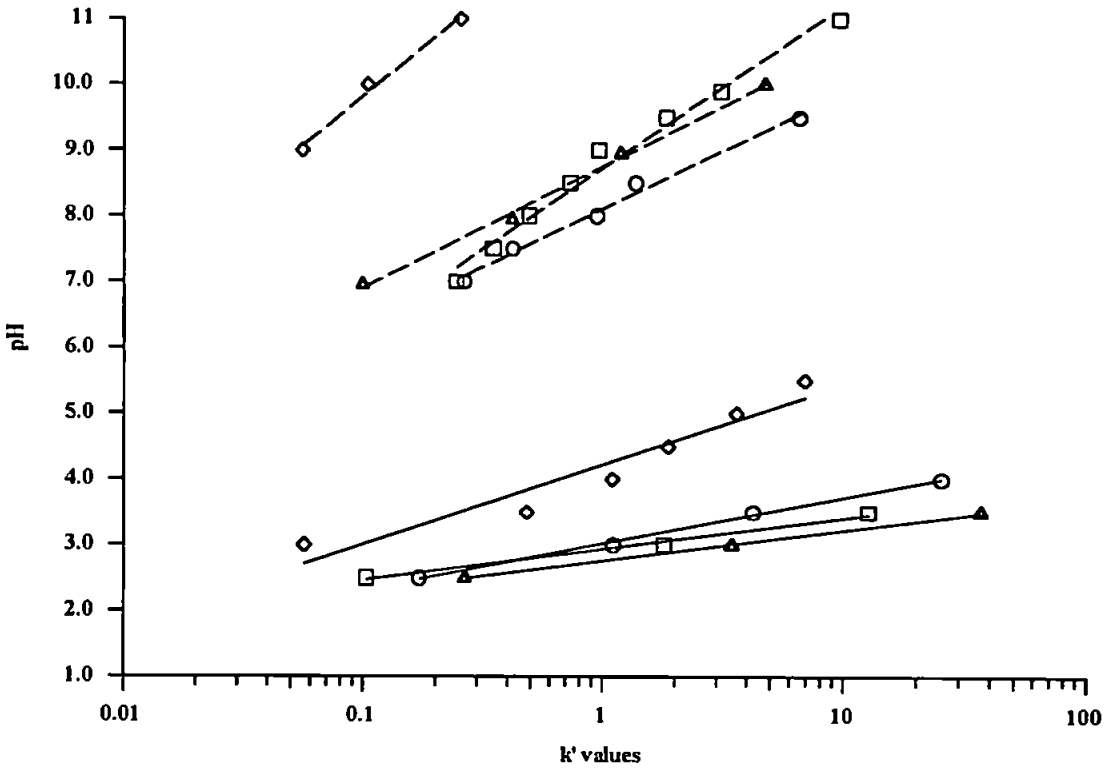

Figure 3.4. A comparison of capacity factor versus pH relationships for Zn(II) and Mg(II) for a range of PAR impregnated polystyrene resins. □ =MN100; ○ = MN200; ◇ = IRA-904; ▲ = XAD-2; — = Zn^{2+}; --- = Mg^{2+}

However, since the data in Table 3.4 illustrates that the actual metal retaining capacity value for XAD-2 was much lower than those for MN100 and MN200, the choice of resin used for the next stage of investigations with small particles was between the macronets. From the macronet resins, it was considered that MN200 was the most suitable as it is a neutral resin, thus eliminating interferences from functional groups in the resin backbone.

For investigations into the separating ability of the MN200 dye impregnated columns, small particle sizes were required to obtain increased efficiency when compared to the columns used for the k' value investigations. A particular property of the hypercrosslinked resins is their high rigidity, which enables them to be crushed easily. Problems were encountered when crushing the standard crosslinked resins since the material was more elastic, thus requiring considerable effort when crushing at room temperature (crushing the particles in liquid nitrogen was considered but not attempted). In addition, when the standard crosslinked resins were relieved of moisture, it was fairly difficult to resolvate them, whereas the macronet resins possessed unexpected hydrophilic properties which enabled them to be wetted immediately. The MN200 particles also settled more readily when agitated in aqueous mixtures. Therefore, the MN200 resin was suitable for investigation at a much smaller particle size than that used in the previous investigation.

3.3.3 Small Particle Size Investigations of the MN200 Resin for Analytical Separations

The main objectives of the investigations were to produce analytical separations, and small particle size resins were essential for this. Small particle size resins are a much improved packing material for HPLC columns and achieve increased separating efficiencies when compared to the larger size resins. An important consideration with the MN200 therefore was that the particle size range must be as small as possible for greatest column efficiency, enabling the separating ability of the dye impregnated resin to be evaluated. A possible problem was that fine particles (< 2 μm), present after crushing, could block the column 'frits' (filters) and care was taken to remove them before the substrates were packed into the column.

A small particle size material was prepared as described in section 3.2.3 and the particle size distribution is displayed in Figure 3.5. The particle size range was relatively large, but the mean particle size was about 20μm which was considerably less than the resin size used for the previous investigations. The particles were therefore known as 20 μm MN200.

Owing to difficulties in handling particles of such extremely small mean diameter, the batch dyeing procedures, used for the large and intermediate particle size resins, could not be used with the smaller particle size resins. A dynamic coating method was therefore employed for a column packed with 20 μm MN200.

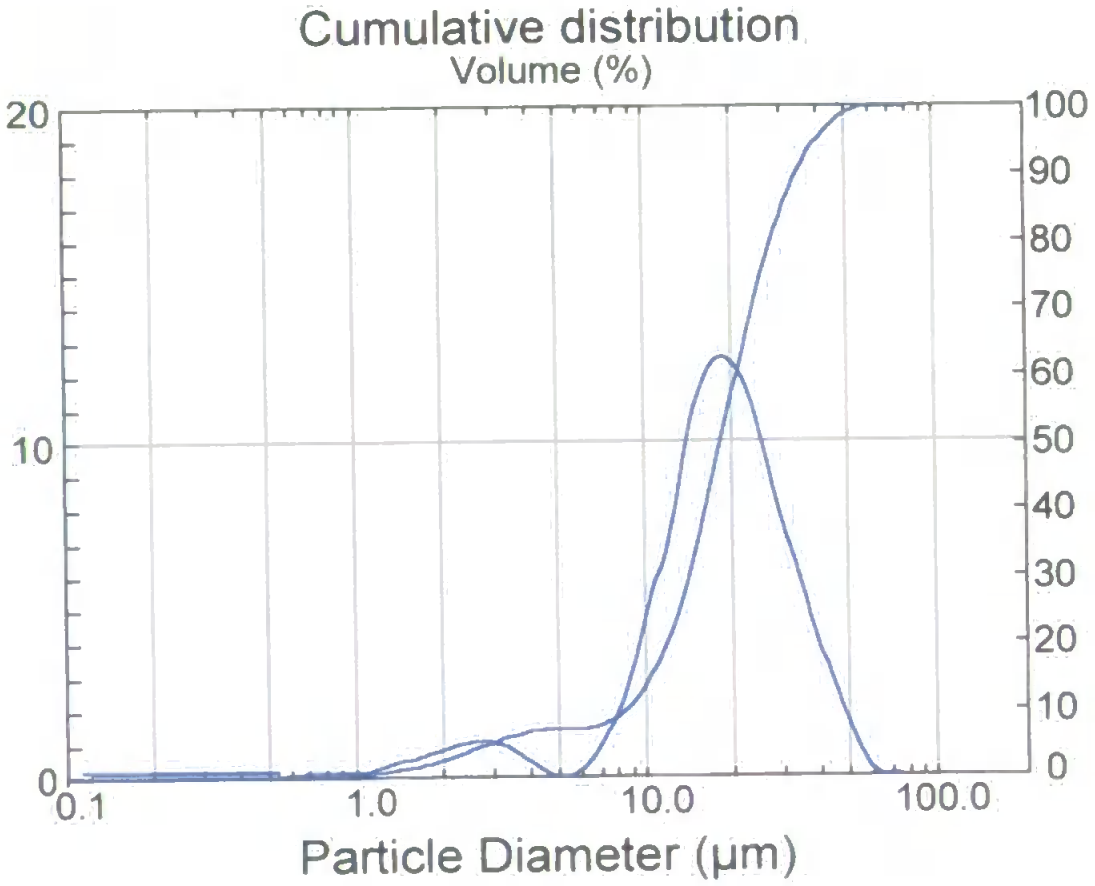

Figure 3.5 Particle Size Distribution of Crushed MN200

3.3.3.1 20 μm PAR column

A PAR column was prepared from 20 μm MN200 resin, using the dynamic coating procedure and its performance investigated. The capacity of the column was found to be 0.078 m moles of Cu(II) per gram of resin. This was lower than that of the larger size resin (0.211 m moles of Cu(II)) and was probably the result of a loss in suitable adsorption sites owing to the attrition of the resin. A recent study by Paull and Jones [110], however, reported a PAR impregnated column with a capacity of 0.019 m moles of Zn(II) per gram of resin which was less than a quarter of the capacity of the dye impregnated macronet resin.

To test the separating capabilities of the column under isocratic conditions, a series of metals were chosen which produced chelates of relatively similar strengths. It was decided that a selection of the alkaline earth metals would clearly display the separating capabilities of the column. Figure 3.6 shows the separation of a 5 μg ml^{-1} Ba(II) , 5 μg ml^{-1} Sr(II), 10 μg ml^{-1} Ca(II) and 10 μg ml^{-1} Mg(II) sample using the PAR column. The eluent was 0.5 mol dm^{-3} KNO_3 with 0.05 mol dm^{-3} lactic acid, adjusted to pH 10 with ammonia. The elution order of the metals from the column was opposite to that observed with simple ion exchange, indicating that the separation was achieved by a chelating mechanism (any simple ion exchange sites would have been overloaded with K^+ ions). The chromatogram shows rapid broadening of the peaks. This may have arisen since the relatively slow kinetics involved with chelating ion exchange mean that greater mass transfer effects are apparent when compared to simple ion exchange.

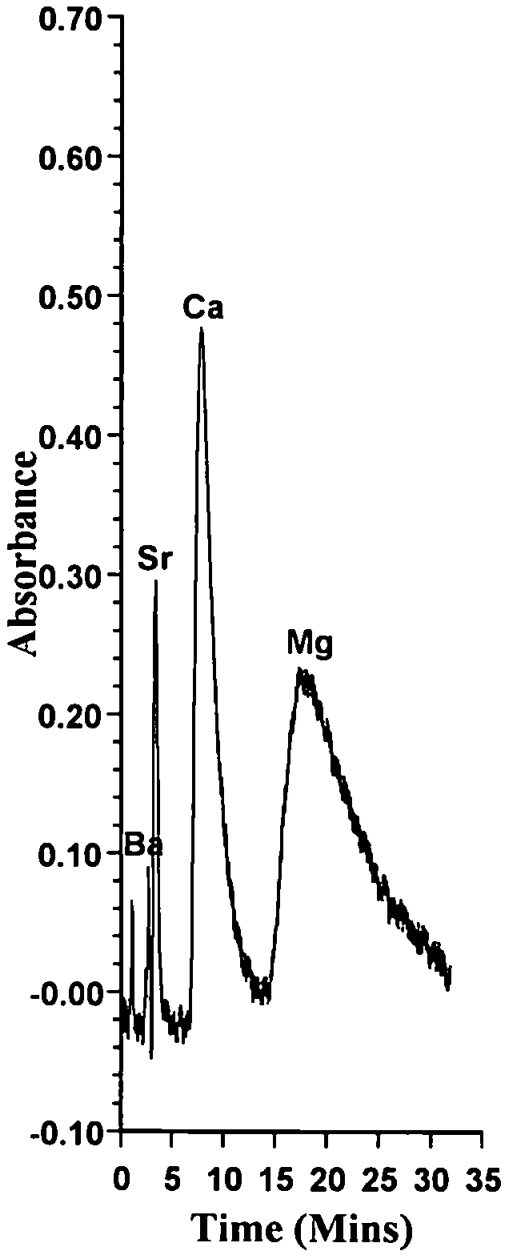

Figure 3.6 A separation of 5 μg ml^{-1} Ba(II), 5 μg ml^{-1} Sr(II), 10 μg ml^{-1} Ca(II) and 10 μg ml^{-1} Mg(II) at pH 10 with the 20 μm MN200 PAR column. The eluent was 0.5 M KNO_3, with 0.05 M lactic acid and the PCR was PAR/ Zn-EDTA with detection at 490 nm.

With increasing retention time the broadening effects are more visible. The peak shapes can be greatly improved if gradient elution is employed [109].

3.3.3.2 Further Investigations Using the 20 μm MN200

In order to further establish the properties of the small particle size MN200 resin, three more dyes were chosen to dynamically coat 10 cm columns of the resin. These were Phthalein Purple (PP), Aluminon and Sudan Orange G (SOG) and are shown in Figure 3.7. By impregnating the MN200 with different dyes, modifications in the selectivity of the columns for certain metal ions should be effected, resulting in both subtle and more distinct differences of metal ion separations between columns. The PP, Aluminon and SOG dyes were chosen since they have relatively different chelating strengths, which are in the order PP > Aluminon > SOG. Separations of Zn(II), Cd(II) and Pb(II) were attempted for each respective column and the capacity factors for In(III), Zn(II) and Mg(II) were also calculated.

3.3.3.2.1 Phthalein Purple Column Investigations

Phthalein Purple is a triphenylmethane based dye containing two iminodiacetic acid chelating groups. It is similar in structure to the Xylenol Orange dye, except that the sulphonate group is replaced with a carboxylic acid functional group. This results in the solubility of the Phthalein Purple dye to be decreased significantly at low pH. The Phthalein Purple dye is colourless below pH 9 whereas both Xylenol Orange and CAS are coloured at all pH's.

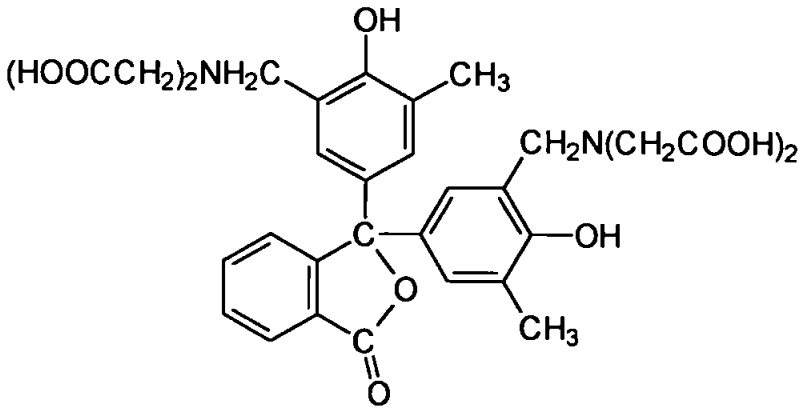

A)

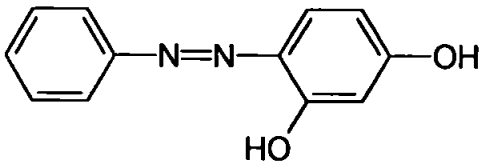

B)

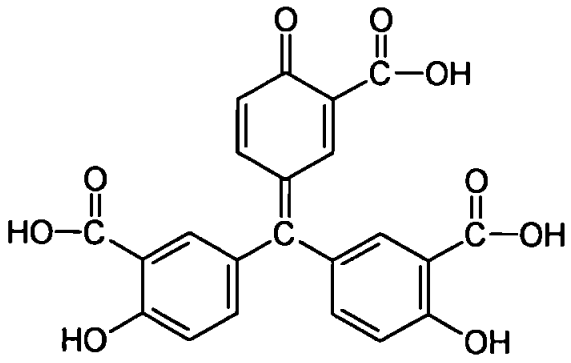

C)

Figure 3.7. Structures of A) Phthalein Purple, B) Sudan Orange G and C) Aurin tricarboxylic acid (Aluminon).

It was considered that Zn(II), Cd(II) and Pb(II) would give an example of a typical separation using the PP impregnated MN200 column since they formed chelates of a similar strength. A separation of 10 μg ml^{-1} Zn(II), 20 μg ml^{-1} Cd(II) and 20 μg ml^{-1} Pb(II) using the Phthalein Purple column is illustrated in Figure 3.8. The eluent was 0.5 mol dm^{-3} KNO_3 and 0.05 mol dm^{-3} lactic acid, adjusted to pH 4 with dilute ammonia. The elution order of the metals, when investigated separately, was Zn(II) < Cd(II) < Pb(II) but, when the metals were injected as a mixture, the Zn(II) and Cd(II) peaks merged into one large peak since they were fairly broad and had similar retention times. The Pb(II) peak was broad and this illustrates the slower kinetics involved in chelation ion chromatography.

Figure 3.9 illustrates the variation of capacity factors (using the Phthalein Purple column) with pH for In(III), Zn(II) and Mg(II). In was chosen since it is a trivalent metal ion which forms strong chelates. Zn(II) and Mg(II) were chosen as they form medium strength and weak complexes respectively. Since the height of the line on the graph is a measure of the column's affinity for a metal ion (with the lower lines being the strongest) the order of In(III) > Zn (II) > Mg(II) was as expected. The 'gap' between the lines is a measure of the selectivity of the columns for the metal ions. The variation in gradient between the lines was unusual and was probably a result of the difference in eluent compositions which were used to obtain different pH's. The increased gradient of the Mg(II) line implies that the likelihood of elution overlap with another metal is increased. Shallow lines imply that there are large changes in retention times with small changes in pH, which can be crucial when optimising a separation.

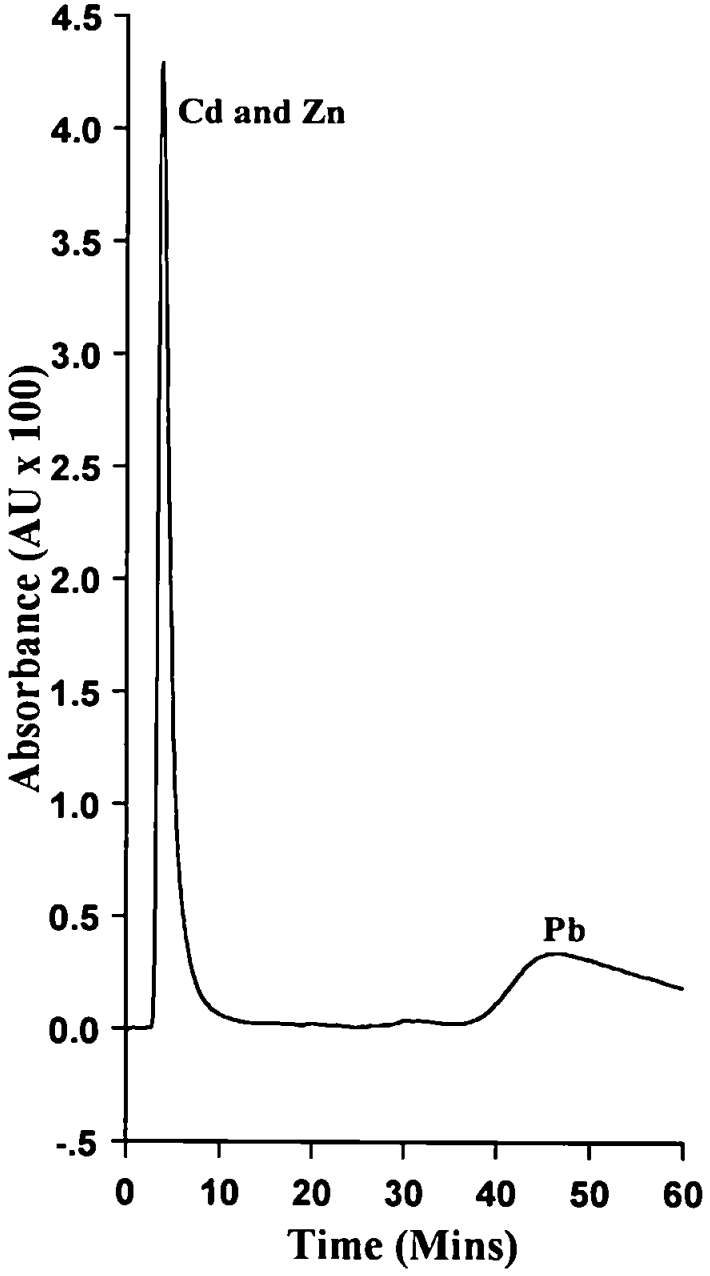

Figure 3.8. 100 µl injection of 10 µg ml^{-1} Zn(II), 20 µg ml^{-1} Cd(II) and 20 µg ml^{-1} Pb(II) using the PP column. The eluent was 0.5 mol dm^{-3} KNO_3 and 0.05 mol dm^{-3} lactic acid, adjusted to pH 4 with dilute ammonia. Detection was with PAR at 490 nm.

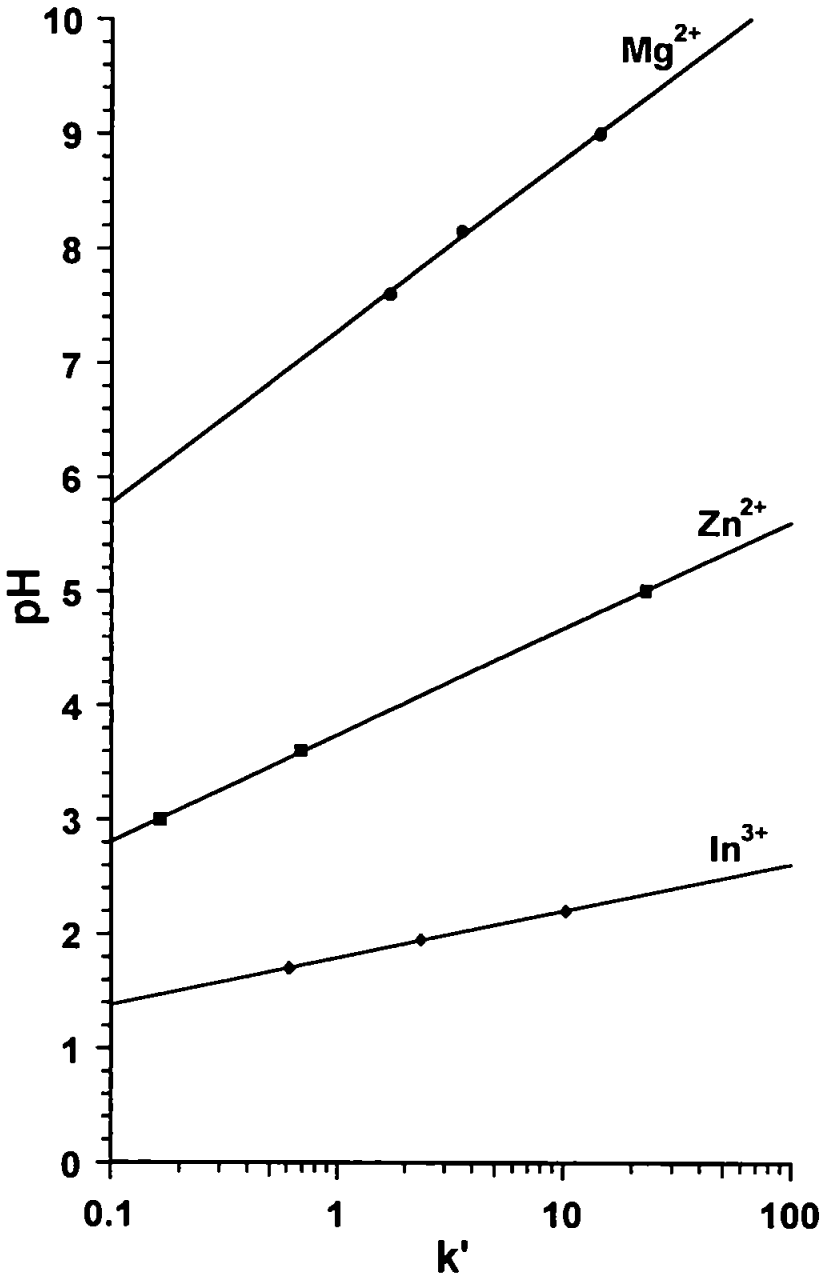

Figure 3.9 The k' values for In(III), Zn(II) and Mg(II) for the 10 cm Phthalein Purple column.

3.3.3.2.2 Aurin tricarboxylic acid (Aluminon) Column Investigations

Aluminon is a triphenylmethane based dye (Figure 3.7) but, unlike Phthalein Purple, it does not have iminodiacetic acid functional groups. The chelating functional groups are carboxylic acid groups with adjacent hydroxyl groups which are directly attached to the benzene rings. The chelating properties of the Aluminon dye may therefore be expected to be weaker than those of Phthalein Purple, since (N,O) chelators are regarded as being stronger than (O,O). However, like Phthalein Purple, Aluminon does not contain any sulphonate functional groups and so is not very soluble in its acid form. It is soluble in dilute solutions of ammonia or sodium hydroxide.

Figure 3.10 displays a separation of 3 $\mu g\ ml^{-1}$ Zn(II), 10 $\mu g\ ml^{-1}$ Cd(II) and 10 $\mu g\ ml^{-1}$ Pb(II) using the Aluminon column. The eluent was 0.5 M KNO_3, 0.1 M hexamine and 0.05 M lactic acid at pH 4.25. The post column reaction detection was achieved using buffered PAR at 490 nm. The separation was better than that recorded for PP since Cd(II) and Zn(II) were fully resolved to the baseline. The Pb(II) peak was fairly broad, however this was expected for all of the columns since the mean particle size was still relatively large (in comparison to the phases used for reversed phase chromatography e.g. 3-5 μm) with a wide particle size distribution. Mass transfer effects could have therefore been greater owing to the slow kinetics involved with chelation. With small and uniform particle sizes, mass transfer effects are reduced since the elution paths of the metal ions do not differ significantly.

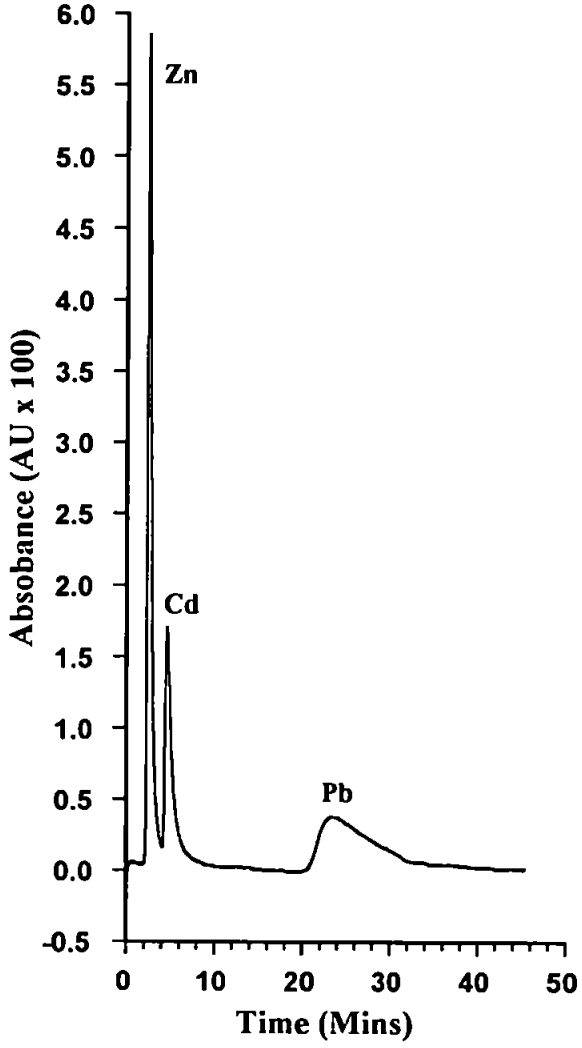

Figure 3.10 A 100 µl injection of 3 µg ml^{-1} Zn(II), 10 µg ml^{-1} Cd(II) and 10 µg ml^{-1} Pb(II) with the Aluminon column. The eluent was 0.5 M KNO_3, 0.1 M hexamine and 0.05 M lactic acid at pH 4.25. The post column reaction detection was with buffered PAR at 490 nm.

Figure 3.11 displays the change in k' with pH for the Aluminon column. For k' values of 1, the corresponding pH values for In(III), Zn(II) and Mg(II) were all higher for the Aluminon column compared to the PP column, indicating that the Aluminon column was weaker. The Mg(II) line for the Aluminon column was unexpectedly steep in comparison to the Zn(II) and In(II) lines which was difficult to explain. It may be that there was slight bleeding of the dye from the column at high pH, although no bleed was observed at the time.

3.3.3.2.3 Sudan Orange G Column Investigations

Sudan Orange G (SOG) is an azo dye and was chosen as it was considered a weaker chelator when compared to Aluminon and PP. It was believed that weaker chelating functional groups could give better reaction kinetics in the chromatographic system and thus yield chromatograms of improved resolution. SOG is similar in structure to PAR except that the pyridyl group present in PAR is replaced with a benzene group. As a result, SOG has a weaker chelation affinity for metal ions compared to PAR since the pyridyl nitrogen utilised for the chelation in PAR is not present in SOG. SOG also has low solubility in the acid form, but is soluble in weak alkaline solutions.

Figure 3.12 displays a separation of 10 $\mu g\ ml^{-1}$ Zn(II), 20 $\mu g\ ml^{-1}$ Cd(II) and 20 $\mu g\ ml^{-1}$ Pb(II). The Zn(II) and Cd(II) peaks show better resolution than for the Phthalein Purple column although there is a serious 'fronting' problem with the Pb(II) peak. It is possible that agglomerated particles of the dye were trapped in the column causing serious broadening of the peaks.

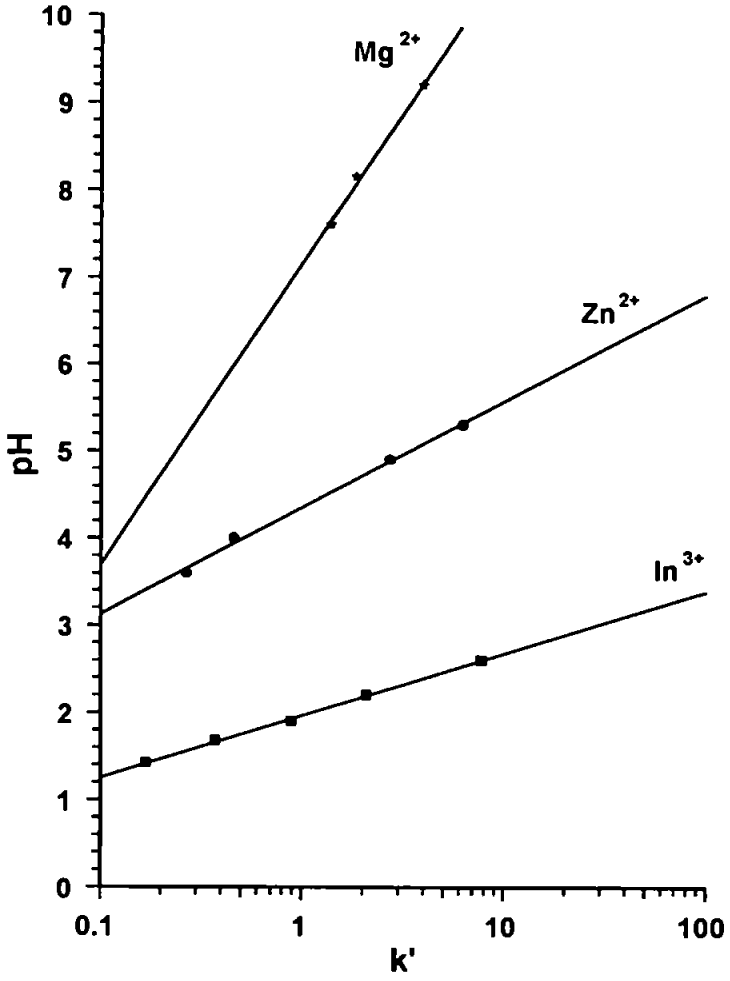

Figure 3.11. Variation of k' with pH for the Aluminon column.

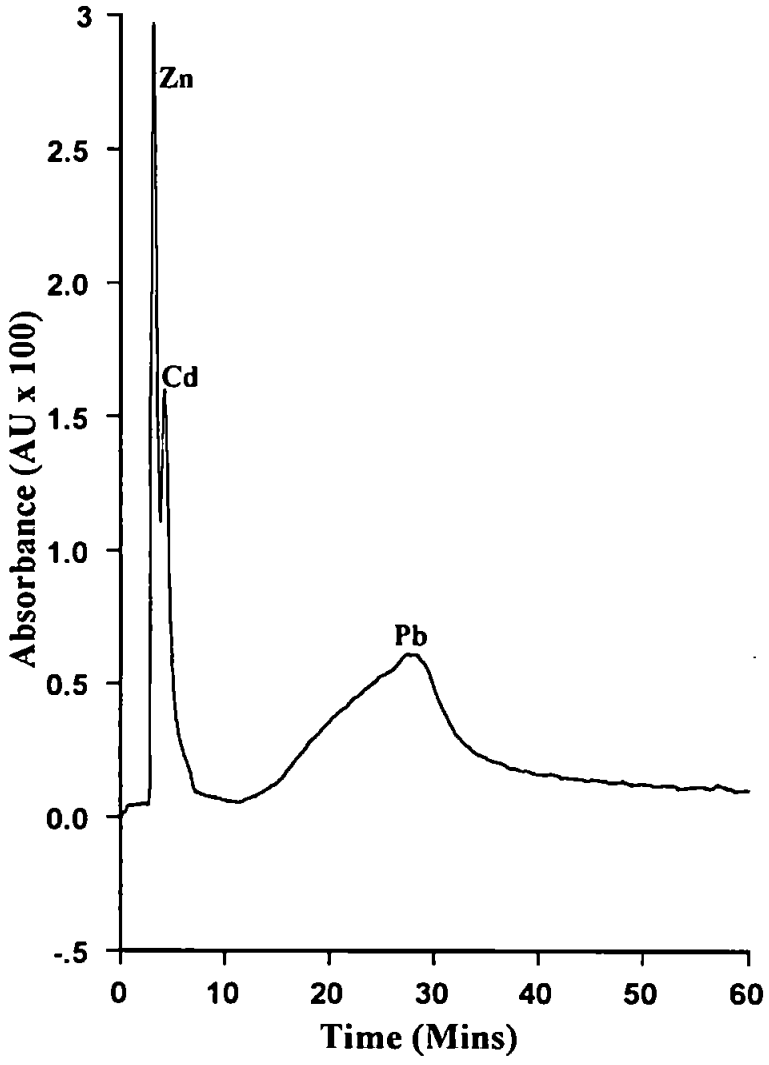

Figure 3.12. 100 µl injection of 10 µg ml^{-1} Zn(II), 20 µg ml^{-1} Cd(II) and 20 µg ml^{-1} Pb(II) using the SOG column. The eluent was 0.5 M dm^{-3} potassium nitrate, 0.05 M dm^{-3} lactic acid adjusted to pH 4 with dilute ammonia. Detection was with PAR at 490 nm.

Figure 3.13 illustrates the variation of k' values with pH for the SOG column. These values were lower when compared to the k' values for the Aluminon and PP columns at a particular pH and this was as expected in terms of their relative chelating strengths, i.e. PP > Aluminon > SOG. The lines are significantly steeper than those of the PP column. This may account for the better separation of Cd(II) and Zn(II) with the SOG column when compared to the PP column. It is possible that the k' values for Cd(II) and Zn(II) are closer to the k' values for Pb(II) with the SOG column compared to the PP column. Therefore, Cd(II) and Zn(II) will be separated whilst the retention time for Pb(II) is fairly low. If the k' values of Cd(II) and Zn(II) are much lower than those for Pb(II) at a chosen pH, the retention time of Pb(II) will be high before Cd(II) and Zn(II) are separated. This appears to be the case with the PP column. The k' values for the SOG column were lower in comparison to the values for the Aluminon and PP columns

The capacity factors for all the dyes were determined in buffered solutions to reduce column equilibration times between different pH eluents. It was thought, however, that competing chelation from the acetate groups present in the buffered solutions could cause a decrease in the observed k' values for the columns. The determination of the k' values for Zn(II) using an unbuffered eluent system was therefore attempted to investigate any differences between the eluent systems. Figure 3.14 shows two lines illustrating the variation of k' values with pH for Zn(II). The upper line corresponds to the use of an ammonium acetate buffer in the eluent whilst the other line is for the same eluent composition, but without the buffer. It appears that the presence of the buffer lowered the affinity of Zn(II) for the column and a higher pH was therefore required with the buffered system to maintain the same retention time of Zn(II).

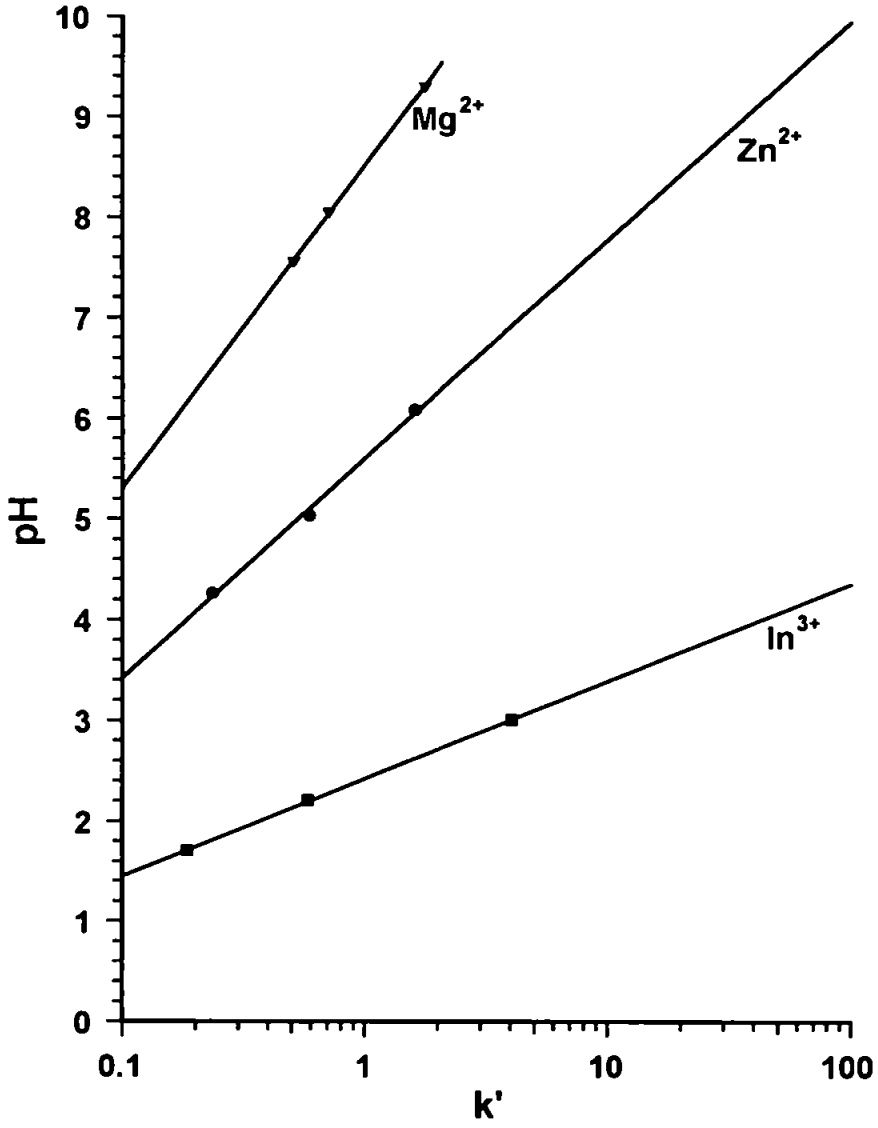

Figure 3.13. Variation of k' with pH for the SOG column

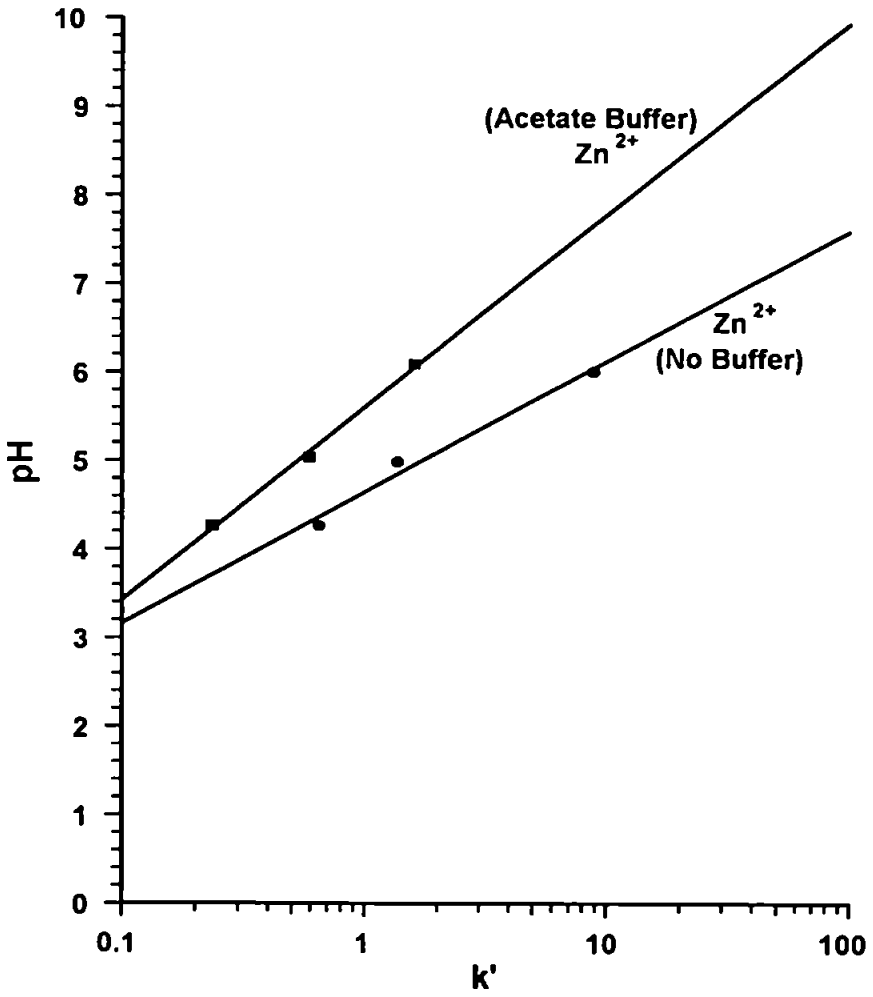

Figure 3.14. Variation of k' values with pH for Zn(II) using a buffered and unbuffered eluent system with the SOG column.

However, since the k' values for the other columns were determined with buffered systems, the upper line for Zn(II) was the one used for comparison.

Although the k' values determined for each column gave the relative chelating strengths of the columns in the expected order, the separations of metal ions obtained from the columns were not remarkably different. The chromatogram for the SOG column, however, was unusual as the Pb(II) peak was fronting and the kinetics were not improved with the weaker column as originally believed. It was considered that there could have been an influence from the resin backbone. If this was true, then it was most likely to affect the separations on the SOG column more than for the Aluminon and PP columns, since SOG had the weakest relative chelating strength. Investigations were therefore required to evaluate the properties of the unmodified MN200 resin.

3.3.3.3 Investigations with Unmodified MN200 Resin

Initially, the unmodified MN200 resin was not suspected to have adsorption properties for metal ions to any degree since the structure consists of bare crosslinked neutral polystyrene resin with no additional chelating groups. However, the results obtained for the SOG column investigations caused concern that the resin backbone may also have an affinity for the metal ions. An alternative explanation could be that one or several organic molecules with chelating functionalities had inadvertently become adsorbed onto the polystyrene resin and were interacting with metal ions passing through the system. It was believed that the most likely molecule that could have

become adsorbed onto the column and was used frequently in the system, was dipicolinic acid. Dipicolinic acid contains a benzene ring which could become adsorbed onto the column in the same manner as the dye molecules, i.e. by π - π interactions.

A 15 cm PEEK column was packed with fresh untreated 20 µm MN200 and it was ensured that elution of complexing agents through the column before use was avoided. Figure 3.15 shows a separation of 5 µg ml^{-1} Zn(II), 20 µg ml^{-1} Cd(II) and 20 µg ml^{-1} Pb(II). The eluent was 0.5 M KNO_3 and 0.05 M lactic acid which was adjusted to pH 4.42 with NH_3. The post column reagent was buffered PAR with detection at 490 nm. The separation between the Zn(II) and the Cd(II) was not baseline resolved but there were two distinct peaks and the Pb(II) was well separated from the Zn(II) and Cd(II), as for the other chromatograms. The resolution of the bare MN200 column should have been slightly better than that of the other columns tested, since it was one and a half times the length, thus increasing the number of separating plates and resultant column efficiency. However, the selectivity of the bare column was not as high as that of the Aluminon column, where Cd(II), Zn(II) and Pb(II) were completely resolved in a shorter time. The Pb(II) peak was very broad, as with the other columns investigated, but there would have been similar mass transfer effects for all the columns as they were packed using the same method with the same substrate.

A 5 cm column was prepared to establish the k' values for the unmodified MN200 resin since the retention times using the 15 cm column would have made the investigations tedious. Figure 3.16 displays the change in k' values with pH for the unmodified MN200 column. The lines for the In(III), Zn(II) and Mg(II) are almost

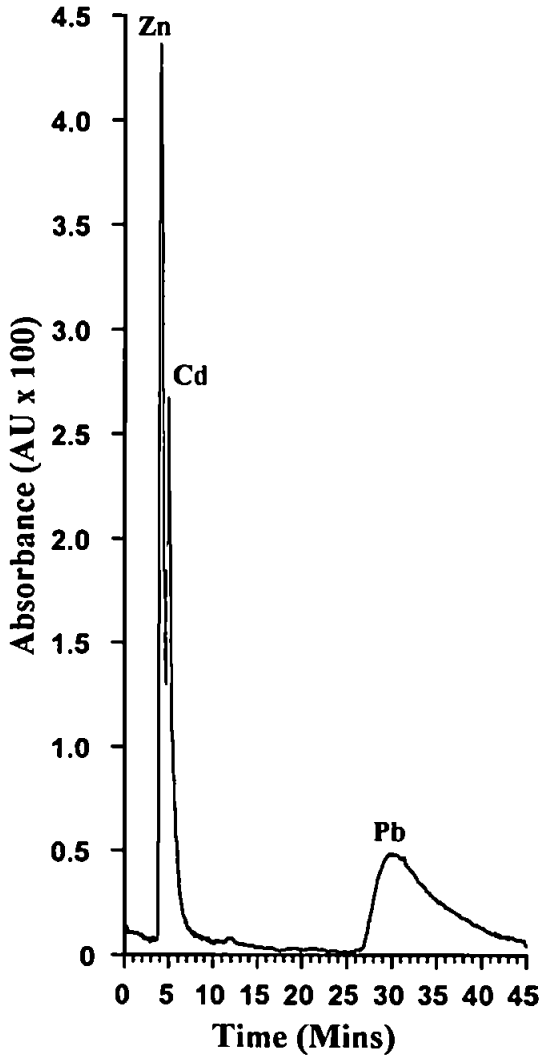

Figure 3.15. A 100 µl injection of 5 µg ml^{-1} Zn(II), 20 µg ml^{-1} Cd(II) and 20 µg ml^{-1} Pb(II). The eluent was 0.5 M KNO_3 and 0.05 M lactic acid which was adjusted to pH 4.42 with NH_3. The post column reagent was buffered PAR with detection at 490 nm

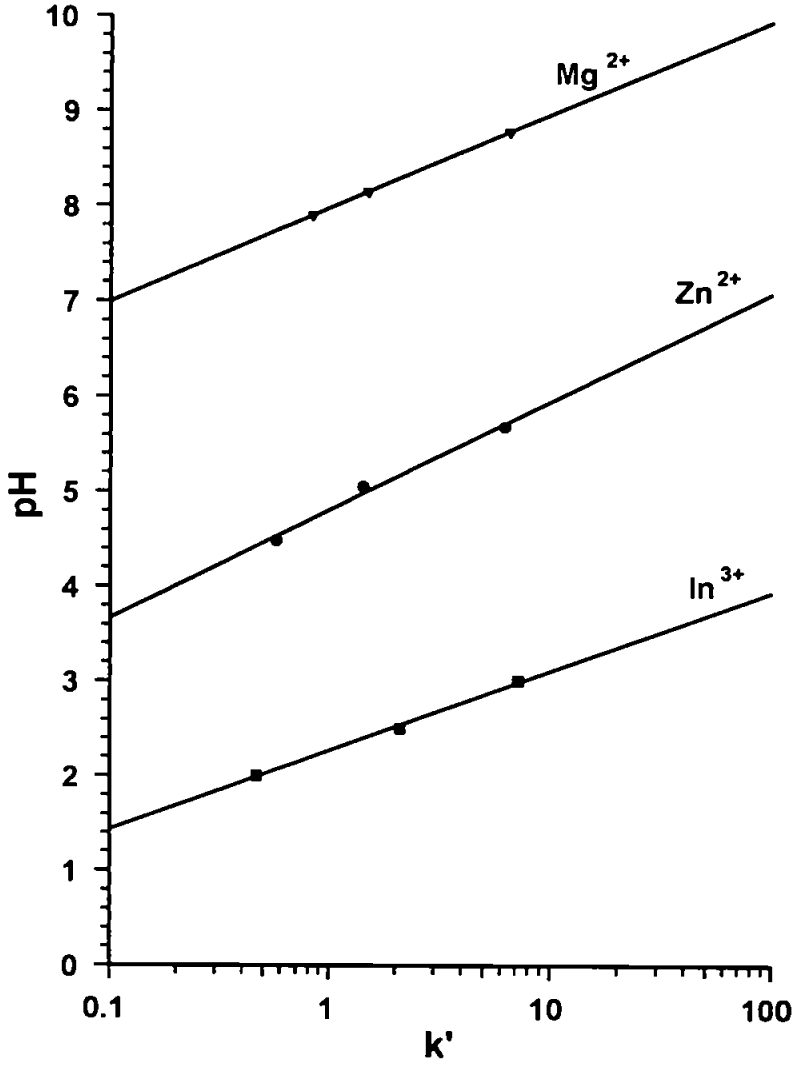

Figure 3.16. Variation of k' with pH for an unmodified MN200 column

parallel and the gradient of the Mg(II) line is less than that obtained using the other columns. It appears that this unmodified column showed weaker affinity for the elements than the dyed columns and should therefore not interfere significantly with the chelating mechanisms.

3.3.3.3.1 10 μm MN200 investigations

In view of the relative ease in which 20 μm material was obtained, it was decided to carry out more crushing which would reduce the mean particle size even further to achieve even greater efficiency columns. Further crushing and fractionation of the MN200 resin led to a mean particle size of approximately 10 μm being obtained with a smaller particle size range when compared to the 20 μm resin. Figure 3.17 displays the particle size distribution graph for the MN200 and it is evident that the mean size is approximately 10 μm. The other maxima occurs at about 2 μm and may be an artefact of the sizing instrument since the instrument was calibrated using known particle size distribution standards. In addition it was assumed that all particles were absorbing light from the laser.

It was decided that a separation of Cd(II), Zn(II) and Pb(II) would be sufficient to compare the column with either a modified or unmodified 20 μm MN200 column. The column chosen for comparison was Phthalein Purple, since an improvement in the separation could be identified simply owing to the lack of resolution between the Cd(II) and Zn(II) peaks with the 20 μm column. A 10 cm PEEK column was packed with the 10 μm MN200 and the column was impregnated with the Phthalein Purple in

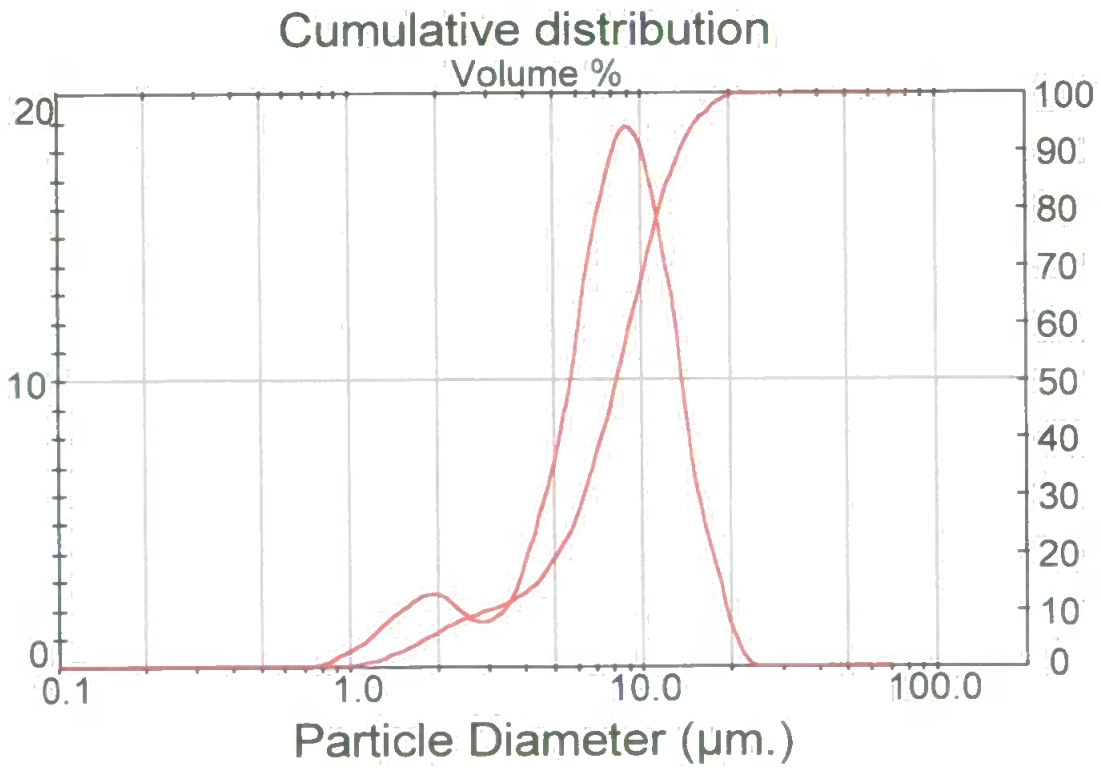

Figure 3.17. Particle size distribution for MN200

the usual manner. The back pressure produced by the column was noticeably higher than that of the previous columns owing to the smaller particle size distribution of the resin.

Figure 3.18 displays a separation of 4 μg ml^{-1} Zn(II), 4 μg ml^{-1} Cd(II) and 20 μg ml^{-1} Pb(II). The eluent was 0.5 M KNO_3 and 0.05 M lactic acid adjusted to pH 4.00 with NH_3. The post column reagent was buffered PAR with detection at 490 nm. When compared to a similar separation performed using the 20 μm column, the resolution appears to be enhanced. There was almost a baseline separation between Zn(II) and Cd(II) using the 10 μm column. It was not possible to compare the two chromatograms directly but, by constructing a graph of plate number against k' values for the 20 μm MN200 Phthalein Purple column, the number of plates may be the same for a particular k' value.

In the case of the 20 μm column, the parameters from two Zn(II) peaks were measured. For the first injection (the actual chromatogram is not shown) a model working for the calculation of capacity factors and theoretical number of plates takes the following form:

The parameters of two peaks obtained from 100 μl injections of Zn(II) were measured:

Retention time of an unretained peak, $t_0 = 2.10$ minutes.

Retention time of the first Zn(II) peak, $t_1 = 2.20$ minutes.

Peak width at half height of the first Zn(II) peak, $W_{½} = 0.38$ minutes.

The theoretical number of plates, N, calculated from the first Zn(II) peak,

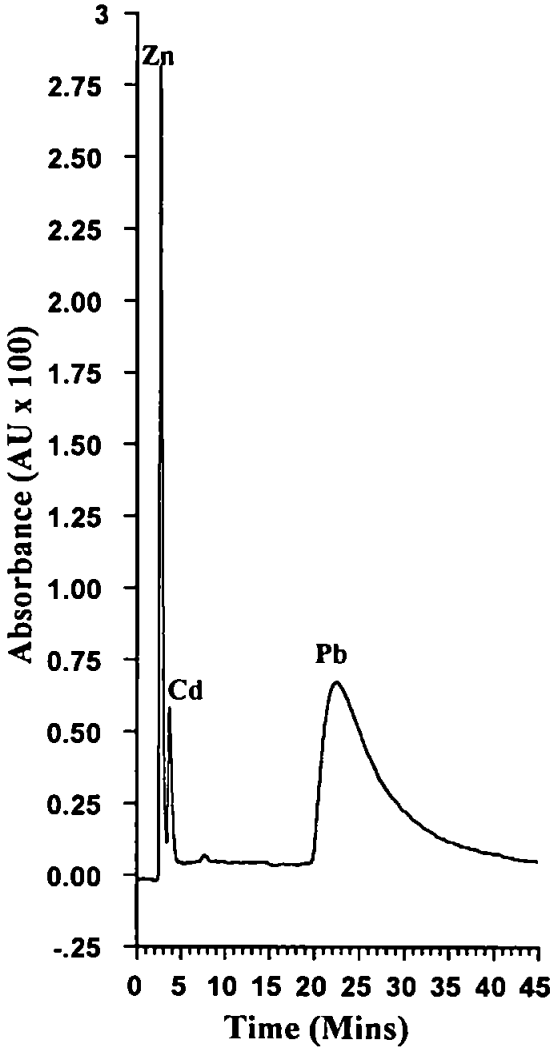

Figure 3.18. A 100 µl injection of 4 µg ml^{-1} Zn(II), 4 µg ml^{-1} Cd(II) and 20 µg ml^{-1} Pb(II). The eluent was 0.5 M KNO_3 and 0.05 M lactic acid adjusted to pH 4.00 with NH_3. The post column reagent was buffered PAR with detection at 490 nm.

$$N = 5.54\left(\frac{t_1}{W_{½}}\right)^2 = \left(\frac{2.20}{0.38}\right)^2 = 185.69$$

Capacity factor, k' value, for the first peak,

$$k_1' = \left(\frac{t_1 - t_0}{t_0}\right) = \left(\frac{2.20 - 2.10}{2.10}\right) = 0.048$$

For the second Zn(II) peak (again the chromatogram is not shown) the capacity factor and theoretical number of plates were calculated in the same manner.

$t_2 = 4.17$ minutes.

$W_{½}' = 1.4$ minutes.

$$N = 5.54\left(\frac{4.17}{1.4}\right)^2 = 49.15$$

$$k_1' = \left(\frac{4.17 - 2.10}{2.10}\right) = 0.986$$

For the 10 μm column, the k' value and plate number were calculated from the Zn(II) peak displayed in the separation in Figure 3.18.

$t_0 = 2.50$ minutes.

$t_{Zn} = 2.70$ minutes.

$W_{½} = 0.30$ minutes.

$$N = 5.54\left(\frac{2.70}{0.30}\right)^2 = 448.74$$

$$k' = \left(\frac{2.20 - 2.10}{2.10}\right) = 0.08$$

Figure 3.19 shows a graph of the theoretical number of plates versus k' values. A line was plotted for the values obtained for the 20 μm column. By interpolation, the plate number at a k' value of about 0.08 can be used to compare the plate number obtained for the 10 μm column. The graph therefore shows that the number of theoretical plates, determined for the 10 μm column was at least twice that of the 20 μm column for a similar interpolated k' value. It may therefore be concluded that the efficiency of the 10 μm column was better than that of the 20 μm column.

3.4 Summary

Preliminary investigations indicated that the hypercrosslinked resins could adsorb higher concentrations of chelating dyes when compared to the lower crosslinked resins. The dye impregnated hypercrosslinked resins also had higher metal retaining capacities. A decision was made to proceed with the neutral macronet resin, MN200, due to superior values for metal retaining capacities and capacity factor values. The PAR impregnated column, prepared from 20 μm MN200, showed good affinity for the alkaline earth metals and a separation of Ba, Sr, Ca and Mg was achieved. For the other three dyes impregnated on the 20 μm MN200 columns, the relative strengths of the columns were as expected from the chelating functional groups present, i.e. Phthalein Purple (N,O) > Aluminon (O,O) > SOG (N,O) (in the case of SOG, the chelating strength was weaker - essentially due to the structure and not the ligating atoms). When the MN200 was crushed further to a mean particle size of 10 μm, a Phthalein Purple column prepared from the resin showed significant improvement in resolution compared to a Phthalein Purple column prepared from the 20 μm resin. Although the efficiency of the 10 μm column was significantly improved, the particle

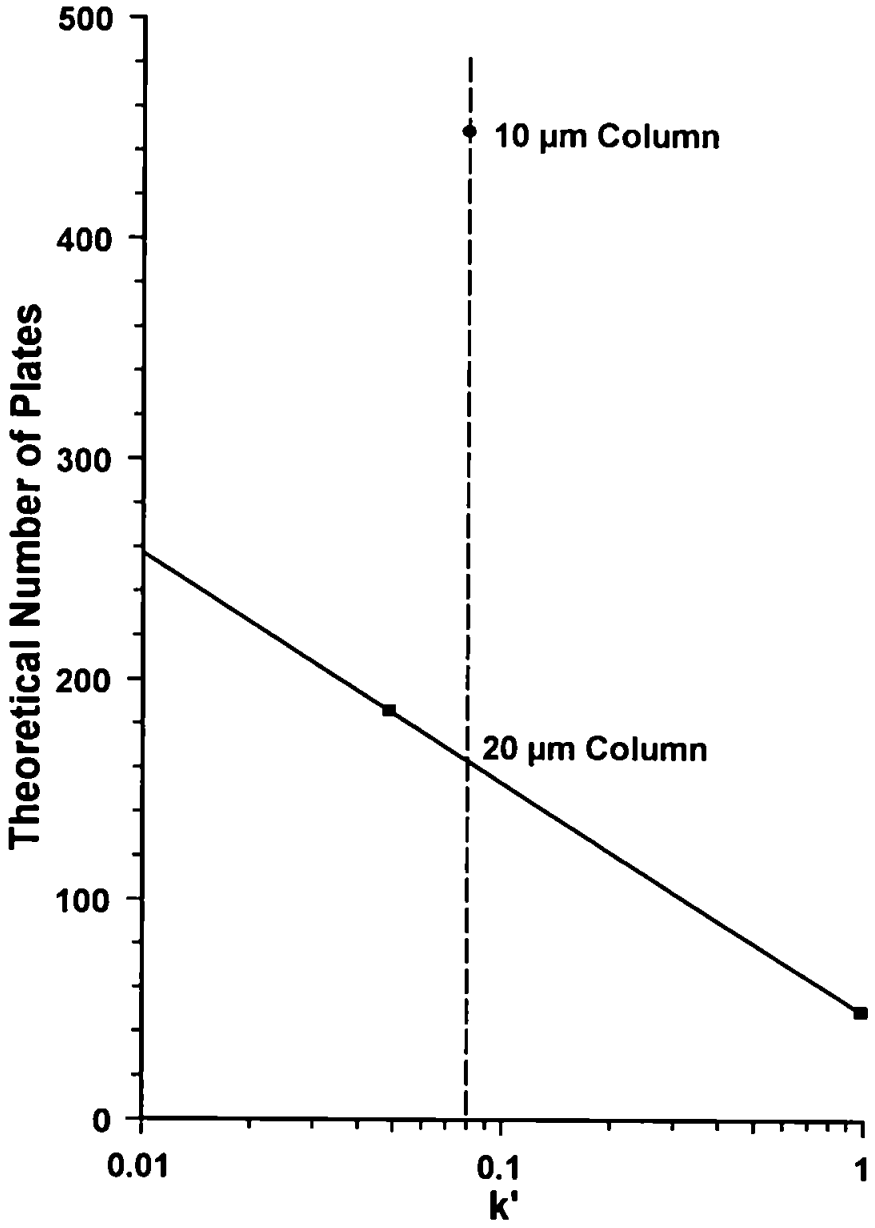

Figure 3.19. A comparison of theoretical plate number versus k' determined from Zn(II) injections using 10 and 20 µm MN200 Phthalein Purple columns.

size distribution of the column was still fairly broad. The efficiency could therefore have been further improved by reducing the mean particle size and narrowing the particle size range.

The chelating ability of the bare MN200 was unexpected. Ion exchange was not considered to be the separating mechanism for the retention of metal ions, since the separations were performed in high ionic strength media which would swamp any ion exchange sites. The peak shapes obtained from the bare column were also comparable to those obtained from a chelating column. A recent paper by Davankov *et al.* [117] discussed the properties of some hypercrosslinked resins and noted metal adsorbing properties of 'Styrosorb' type resins. It was postulated that the adsorption of mercury was caused by a complexation of mercury ions with two or more benzene rings of the polystyrene sorbent. The slow kinetics involved with the complexation were believed to result from a slow conformational rearrangement of the network in accordance with requirements of the metal ion co-ordination sphere. Using aqueous acetate buffers and nitric acid solutions, 440 mg g^{-1} Hg(II) were loaded onto a 'Styrosorb 2' resin with a surface area of 1500 m^2 g^{-1}. Ag(I), Pb(II) and Bi(III) were also found to adsorb into Styrosorbs, although with smaller sorption capacities. Styrosorb resins, however, are different to 'macronet' resins as they are microporous whereas macronets are macroporous. The pore diameter of the Styrosorb resins was 2-3 nm, whereas the macronets are 'bimodal', with pore diameters of 2-3 nm and 30 or 100 nm. The metal adsorbing properties of the Styrosorb resins may therefore not be identical for all of the hypercrosslinked polystyrenes but may give an indication of the possible characteristics of the macronet resins.

CHAPTER 4 - The Separation of Traces of Strontium From Calcium Sulphate For High Resolution Mass Spectrometric Analysis

4.1 Introduction

4.1.1 Isotope Ratio Determinations

The study of the relative proportions of radioactive isotopes and their stable 'daughter' isotopes can yield important information, which enables the age of formation of certain artefacts and natural minerals to be calculated. It is crucial, however, that none of the daughter isotope has been lost during the radioactive decay process, for instance as a gas. This information may also be used as a 'fingerprint' to determine the geographical source of various objects or foodstuffs. Isotopes of Rb and Sr have been the most widely used in this procedure although much research has been done using U and Pb isotopes. Isotopes of Sm and Nd and more recently, Lu and Hf have also been used with much success [118].

Rubidium is a soft, extremely reactive white metal with an ionic radius of 1.48 Å, similar to that of potassium (1.33 Å). Consequently, rubidium occurs substituted in many potassium bearing minerals, such as micas, potassium feldspar, some clay minerals and evaporites such as sylvite and carnallite. Rubidium has 27 isotopes, two of which are found in nature, namely $^{85}_{37}Rb$ and $^{87}_{37}Rb$, with isotopic abundances of 72.17% and 27.83% respectively [119]. The heavier of the two Rb isotopes, ^{87}Rb decays by emission of an electron to stable ^{87}Sr according to the following equation:

$$^{87}_{37}Rb \rightarrow {}^{87}_{38}Sr + \beta^{-} + \bar{\nu} + Q$$

where β^{-} is a beta particle, $\bar{\nu}$, is an anti-neutrino and Q is the decay energy (0.275 MeV).

Strontium is a reactive alkaline earth metal with an ionic radius of 1.13 Å. It is able to replace calcium in many minerals (even though the calcium ion is smaller, with a radius of 0.99 Å). Consequently, although there are minerals where strontium is the major cation, such as celestine, $SrSO_4$, it usually occurs as a dispersed element, especially in calcium bearing minerals such as plagioclase, apatite, calcium carbonate and calcium sulphate (gypsum). There are 23 isotopes of strontium, of which four occur naturally. These are stable and comprise $^{84}_{38}Sr$, $^{86}_{38}Sr$, $^{87}_{38}Sr$ and $^{88}_{38}Sr$, which have the following abundances: 0.56, 9.86, 7.00 and 82.85% respectively. The isotopic abundances, however, are variable, reflecting the formation of radiogenic strontium-87 through the decay of naturally occurring ^{87}Rb. Thus, the exact isotopic composition of strontium in a mineral or rock which contains rubidium, will depend upon the age and the Rb/ Sr ratio of that rock.

The decay of radioactive substances follows the exponential relationship:

$$N = N_0 e^{-\lambda t}$$

where N is the number of unchanged atoms at time t, N_0 is the number present when

$t = 0$ and λ is a constant, characteristic of the particular radioactive species. λ is called the decay constant and has the dimensions of reciprocal time. The rate of radioactive decay is expressed in terms of the half-life $t_{1/2}$ and is the time required for an initial number of atoms to be reduced to half that number by the decay process, i.e. when $t = t_{1/2}$, $N = N_0 / 2$.

Therefore: $t_{1/2} = \ln 2 / \lambda$

In the case of strontium, the ratio of the parent isotope, ^{87}Sr, to the stable daughter isotope ^{86}Sr can be determined and used to give the equation [120]:

$$\frac{^{87}Sr}{^{86}Sr} = \left(\frac{^{87}Sr}{^{86}Sr}\right)_0 + \frac{^{87}Rb}{^{86}Sr}(e^{\lambda t} - 1)$$

^{86}Sr is a suitable isotope to use in time dependent calculations since it is fairly abundant, constituting 9.9% of natural strontium and, in addition, it is not the product of any known radioactive decay series The equation can be used to determine the age, t, of the sample and the initial ratio of strontium $(^{87}Sr/^{86}Sr)_0$ at t years ago, by the analysis of $^{87}Sr/^{86}Sr$ and $^{87}Rb/^{86}Sr$ for two or more minerals, with differing rubidium contents, from the same rock system. Very high precision of the isotope ratios is required and high resolution mass spectrometry can be used to give results with up to six figure precision.

A major advance in the application of Rb-Sr isotope dating was the realisation that two variables were involved with any system of related rocks or minerals [121]. One

variable is the age, or length of time that a mineral or rock has remained in a closed chemical system with respect to Rb and Sr. The second variable is the composition of common strontium (expressed as $^{87}Sr/^{86}Sr$) that existed when t = 0. This composition changes between "systems" that experienced homogenisation of Sr isotopes at a unique time. The geographical origin of mineral or food samples may therefore be determined as well as the age of the samples. An example of this is illustrated in the determination of the provenances of a range of wines by Horn *et al.* [122]. The movement of strontium isotopes from rocks and soils into vines, gives wines in each provenance specific strontium ratios. The determination of these ratios enables the provenance of certain wines to be determined and the information can be used to uncover practices such as illegal blending. Horn *et al.* [123] have also determined the habitat of a 'fossil stag's mandible' to be from the site of *Homo erectus heidelbergensis* at Mauer by the use of $^{87}Sr/^{86}Sr$ calculations.

In a typical sample of naturally abundant gypsum ($CaSO_4.2H_2O$), strontium is usually present as a trace impurity. High resolution mass spectrometry can be used to determine the ratio of ^{87}Sr to ^{86}Sr in the rock and the age of the rock can then be calculated. In order to analyse the total concentration of strontium in the rock, however, it must first be separated from the calcium matrix and any rubidium and barium that may be present. More than a 1% impurity of other metal ions could impair the complete ionisation of the strontium in the mass spectrometer. A lengthy wet chemistry method has been described by Horn *et al.* for the isolation of strontium from a stag's mandible fossil [123] and a flow diagram for the procedure is given in

Appendix 1. Ion chromatography, however, offers an alternative and faster approach to this problem.

4.1.2 The Isolation and Determination of Strontium

In dilute solutions, strontium can be separated from other metal ions as a simple ion by cation exchange or, if in the form of a negatively charged complex, by anion exchange. Haddad *et al.* [124] discussed the separation and determination of strontium from alkaline earth metals using a silica based cation exchange column and Gautier *et al.*[125] have reported the separation of strontium from copper and lanthanum, as EDTA complexes, using an anion exchange column. In the presence of a high concentration of calcium, however, the isolation of strontium may not be facilitated using simple ion-exchange methods. Using cation exchange, Mg, Ca, Sr and Ba may be separated in accordance with the hydrated radii of cations, i.e. Mg < Ca < Sr < Ba [126]. Therefore, when Ca is present in concentrations of up to one thousand times in excess of the Sr concentration, not only will the separation be challenged by Ca 'swamping' the sites of exchange for the strontium, but also the strontium peak will fall in the "tail" of the calcium peak [127].

When using chelation ion exchange, stability constants decrease with the increase in crystalline radii of the cations and the resultant elution order is reversed when compared to simple ion exchange, i.e. Mg > Ca > Sr > Ba. In these instances the strontium elutes before the much larger calcium peak and may therefore be isolated. Some highly specific chelating resins for strontium have been prepared from crown

ethers but are costly and their efficiencies can still be affected by high concentrations of competing metal ions [128,129,130]. In addition, the resins were not high performance chelating resins. Jones *et al.* [109] developed a system using a dye impregnated column for the separation and determination of barium and strontium in mineral waters and milk powder. The metal retaining capacity of the columns used, however, is not believed to be high enough to cope with the levels of calcium in gypsum rock samples. By using a similar dye impregnated resin column with a different substrate to obtain a higher metal retaining capacity, the system can be modified to completely isolate strontium from gypsum samples containing high calcium concentrations. The resolution must also be good enough to completely separate strontium from rubidium and barium, which are present at much lower levels and will have a drastic effect on the strontium isotope ratio.

The principal aim of this work is to obtain a strontium aliquot from gypsum rock samples in a form suitable for introduction into a high resolution mass spectrometer, free from rubidium, barium and calcium. In this way, the precise ratio of ^{87}Sr to ^{86}Sr may be obtained and thus the information can be used to calculate the age and/or the source of the minerals. Four gypsum samples from Northern Africa were acquired from a research group in Munich and identified as B5, F5, F6 and G4 according to the area from which the sample of gypsum rock had been retrieved. The rock samples had been homogenised previously and were ready for sample pre-treatment and dissolution.

4.2 Experimental

4.2.1 Instrumentation

The HPCIC system was as described in Section 3.2.1 except that a three way valve was added after the column in order to obtain fractions eluting from the column at the appropriate times. Inductively coupled plasma mass spectrometric determinations were made using a PlasmaQuad II instrument (Fisons, Cheshire, UK). High resolution thermal ionisation-mass spectrometry (TI-MS) was performed by a collaborating research group in the University of Munich (Dept. of Petrology), Germany.

4.2.2 Reagents

The reagents and eluents used in this study are as described in Section 2.2.2 with the exception that 'Aristar' hydrochloric acid, nitric acid and ammonia solutions were used (BDH, Poole, UK).

4.2.3 Samples

A satin gypsum sample (Geology Dept., University of Plymouth) was used for preliminary investigations and method evaluation. Four gypsum samples (crushed and homogenised), namely, B5, F5, F6 and G4 originating from Northern Africa were obtained from a collaborating research group in Munich.

4.2.4 Procedures

Crushed gypsum was dissolved in 25 ml PTFE vials using 1 ml of HCl and 9 ml of distilled de-ionised water (DDW). The vials were placed in a microwave oven at full power, until boiling, in fifteen second cycles. The vial was then sonicated for ten minutes with intermittent shaking and 1 ml of NH_3 was added with DDW to 25 ml. Strontium retention times were determined using the HPCIC system with 100 µl injections of the sample. Dipicolinic acid (2×10^{-3} M), at pH 2, was used to remove calcium from the column between runs. In subsequent injections, the strontium was collected from the column at the calculated time from the three way valve positioned after the column. Water was removed from the vial by vacuum dessication under P_2O_5 and the remaining ammonium nitrate was volatilised in a muffle furnace at 270°C (under cover). The sealed vials were then transported to Munich for analysis by high resolution TI-MS.

4.3 Results and Discussion

The main objective of this work was to obtain completely isolated fractions of strontium from selected gypsum samples. The ratio of strontium isotopes in the fractions could then be determined by high resolution mass spectrometry. The presence of other metal ions, such as barium and rubidium, in concentrations of greater than 1% of the total strontium concentration, could cause ionisation problems of the strontium in the mass spectrometer and lead to erroneous isotope ratio determinations. These interfering metals therefore have to be completely separated from the strontium.

Rubidium, present in the strontium fraction, may also cause problems in mass spectrometric strontium isotope ratio determinations, owing to isobaric interferences. It was therefore required that the eluent volume for each fraction collection was as small as possible in order to reduce effects from background contamination. In addition, the complete removal of the eluent components from the strontium fraction was required before introduction of the strontium into the mass spectrometer.

4.3.1 Choice of chelating column

Owing to the high concentration of calcium in the gypsum samples, a column with a high capacity was required to perform the separation, and effective isolation, of strontium from the other components. When the separation conditions for the strontium were established, the column could then be used to isolate the strontium for collection as fractions in small vials.

Preliminary studies with dye impregnated 20 μm MN200 columns revealed that the phthalein purple column had the highest metal retaining capacity. Previous studies by Paull *et al.* [110] showed that Phthalein Purple also had good selectivity between Sr and Ca compared to Xylenol Orange and Methyl Thymol Blue. From this information, it appeared that the Phthalein Purple column was the most suitable for these particular experiments and it was subsequently utilised in further investigations to establish whether the column possessed the required selectivity between strontium and calcium, barium and rubidium.

4.3.2 Preliminary separation investigations

A 10 cm phthalein purple column, which had previously been prepared using 20 μm MN200, had a measured capacity of 9.9×10^{-2} m moles of Cu(II) per gram of dye impregnated resin. To increase the capacity of the separation column, a 15 cm column was packed with 20 μm MN200 and impregnated with phthalein purple, following the same method for the previous column. However, the expected capacity of approximately 0.14 m moles of Cu(II) per gram of resin for the column was not achieved and, in fact, it was found that only 0.075 m moles of Cu(II) per gram of resin was loaded onto the entire column. For this reason, subsequent investigations were continued with the 10 cm column. It was not clear why there was a difference in capacity between the columns but variations in dye loadings for similarly prepared columns have been described by Paull and Jones [110].

Although the separation of Rb from Sr was extremely important for the investigations, the separation of Sr from the high concentrations of Ca was considered more challenging and was attempted first. A sample of 0.5 g of 'satin' gypsum rock was dissolved in 50 ml of hydrochloric acid solution and the pH neutralised with NH_3, for analysis using this system. The eluent was 0.5 M KNO_3 and 0.1 M HNO_3 which was adjusted to pH 10 with NH_3. It was found that not even a partial separation of strontium and calcium was achieved using the 10 cm column. Even though the measured capacity was lower, a similar separation was attempted using the 15 cm column.

Figure 4.1 illustrates a 100 µl injection of Sr and Ca from the 0.5 g 'satin' gypsum sample using the 15 cm phthalein purple column. The eluent was 0.5 M KNO_3 and 0.3 M HNO_3 which was adjusted to pH 10 with NH_3. The post column reagent was PAR/ZnEDTA with detection at 490 nm. Only part of the Ca peak is shown in order that the Sr peak can be seen more clearly. A baseline separation was not achieved indicating that the high Ca concentration was overloading the column. For this reason, the sample was diluted to half the concentration for the next injection. As Ba is often present in gypsum samples, Ba (5 mg l^{-1}) was also added to the sample since it was necessary to verify that Ba would not elute with Sr. Ba contamination of the system could lead to ionisation problems for Sr in the mass spectrometer. Rb should not pose a significant problem as it should not be retained on the column and thus will elute on the solvent front.

A separation of the further diluted sample, 0.5 g of gypsum in 100 ml, with 5 mg l^{-1} Ba is illustrated in Figure 4.2. The same eluent conditions were used as described for the previous separation. It can be seen that a baseline separation was achieved between Ba and Sr, and the retention times for both Sr and Ca were increased. This may be explained by the lower concentration of Ca not overloading the column as much as in the previous separation and, in this case, Sr was not forced from the column as quickly. Owing to the increase in retention time on the column, the peak was slightly broader than that obtained previously but was still suitable for collection as a fraction without significant contamination from the eluent. In an ideal scenario the strontium peak would be as narrow as possible, therefore less eluent would have to be evaporated from the fraction and background contamination would be minimised.

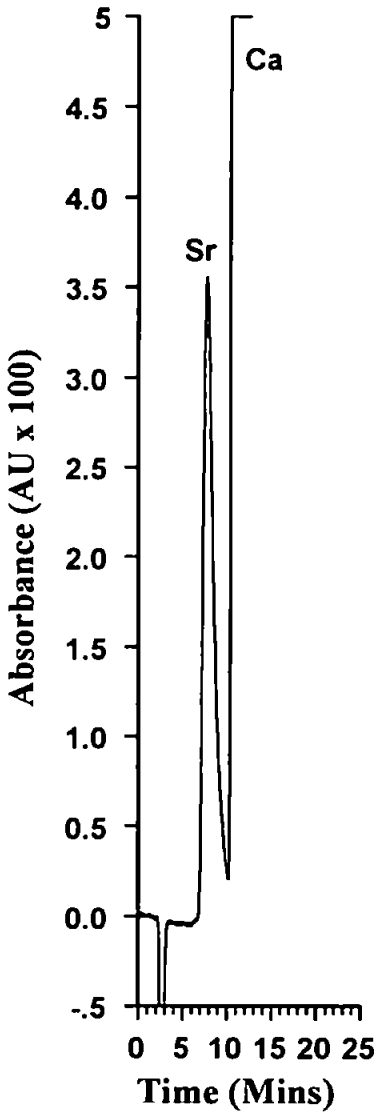

Figure 4.1. A 100 µl injection of 0.5 g gypsum dissolved in 50 ml of acid solution and the pH neutralised with NH_3. The column was 15 cm phthalein purple. The eluent was 0.3 M HNO_3 which was adjusted to pH 10 with NH_3. The post column reagent was PAR/ ZnEDTA with detection at 490 nm.

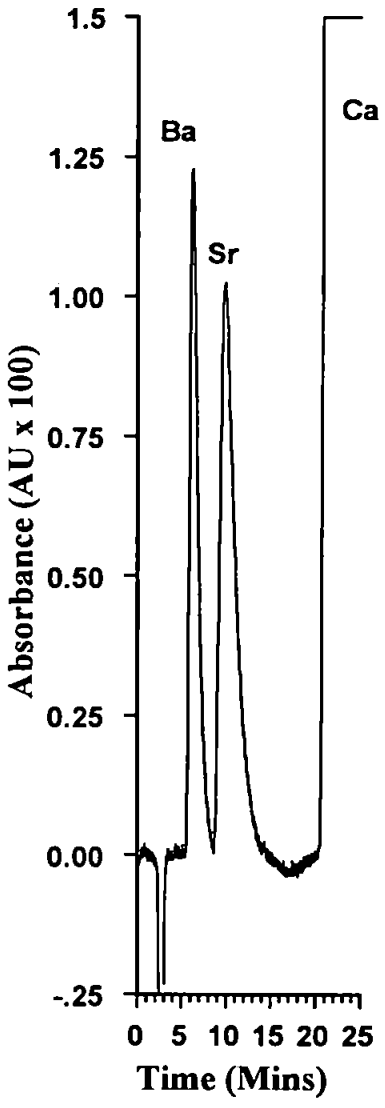

Figure 4.2. 100 µl injection of 0.5 g gypsum dissolved in 100 ml of acid solution and the pH neutralised with NH_3 (5 mg l^{-1} Ba added). The column was 15 cm phthalein purple. The eluent was 0.5 M KNO_3 and 0.3 M HNO_3 which was adjusted to pH 10 with NH_3. The post column reagent was PAR/ ZnEDTA with detection at 490 nm.

4.3.3 Choice of eluent

KNO_3 was present in the eluent in order to saturate any ion exchange sites and to ensure that the separation of metal ions proceeded only via a chelation mechanism. After the isolation of Sr, it was important that all traces of the eluent were removed and the purest possible fraction of Sr obtained. After evaporation of any water from the Sr fraction collection, however, crystals of KNO_3 would cause serious contamination with the mass spectrometric analysis.

The possibility of employing an ammonium nitrate eluent was investigated due to the relative ease of sublimation of ammonium salts. Several factors were assessed concerning the nature of the NH_4^+ ion compared to the K^+ ion. Two considerations led to the conclusion that a high concentration of NH_3 was required to attain similar effectiveness of the NH_4^+ to the K^+ ions; first, NH_4^+ was weaker than K^+ in terms of cation exchange; and second, the amount of NH_4^+ present, relative to the total ammonia concentration at pH 10, was rather small. Figure 4.3 illustrates the pH speciation diagram for NH_3 and NH_4^+. The concentration of NH_4^+ ions at pH 10 is about 15 %. Therefore, the concentration of NH_3 required to give a level of NH_4^+ equivalent to that of 0.5 M K^+ was about 4 M NH_3. For this reason, an eluent of 4 M NH_3, which was adjusted to pH 10 with HNO_3, was prepared for further Sr separations.

Investigations concerning the removal of the ammonium nitrate eluent from column fraction collections were made and it was discovered that, after the water was evaporated from the eluent, the ammonium nitrate crystals could be volatilised in a

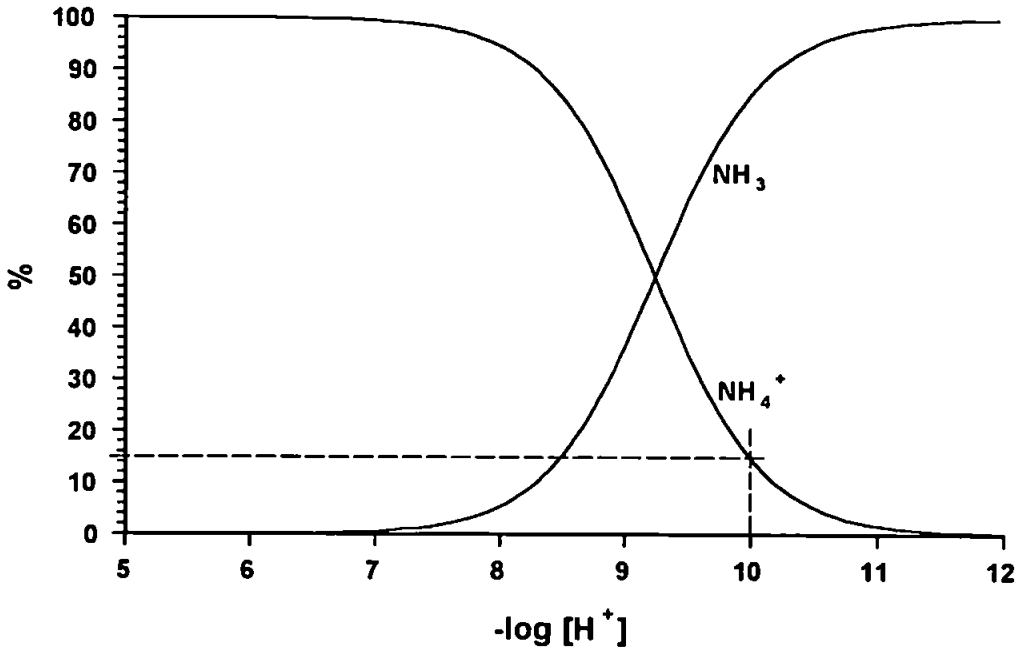

Figure 4.3. A speciation diagram for NH_3 and NH_4^+.

muffle furnace at 270°C. The ammonium nitrate was therefore suitable as an eluent provided that the separation capabilities of the column were not impaired during its use.

A separation using 4 M NH_3, adjusted to pH 10 with HNO_3 eluent, was attempted with the previous sample of 0.5 g gypsum in 100 ml with 5 mg l^{-1} Ba added. Figure 4.4 displays the result of a 100 µl injection of the sample and it is evident that there is an improvement in the resolution of the peaks and a decrease in the retention times for Ba, Sr and Ca. The actual peak heights and areas obtained in the chromatogram are less than those obtained with the previous eluent since the increased concentration of NH_3 suppresses the colorimetric reaction with the PAR/ZnEDTA post column reagent. This was not important, however, as sufficient Sr was present to ascertain the exact place where a column fraction could be taken. Figure 4.5 displays the same chromatogram but with the scale increased in order that a comparison of the Sr and the Ca peaks may be made.

After further sample separations with the 15 cm column, the selectivity ratio of the separations decreased over a period of time. It was thought that the high pH conditions removed some of the loosely bound phthalein purple from the resin, causing a slight decrease in the capacity of the column. Therefore, the 10 cm phthalein purple column was added to the system in line with the 15 cm column, effectively giving a column of 25 cm in length. This measure was used to guarantee complete separation of Sr from Ca. As expected, the resultant retention times were found to increase and the peaks were marginally broader owing to further dead volume in the system. Figure

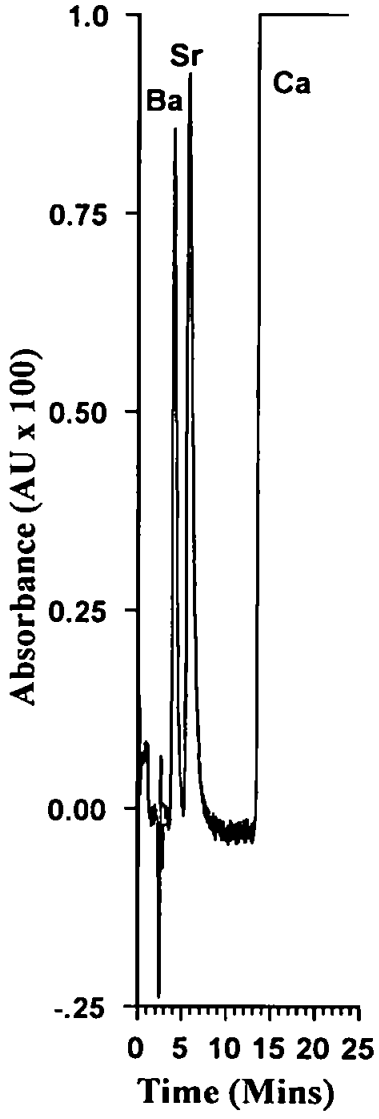

Figure 4.4. A 100 µl injection of 0.5 g gypsum dissolved in 100 ml of acid solution and the pH neutralised with NH_3 (5 mg l^{-1} Ba added). The column was 15 cm phthalein purple. The eluent was 4 M NH_3 which was adjusted to pH 10 with HNO_3. The post column reagent was PAR/ZnEDTA with detection at 490 nm.

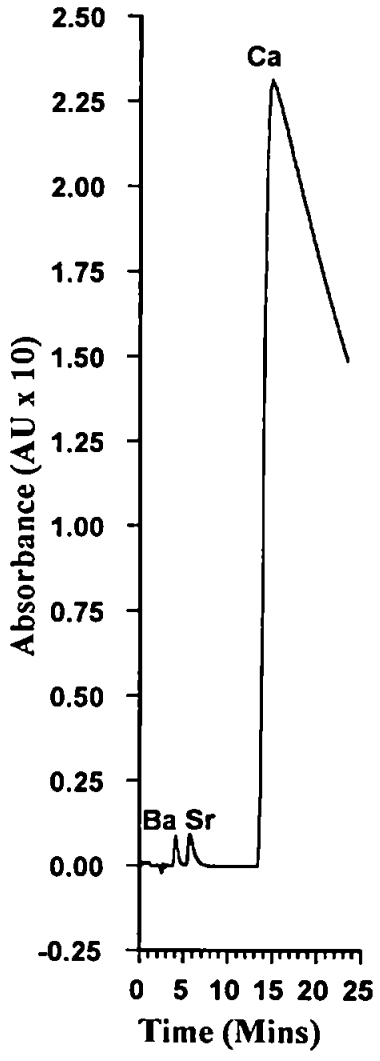

Figure 4.5. A 100 µl injection of 0.5 g gypsum dissolved in 100 ml of acid solution and the pH neutralised with NH_3 (5 mg l^{-1} Ba added). The column was 15 cm phthalein purple. The eluent was 4 M NH_3 which was adjusted to pH 10 with HNO_3. The post column reaction was with PAR/ZnEDTA with detection at 490 nm

4.6 displays a separation with the combined 10 and 15 cm phthalein purple columns using a standard mixture of 2 mg l^{-1} Ba, 5 mg l^{-1} Sr and 5 mg l^{-1} Ca, which illustrates the difference in retention times between Sr and Ca when the system is not partially overloaded. The Ca peak shows slight tailing but the Ba and Sr peaks are fairly symmetrical and well separated. As the concentration of Ca massively increases it reduces the separating power of the column and the retention times of all of the peaks are significantly reduced. There is therefore an optimum total concentration of metal ions where the maximum sample throughput is achieved, whilst maintaining a separation between Sr and Ca. This optimum sample loading was hoped to be sufficient to obtain enough Sr in the Sr fraction collections for MS analysis.

4.3.4 Strontium Isolation From Gypsum Rock Samples

The concentration of Sr in the rock samples had been determined previously by the Munich group using inductively coupled plasma optical emission spectroscopy (ICP-OES) and the results are displayed in Table 4.1. Sample G4 had the highest amount of Sr and B5 the lowest. It was decided that a concentration of 6 g l^{-1} samples of the gypsum samples could be used in the system to yield completely isolated fractions of Sr.

The actual sample volume required for introduction onto the Re-filaments in the mass spectrometer was about 1-3 µl which contains about 400 ng of Sr. It was intended that sufficient Sr would be collected to allow three separate runs on the mass

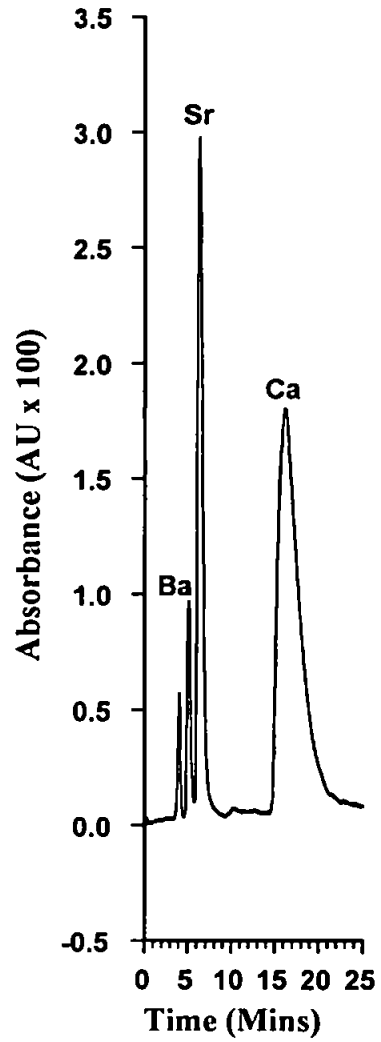

Figure 4.6. A 100 µl injection of 2 mg l^{-1} Ba, 5 mg l^{-1} Sr and 5 mg l^{-1} Ca using the 10 and 15 cm phthalein purple columns. The column was (10 + 15) cm phthalein purple. The eluent was 4 M NH_3 adjusted to pH 10 with HNO_3. The post column reagent was PAR/Zn EDTA with detection at 490 nm.

Sample	Concentration of Sr by ICP-OES $\mu g\ g^{-1}$
B5	**257 ± 35**
F5	**735 ± 35**
F6	**681 ± 35**
G4	**1130 ± 35**

Table 4.1. The concentration of Sr in gypsum samples

determined by ICP-OES

spectrometer requiring that the total collection of Sr was approximately 1.2 μg for each sample.

From the estimated concentrations of Sr in the samples, the number of runs required to give the concentration of Sr, suitable for three separate determinations using the mass spectrometer, were calculated. A specimen calculation for the G4 sample is given below:

Amount of Sr in G4 sample determined using ICP-OES = 1130 μg g^{-1}

Concentration of sample solutions prepared = 6 g l^{-1}

In 1 litre of sample there are (6 x 1130) = 6780 μg of Sr

In 100 μl (injection volume) = 678 ng of Sr

Therefore, for two injections (two runs) = 1.36 μg of Sr

It was found that two runs were required for the G4 sample to ensure a total Sr collection of 1.2 μg (complete recovery of Sr from two 100 μl injections of the 6 g l^{-1} G4 solution would have given 1.36 μg of Sr) and more collections were required for the samples of lower Sr concentration.

Figure 4.7 illustrates the separation of Sr from Ca in the G4 sample. The flow rates for both the eluent and the post column reagent pumps were reduced to 0.5 ml min^{-1} to increase the time period for the Sr fraction collections. The dead time from the end of the column to the detector was measured using a 0.1 M KNO_3 eluent at 270 nm and was found to be 36 seconds. This time was subtracted from the recorded integrator time to give the Sr elution time from the column. In the case of the G4 sample, the Sr

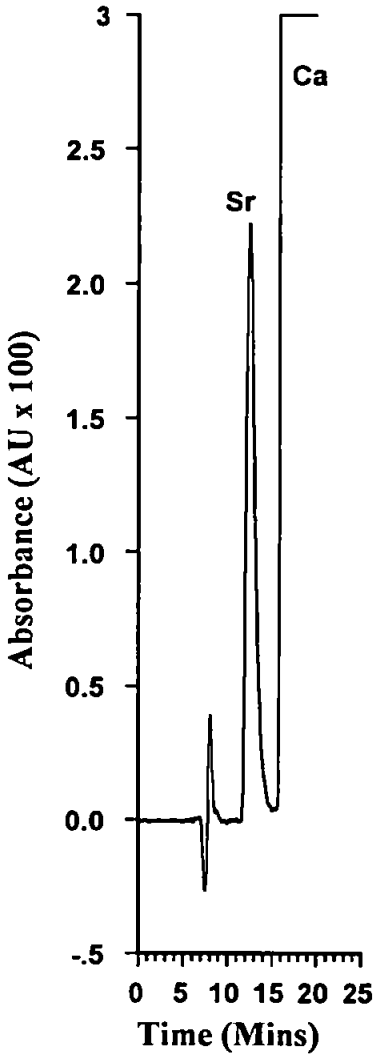

Figure 4.7. 100 µl injection of 6 g l^{-1} G4 gypsum rock sample. The column was (10 + 15) cm phthalein purple. The eluent was 4 M NH_3, adjusted to pH 10 with HNO_3 (eluent and post column reagent pumps at 0.5 ml min^{-1}). PCR was PAR/ ZnEDTA at 490 nm.

peak eluted between 12 and 14 minutes and so, for the next run, the Sr fraction was collected between 11 min.:24 seconds and 13 min.:24 seconds. The Sr fractions were collected in PTFE vials. It was important that there was no overlap with the calcium peak since contamination of the collected fractions could occur. In order to prevent such occurrence, the system was checked between fraction collections for fluctuations in the Sr retention times. However, no significant changes were recorded.

This exact procedure was followed for each of the gypsum rock samples with the lower Sr concentration samples requiring more fraction collections than the higher Sr concentration samples. Since more eluent volume was collected for the lower Sr concentration samples there was the possibility of increased contamination effects. A blank injection of DDW was injected into the system and a blank fraction was collected into a PTFE vial for determination of the level of contamination in the system using the mass spectrometer.

Once the fractions of all the samples had been collected, the water was evaporated by placing the open PTFE containers in a vacuum dessicator overnight in the presence of P_2O_5. This measure prevented any 'spluttering', and thus loss of sample, by rapid drying in an oven or furnace. Once the water was removed from the fractions, the samples were placed in a muffle furnace at 270°C to volatilize the ammonium nitrate. The ammonium nitrate left the PTFE vials as a dense white vapour and the samples were therefore clear when the sublimation was complete. The PTFE vials were placed in the furnace under a glass cover, with an outlet on top of the vessel which faced down, to prevent any dust entering the vials which could cause contamination (Figure

4.8). In addition, the eluents were prepared in laminar flow cabinets and all containers were sealed to ensure background contamination levels were kept at a minimum. The HPCIC system was utilised in standard laboratory conditions but atmospheric contamination was not believed to be a problem since the system was totally enclosed.

Two Sr fractions from the F6 gypsum rock sample were collected. One of the fractions had the eluent removed to yield only the Sr nitrate. The other fraction was left in the eluent and the levels of contamination were examined using ICP-MS. The results obtained by ICP-MS for the F6 fraction showed that the levels of Ba and Rb were below the detection limit of the instrument and were therefore effectively isolated from the Sr. The results for Ca, however, were erratic. Ca determinations can be problematic owing to isobaric interferences with regard to the most common isotope (^{40}Ca). A fairly high level of Ca, i.e. about 1.4 mg l^{-1} (in the 3 ml sample) was recorded. It was believed that Ca in the eluents were the cause of this and it was decided that the collected fractions should be passed through the HPCIC system again, before their introduction into the high resolution mass spectrometer.

Sr nitrate, prepared from each of the fractions collected, was very soluble in water, but to ensure maximum dissolution the samples (including the blank sample) were heated in a microwave with approximately 1 ml of 0.1 M HNO_3. A similar chromatographic system was used as for the previous fraction collection procedures, but the whole sample was injected by means of a 1 ml sample loop instead of the 100 µl injection. In an attempt to reduce the contamination effects the eluents used in this repeat experiment were of 'Aristar' grade instead of 'Analar'.

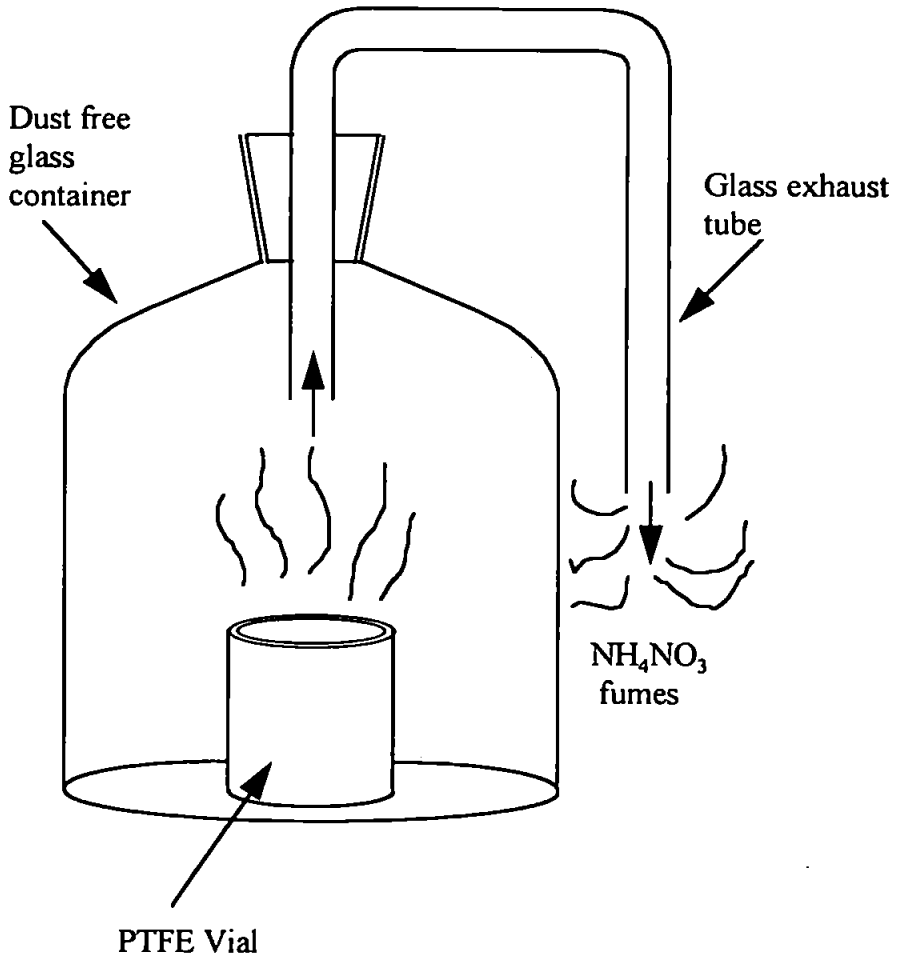

Figure 4.8. The glass cover used to protect the PTFE vials from contamination in the muffle furnace.

The Sr fractions were again collected in their respective PTFE vials and the eluent was removed by dessication followed by sublimation, as before. These samples were then in a form suitable for introduction into the high resolution mass spectrometer. The mass spectrometric analyses of the samples were performed in Munich. Table 4.2 compares the results of the Sr isotope ratios from the fractions isolated using HPCIC with the ratios found using the Munich laboratory's original (more laborious) method for Sr isolation. The results compare well, although slight differences in the values may indicate that there was possible heterogeneity of the samples. It is likely that if high purity reagents had been used initially, the second series of fraction collections using the HPCIC system would not have been necessary. The eluent fraction (blank) collected for the mass spectrometric determination of Sr in the eluent (6.55 ng) was slightly higher than normally found by the classical method, but did not appear to affect the results significantly.

4.4 Summary

The phthalein purple impregnated columns were found to be suitable for separating, and isolating traces of Sr from much higher concentrations of Ca. There was a minor problem with the capacity of the 15 cm column becoming reduced over time but this did not significantly affect the separation ability of the column. The ammonium nitrate eluent system proved to be successful and was easily removed from the Sr. One major problem with the method was contamination in the eluents. This was overcome by using higher purity eluents and, it should be noted that only one isolation step of the Sr would have been required if these eluents had been used for the first collections. There is room for further improvement in the system and the most obvious change

Gypsum Sample	$^{87}Sr/^{86}Sr$ New	Error (±)	Sr Conc. (μg)	$^{87}Sr/^{86}Sr$ Old	Error (±)
B5	0.709086	0.000011	0.327	0.708703	0.000016
F5	0.707275	0.000015	1.10	0.707204	0.000011
F6	0.707331	0.000009	1.78	0.707246	0.000014
G4	0.709125	0.000012	1.31	0.709177	0.000011

Table 4.2. Results obtained from the high resolution mass spectrometer. The old method was a classical wet chemical method while the new method used HPCIC.

would be to use larger diameter columns which would cut down on the number of fraction collections and therefore further reduce potential contamination. As mentioned previously, the results obtained from the high resolution mass spectrometer were reasonably consistent with the Munich group's method, displaying good potential for the system, not only for the separation of Sr from Ca in gypsum rocks but, also in other matrices such as wines, milk and mineral waters.

CHAPTER 5 - The Determination of Trace Bismuth in Lead

5.1 Introduction

5.1.1 Properties of Bismuth

Bismuth is a brittle, diamagnetic, reddish-white metallic element with interesting physical properties [131]. It is considered to be the poorest conductor of all metals and, unlike most metals, expands on solidifying from the melt. The major isotope of bismuth is ^{209}Bi, although several other isotopes occur as daughter products in the decay chains of uranium and thorium. In the environment, Bi is found in basaltic and granitic rocks in typical concentrations of 2×10^{-3} μg g^{-1} and 10^{-2} μg g^{-1} respectively [132]. The concentration of Bi in ocean water is 2×10^{-5} μg g^{-1} [132,133].

Bismuth occurs naturally as the basic oxide Bi_2O_3 in sulphide ores or in secondary alteration products of sulphides and related compounds. The oxide is reduced by carbon, after roasting, to form the elemental bismuth. Bismuth is a by-product of lead refining and is also obtained from the anode sludge produced during the electrorefining of copper [131]. Commercial ore minerals of bismuth are native bismuth, bismuthinite (the most important hydrothermal mineral of bismuth) and bismuth ochre.

Bi metal will readily dissolve in 6 M HNO_3 but, not in HCl:

$$Bi_{(s)} + 6\ H^{+}_{(aq)} + 3\ NO_3^{-}{}_{(aq)} \leftrightarrow Bi^{3+}_{(aq)} + 3NO_{2(g)} + 3H_2O$$

In aqueous solutions, bismuth favours the +3 oxidation state and rarely occurs in the +5 state. The metallic ion exists only in strong acidic solution; in water it will hydrolyse to form an insoluble basic salt:

$$Bi^{3+}_{(aq)} + Cl^{-}_{(aq)} + H_2O \leftrightarrow BiOCl_{(s)} + 2\ H^{+}_{(aq)}$$

Solutions containing Bi(III) ions are therefore kept in acidic conditions to keep the cations from precipitating. In the presence of halides, however, stable complexes such as $BiCl_4^-$ may be formed.

There is no evidence for the simple bismuth aquo ion $[Bi(H_2O)_n]^{3+}$. In neutral perchlorate solutions, the main species is $[Bi_6O_6]^{6+}$ or its hydrated form $[Bi_6(OH)_{12}]^{6+}$ and, at higher pH, $[Bi_6O_6(OH)_3]^{3+}$ is formed. The $[Bi_6(OH)_{12}]^{6+}$ species contains an octahedron of Bi^{3+} ions with an OH^- bridging on each edge [134].

Bismuth is of interest because it is one of the few metals which expands on solidification. It is used in the manufacture of fusible alloys, for example in Rose's alloy (50% bismuth, 28% lead and 22% tin; m. p. 100°C) and Wood's alloy (50% bismuth, 24% lead, 14% tin and 12% cadmium; m. p. 71°C). Owing to its expansion properties, bismuth alloys have been developed for dental amalgams and for setting process tools in their holders [135].

Although bismuth has many important applications, perhaps a more important concern is the problems that bismuth can cause when present in lead. Bismuth is considered a

major impurity, particularly in Canadian lead ores [136]. Other metals present in lead ores e.g. zinc and copper can be removed by flotation, smelting and refining procedures, but bismuth is harder to remove owing to its lead-like properties. Electrolytic procedures are available for the removal of bismuth from lead [136], but recent developments have used the introduction of magnesium-calcium alloys (Mag-Cal™) into a vortex of lead at 480 - 500°C [137]. There is therefore a requirement to monitor the concentration of trace amounts of bismuth in high concentrations of lead.

An area where bismuth determination is of crucial importance is in the development of lead-lithium alloys as a source of tritium for use in future power stations [138]. Pb-17Li (83 atomic % lead and 17 atomic % lithium) serves as a stable source of lithium for the production of tritium by neutron bombardment. However, trace bismuth present in the lead and bismuth, produced during the decay of lead isotopes, could lead to the production of radioactive polonium:

$$^{208}Pb \xrightarrow{n,\lambda} {}^{209}Pb \xrightarrow{\beta^-} {}^{209}Bi \xrightarrow{n,\lambda} {}^{210}Bi \xrightarrow{\beta^-} {}^{210}Po$$

Bismuth must therefore, be continuously separated from the Pb-17Li and an assay of bismuth is required for small amounts of the blanket material.

Another important requirement for the determination of trace bismuth in high concentrations of lead is in the area of forensic chemistry. A lead shotgun pellet consists of 95-99% lead and 1-5% antimony is added to harden the pellets. However, lead pellets from different origins have been found to have different concentrations of

trace elements present e.g. bismuth. It may therefore be possible to determine the source of the pellets by determining the concentration of trace metals present in a pellet recovered from the scene of a crime [139].

5.1.2 The Determination of Trace Bismuth In Lead

The determination of certain trace metals in complex matrices may present problems for the analytical chemist in terms of attaining the required limits of detection and the resultant interferences that may occur. This problem is particularly difficult when the matrix contains massive amounts of major metals. The determination of bismuth in lead is a good example of this, as previously mentioned. In this instance some analytical methods require the removal of the lead matrix prior to bismuth analysis. Suzuki *et al.* [139] reported the determination of bismuth in lead shotgun pellets using ICP-MS where the lead matrix was eliminated as a lead sulphate precipitate in order to avoid isobaric interferences. This approach, however, can be time consuming and there is a possibility of entrainment effects, resulting in poor analytical recovery. A classical spectrophotometric method has also been described for the determination of bismuth in lead as an iodide complex, but again the matrix is removed before the analysis to prevent the formation of a heavy precipitate of lead iodide [140]. Judex *et al.* [138] developed a stripping voltammetric procedure for the study of bismuth in lead lithium alloys. In the method described, the lead matrix appeared to have no affect on the bismuth determination, but copper present in concentrations of greater than 140 times results in a significant interference effect.

High performance chelation ion chromatography (HPCIC) offers an alternative approach for the determination of bismuth in lead. Simple ion exchange columns would be 'swamped' by the lead matrix leaving little capacity to separate the bismuth. However, chelating ion exchange has the potential to separate several metal ions from much greater concentrations of other metals and, in this case, trace amounts of bismuth need to be separated from very high concentrations of lead. The selectivity of the column does not have to be too great since there is a large difference in potential chelating properties between bismuth and lead. This is largely due to the fact that lead is present as a divalent ion and bismuth is trivalent. In general, the conditional stability constants for trivalent metal ions are much greater than those for divalent ions and separations between them may be easily achieved.

The main aim of this study was to develop an HPCIC system for the determination of trace bismuth in lead. A suitable chelation separation column is required prior to spectrophotometric detection of the bismuth species. Rapid analysis times and low detection limits for bismuth are required to make the system viable for routine analysis. The system will also need to be tested for reproducibility and reliability.

5.2 Experimental

5.2.1 Instrumentation

The HPCIC system used was as described in Section 3.2.1 except that, for the halide work, no post column reagent pump was required.

5.2.2 Reagents

The reagents used were as described in Section 2.2.2 except that hydrobromic acid (48%) (Aldrich, Milwaukee, USA) and hydrochloric acid (BDH, Poole, UK) were also used as eluents. Bismuth standards were prepared in 0.1 M 'AnalaR' nitric acid (BDH,) by serial dilution of a commercially prepared 1000 $\mu g\ ml^{-1}$ bismuth nitrate standard (BDH). A Xylenol Orange (2×10^{-4} M) post column reagent was also used (detection at 565 nm).

5.2.3 Sample Preparation

Lead pellets (1 g, CRM 288B, BAS) were dissolved in 10 ml of 12.5 M nitric acid on a hotplate and diluted to 50 ml. 10 ml aliquots of the solution were diluted further to 100 ml with concentrations of 0.5, 1.0 and 1.5 $\mu g\ ml^{-1}$ of bismuth added respectively to three of the four samples as part of a standard addition procedure.

5.3 Results and Discussion

5.3.1 Choice of column

Since bismuth is present as Bi(III) in acid solutions, as is the case for most trivalent metals, it forms very strong complexes with some chelating groups. From determinations of stability constants of EDTA complexes in 1 M $NaClO_4$ at 25°C using voltammetry, for Bi the log K_1 value = 26.41 and for Cu, log K_1 = 17.28 [141]. The formation of very strong complexes can lead to metal ions being eluted from a chelating column as a very wide band owing to the slow kinetics involved with chelation. Preliminary investigations for the determination of bismuth were therefore performed on a column impregnated with a triphenylmethane based dye with relatively weak chelating functional groups. The dye was aurin tricarboxylic acid (Aluminon), impregnated onto MN200 with a mean particle size of 20 µm, after packing in a 10 cm PEEK column. The capacity factors for three metals with the Aluminon column and the structure of the dye have been described previously in Chapter 3.

After testing the Aluminon column with various eluents, a suitable retention time for bismuth (III) was obtained for an eluent comprising 0.2 M HNO_3 and 0.5 M KNO_3. The bismuth peaks were considered too broad, however, and the column was deemed unsuitable for further investigations. Figure 5.1 illustrates the chromatogram for a 100 µl injection of a 100 mg l^{-1} Bi standard using the Aluminon column with the eluent described. The post column reaction was with Xylenol Orange and detection was at 565 nm. The peak was more than ten minutes in duration and was tailing badly with a

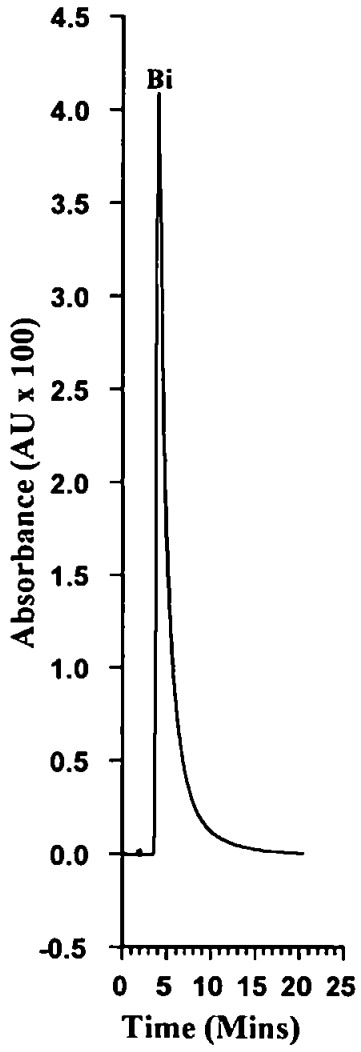

Figure 5.1 100 µl injection of 100 mg l^{-1} Bi using the 10 cm Aluminon column. The eluent was 0.5 M KNO_3 with 0.2 M HNO_3. A Xylenol Orange post column reagent was used with detection at 565 nm.

high degree of asymmetry. This seemed typical of the behaviour of bismuth on chelating columns, as described by Jones and Schwedt [101].

Similar eluent and post column detection conditions were used for a 10 cm Phthalein Purple coated MN200 column (also described in Chapter 3). Figure 5.2 displays the chromatogram for a similar injection of 100 mg l^{-1} Bi. Although the peak was slightly more symmetrical than the peak for the Aluminon column, it was far broader. The Phthalein Purple column was therefore also regarded as unsuitable for further investigation. The difference in the adsorption behaviour of the Bi(III) between the two columns is due to the fact that Aluminon is a O,O chelator whereas Phthalein Purple is a N,O chelator.

Previous investigations (discussed in Chapter 3) revealed that the bare MN200 column had some form of metal adsorbing capacity. The capacity factors of the unmodified resin were lower when compared to the dye impregnated resins. It was believed that weaker complexes of the Bi(III) with bare MN200 may improve the kinetics of the system and sharpen peak shapes. It was therefore decided that the affinity of bismuth for the bare MN200 column should be tested since the performance of the dye impregnated columns with Bi(III) was poor. A 5 cm column of 20 µm MN200, which had already been prepared and utilised in the k' investigations in Chapter 3, was tested with a 100 µl injection of the 100 mg l^{-1} Bi standard. The 0.2 M HNO_3 with 0.5 M KNO_3 eluent was used with the Xylenol Orange post column reaction system described previously.

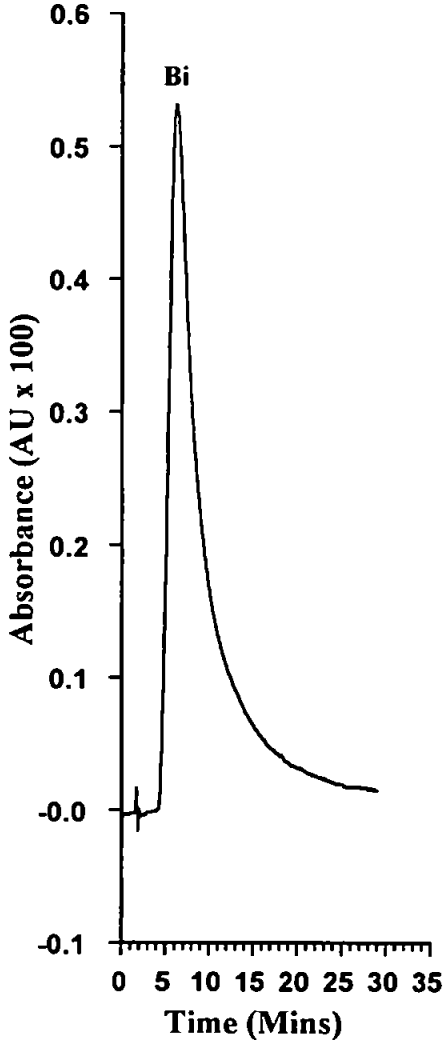

Figure 5.2 100 µl injection of 100 mg l^{-1} Bi using the 10 cm Phthalein Purple column. The eluent was 0.5 M KNO_3 with 0.2 M HNO_3. A Xylenol Orange post column reagent was used with detection at 565 nm.

Figure 5.3 displays the first chromatogram recorded for a 100 µl injection of 100 mg l^{-1} Bi using an MN200 column and the results were far more impressive than previously obtained using the dye impregnated substrates. The peak width was less than that of the other columns and thus peak height was improved which would aid in improving the detection limit for Bi. An important feature of the MN200 column compared to the other columns, however, was that it was very stable in strong acid solutions, which were required owing to the high stability constants for Bi. With the dye impregnated columns there was a possibility of the dyes bleeding from the columns or becoming denatured when exposed to strong acids for extensive periods of time. Therefore, from the positive information obtained, it was apparent that the MN200 column was suitable for further investigation for the determination of trace bismuth in lead.

5.3.2 Post Column Reaction Detection of Bismuth

Previous investigations using dye impregnated chelating columns have incorporated chelating dyes in post column reactions for spectrophotometric detection of the eluted metal components, as mentioned in Chapter One. It was therefore considered that this procedure would also be suitable for the bismuth investigations, utilising Xylenol Orange as the post column reagent. The main problem with the system was that the use of acid eluents requires that Xylenol Orange be buffered in order to produce a colourimetric reaction with the bismuth. Owing to the high strength of the acid, however, it was difficult to obtain the optimum pH (about pH 2 to 3) of the reaction and ammonia was added to counteract eluents of increased acid strength.

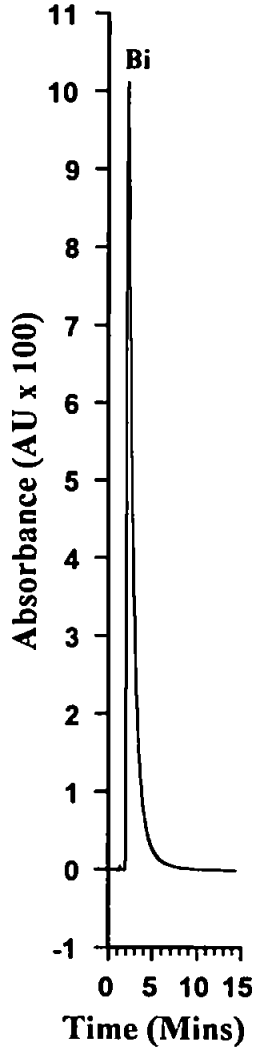

Figure 5.3. A 100 µl injection of 100 mg l^{-1} Bi using the 5 cm MN200 column. The eluent was 0.5 M KNO_3 and 0.2 M HNO_3 with Xylenol Orange detection at 556 nm.

Preliminary investigations were performed using the Xylenol Orange post column reagent system, using detection at 556 nm. The 5 cm MN200 column was utilised to test the system, for a separation of 1 mg l^{-1} Bi from 100 mg l^{-1} Pb. An eluent of 0.5 M KNO_3 and 0.05 M HNO_3 was used. Figure 5.4 illustrates that there was no interference from the 100 mg l^{-1} Pb, however the Bi peak was broad and the sensitivity for Bi was too low. Xylenol Orange solutions were analysed at pH 2 and pH 3 using UV/VIS spectrophotometry and the results indicated that the background absorbance from the dye alone was very low. However, since the absorbance with the Bi complex was also low, the baseline for the chromatogram was poor. The results obtained indicated that the detection limits for Bi, from the MN200 column with Xylenol Orange post column reaction system, were too high and that optimisation of the system would not yield significant improvement. The possibility of the use of a different detection system for Bi was therefore considered.

5.3.3 Separation and Determination of Bismuth as Halide Complexes

Studies in the literature have already determined that Bi may be detected as an iodide complex for spectrophotometric detection [140]. A problem with the method is that chloroform is used to remove the bismuth as cupferrate (N-nitroso-N-phenylhydroxylamine) from the lead matrix, owing to the insolubility of lead iodide. It was considered that, if a smaller halogen ion was used to complex with Bi, the formation of a Pb precipitate could be avoided.

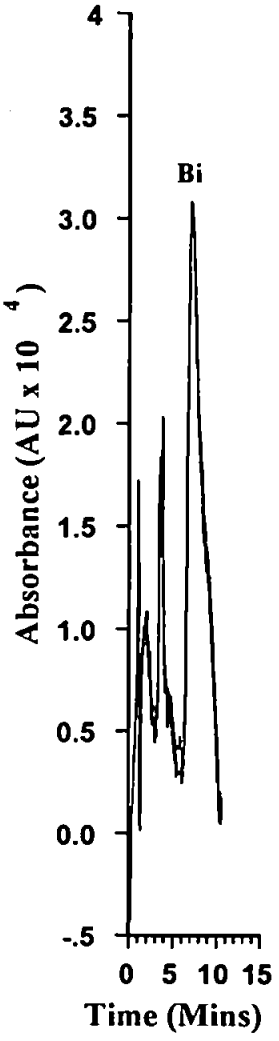

Figure 5.4 100 µl injection of 1 mg l^{-1} Bi and 100 mg l^{-1} Pb using the 5 cm MN200 column. The eluent was 0.5 M KNO_3 and 0.05 M HNO_3. Post column reaction was with Xylenol Orange at approx. pH 2 (detection at 556 nm).

Sandell and Onishi [142] reported that chloride and bromide may also be used to form complexes with Bi, which can then be detected by UV/Visible spectrophotometry. The sensitivity of the complexes varies with the halide concentrations, with high halide concentrations enabling the greatest sensitivity. It was therefore possible that, by using an eluent of either hydrochloric or hydrobromic acid, the need for a post column reaction detection system would be eliminated. A single pump system could be used and time would also be saved in reagent preparations. In effect, hydrobromic acid may be used for both elution and detection of Bi.

Figure 5.5 displays the sensitivity indexes, *S*, of bromide and chloride complexes in the far UV region of the electromagnetic spectrum for Bi, along with a range of other metals. The sensitivity indexes ($\mu g\ cm^{-2}$) indicate the amount of metal required to obtain a complex with an absorbance of 0.01.

Figure 5.6 displays the speciation curves for bromide and chloride complexes of bismuth for a ligand to metal concentration of up to 5000, based on stability constants obtained using similar conditions [141]. It is clear that the predominant species at the high level ratios are the $BiBr_6^{3-}$ and $BiCl_6^{3-}$ complexes. In the following investigations, the high acid eluent conditions used meant that the ligand to metal concentrations were far in excess of 5000 times and it was safe to assume that the major species of bismuth present were the octahedral $BiBr_6^{3-}$ and $BiCl_6^{3-}$ complexes. Table 5.1 displays data for the overall stability constants ($\beta 6$) for the aforementioned complexes and it is apparent from these values that the bromide complexes are stronger than the respective chloride complexes. Since the halogen complexes of Bi(III) will be competing with the

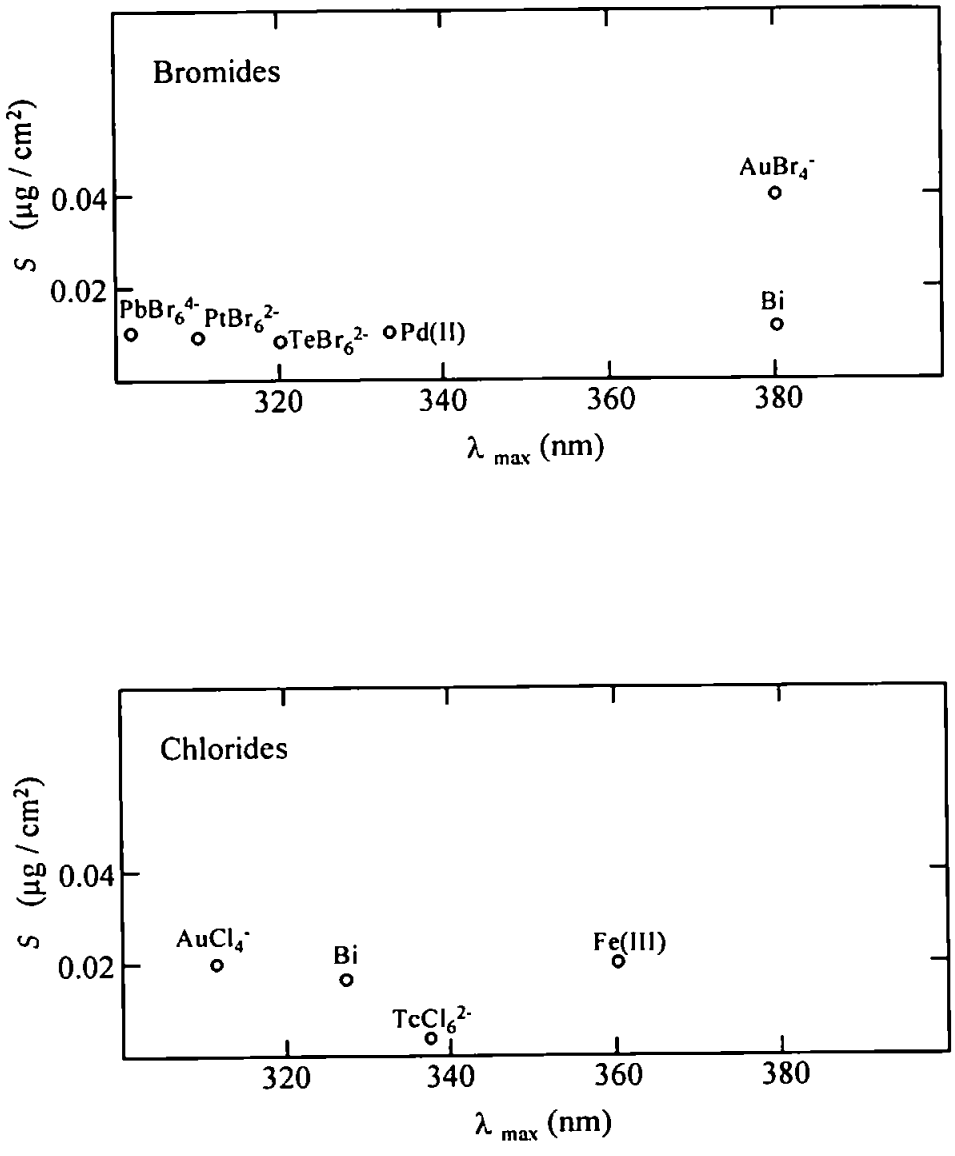

Figure 5.5. The sensitivity indexes, *S*, of chloride and halide complexes for bismuth and a range of other metals.

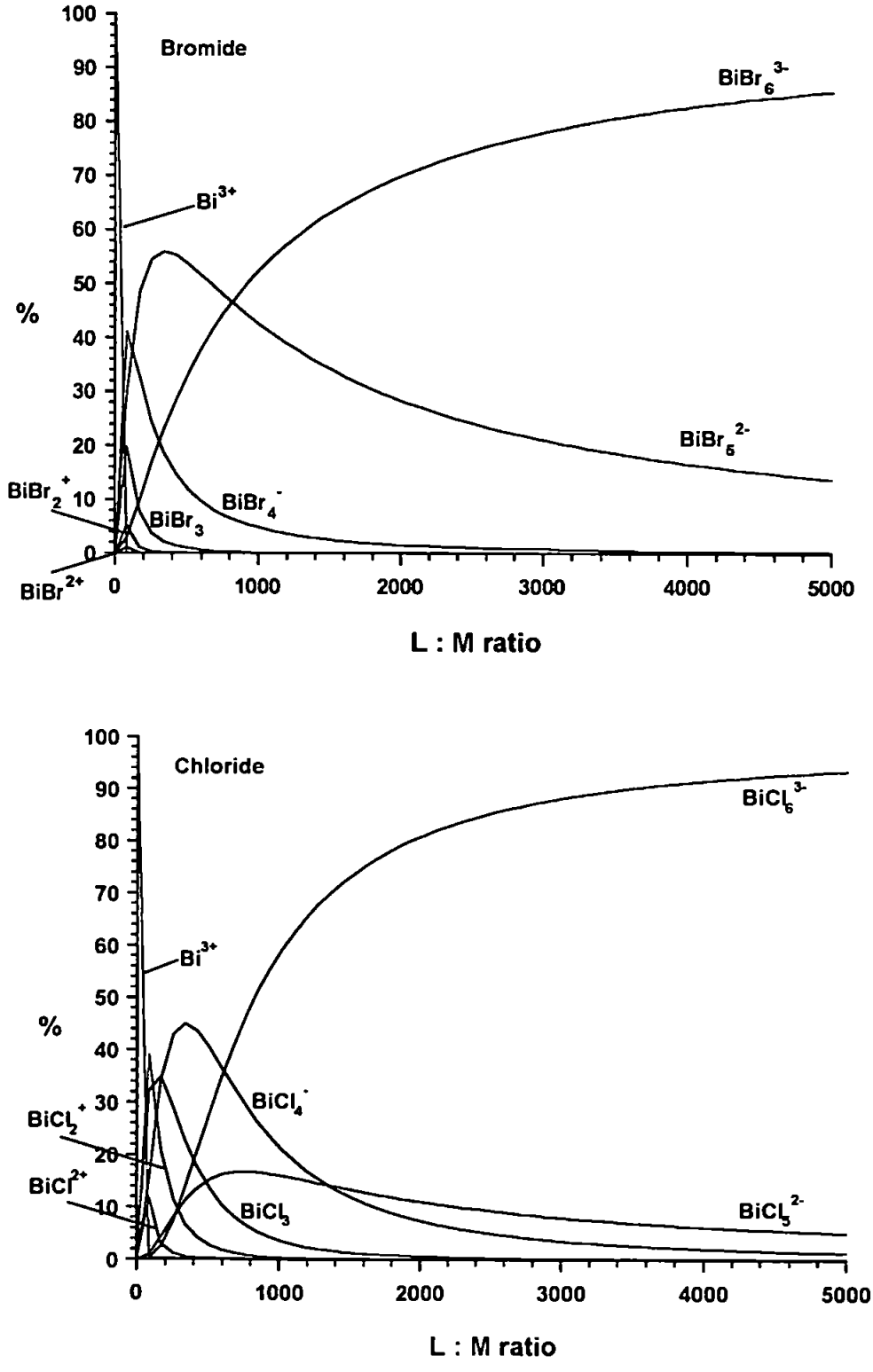

Figure 5.6. Bismuth speciation diagrams for bromide and chloride complexes.

Temperature (°C)	Concentration $NaClO_4$, M	β_6 (Overall formation constants for BiX_6^{3-}) X = Br	X = Cl
25	0.50	8.34*	6.68‡
25	3.0	9.75†	-
20	3.0	-	6.56*

Table 5.1. A comparison of the overall formation constants for bromide and chloride complexes of bismuth determined in a perchloric acid medium [141]. The methods of determination were: * specific ion EMF measurements, † glass electrode and ‡ ion selective electrode.

chelating groups on the column, it would appear that a lower concentration of hydrobromic acid eluent would be required, compared to the concentration of hydrochloric acid, to give the same retention time. An important consideration was that the concentration of halide must be as high as possible in order to obtain the optimum sensitivity. Subsequently, initial investigations were performed using hydrochloric acid.

5.3.3.1 Hydrochloric acid investigations

From the data reported by Sandell and Onishi [161], Au(III) and Tc(IV) chloride complexes may cause interference at 325 nm, but were unlikely to be present and should not co-elute with Bi(III). A preliminary investigation using a 6 M hydrochloric acid eluent was made with detection at 325 nm. Figure 5.7 displays a 100 µl injection of a 1 mg l^{-1} Bi standard using the system described. There was a large solvent disturbance, in relation to the size of the Bi peak. The Bi peak was affected by the solvent disturbance, but this could be prevented by lowering the concentration of the eluent which would, in turn, increase the retention time of the Bi peak. The signal to noise ratio was much improved in comparison to the Xylenol Orange system. One reason for this was that the dead volume after the column was reduced and, in addition, there was no dilution of the eluent which occurs with a post column reaction system.

After testing the system with a series of different concentrations of HCl, it was found that an eluent of 0.6 M HCl gave the optimum concentration for Bi elution from the

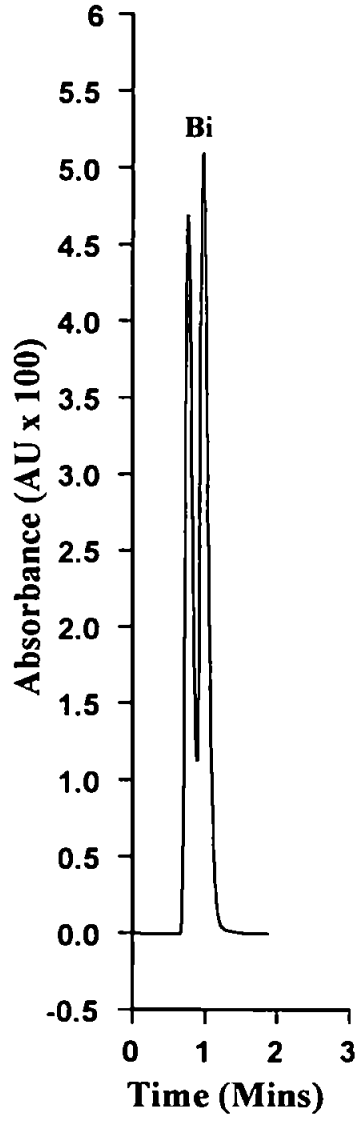

Figure 5.7 A 100 µl injection of 1 mg l^{-1} Bi with the 5 cm MN200 column.

The eluent was 6 M HCl with detection at 325 nm.

column i.e. the Bi peak was eluted slightly after the solvent front and was thus free of disturbance. Figure 5.8 displays the chromatogram for a 100 µl injection of 1 mg l^{-1} Bi into the system with an eluent of 0.6 M HCl. However, sensitivity of the system for Bi was greatly reduced in comparison to the 6 M HCl system and the peak was broader with the 0.6 M HCl eluent. The lack of sensitivity may be explained by the decrease in chloride concentration, and thus a lower concentration of the $BiCl_6^{3-}$ complex, which appears to responsible for the absorbance at 325 nm. The increase in broadness of the peak may be explained by an increase in retention time, which was a result of lower acid concentration and less competition from the halide complexes in the eluent. Nevertheless, the sensitivity was still much better than that of the Xylenol Orange post column reaction system. With the Xylenol Orange system, a 100 µl injection of a 1 mg l^{-1} standard gave a peak height of about 3×10^{-4} Absorbance units, whereas, with the halide system, a peak height of about 3×10^{-3} Absorbance units was obtained.

In order to obtain a peak for Bi retained just after the solvent disturbance, a compromise had been made with regard to the sensitivity of the system. It was considered that a possible solution to this problem could be the use of gradient elution of Bi from the column. By using a low concentration of HCl, the residence time of Bi on the column would be longer and then a high concentration of HCl could be used to 'sweep' the Bi from the column with an increase in sensitivity. A number of different eluent combinations were attempted e.g. 0.1 M HCl to 3 M HCl, but in each case there was a steep drop in the baseline making quantification of the peak more difficult and there was no significant increase in sensitivity. It was therefore decided that the

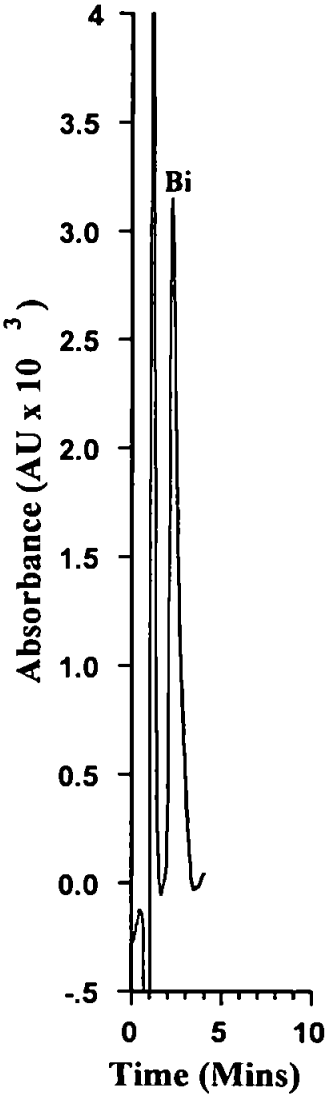

Figure 5.8. A 100 µl injection of 1 mg l^{-1} Bi with the 5 cm MN200 column.

The eluent was 0.6 M HCl with detection at 325 nm.

isocratic elution of Bi from the 5 cm MN200 column, using the 0.6 M HCl eluent was the best approach and should be evaluated with the lead samples.

A 1000 mg l^{-1} lead standard was spiked with 1 mg l^{-1} Bi and a 100 µl injection was made into the system with a 0.6 M HCl eluent. Pb was not detected at 325 nm and thus did not interfere with the Bi peak. However, after a series of UV/Visible spectrophotometric investigations with the eluent and samples to check for any components which could interfere at 325 nm, nitrate was found to be weakly absorbing in this region. Since concentrated HNO_3 was to be used to digest the lead samples, further investigations were made. 100 µl injections of 0.1 M HNO_3 were made using the 0.6 M HCl eluent with detection at 325 nm. Large peaks were obtained for the nitrate, which could overlap with bismuth peaks. Therefore, before proceeding further with the digested lead samples, a different elution system needed to be investigated. A consideration of the halide data given by Sandell and Onishi [161] indicated that HBr may be a better alternative for this particular application.

5.3.3.2 Hydrobromic acid investigations

The detection of the bismuth chloride complex at 325 nm was strongly affected by the presence of a high nitrate concentration (from the sample) which was absorbing in the same region. The detection of a bismuth bromide complex, at 380 nm, was therefore more favourable, as it was free from nitrate interference. It appeared from stability constant data, however, that bromide complexes more strongly with Bi than chloride. There was concern that Bi would elute from the column at a lower acid concentration

causing a loss in sensitivity. Figure 5.5 illustrates that the [$AuBr_4^-$] complex was the only metal complex which could interfere with the Bi. However, the sensitivity was very weak in comparison to the Bi complex, similar elution times were very unlikely and the species was not present in the lead system investigated. There was another absorption peak for the Bi bromide complex which could be detected at 220 nm but this would have been 'swamped' by absorption from the nitrate.

Preliminary investigations with the 5 cm MN200 column used an eluent of 0.25 M HBr with detection at 380 nm. A 100 µl injection of a 5 mg l^{-1} Bi standard was made and there was no sign of any peaks. The column was removed and a similar injection was made resulting in a very large peak. This confirmed that the HBr was reacting with the Bi, producing complexes which could be detected at 380 nm. The MN200 column was replaced and the eluent concentration was increased to 0.6 M HBr. After a 100 µl injection of 10 mg l^{-1} Bi, a peak with a retention time of about 10 minutes was obtained. This meant that, although the HBr was a stronger complexing agent than HCl, the retention time of Bi was longer with HBr than for a similar concentration of HCl. This was the opposite effect to what was previously thought to occur when considering stability constant data. An increase in concentration of hydrobromic acid would be beneficial as the sensitivity of bismuth halide complexes increases with the concentration of Br^-. The HBr concentration was increased further to a concentration of 1.8 M HBr but not greater than 1.8 M since there was concern regarding the long term effect of high acid concentrations on the eluent pump. After a long period of use, there was no deterioration in the behaviour of the pump (PEEK).

Figure 5.9 illustrates a 100 µl injection of 10 mg l^{-1} Bi with an eluent of 1.8 M HBr and detection at 380 nm. The chromatogram indicated that the sensitivity is higher with the 1.8 M HBr eluent than with the HCl and much higher than for the Xylenol Orange post column reaction system. The same injection of 10 mg l^{-1} Bi was made and chromatograms were obtained for different wavelengths. It was found that the optimum wavelength for the Bi was 370 nm and all further investigations were to be made using 370 nm detection. Since the sensitivity changed with varying concentrations of HBr it was also necessary to examine the linearity of the system for different concentrations of HBr.

5.3.3.3 Linearity of the system

A range of bismuth standards from 40 µg l^{-1} to 2 mg l^{-1} were prepared and 100µl injections were made to test the linearity of the detection system. The eluent was 1.8 M HBr with detection at 370 nm. Figure 5.10 displays the chromatogram for a 100 µl injection of 200 µg l^{-1} Bi. The standards were injected twice and a calibration curve was plotted from the peak areas (Figure 5.11). The correlation coefficient, r = 0.99991 for the calibration indicated that the system was linear up to 2 mg l^{-1}, although the determinations made at 40 µg l^{-1} were close to the determination limits.

5.3.3.4 System blanks

Since nitric acid was to be used to digest the lead samples, it was also used as an experimental blank for the system. UV/Visible spectrophotometric analysis of nitric acid indicated that there was no absorption above 350 nm. Therefore, with the 1.8 M

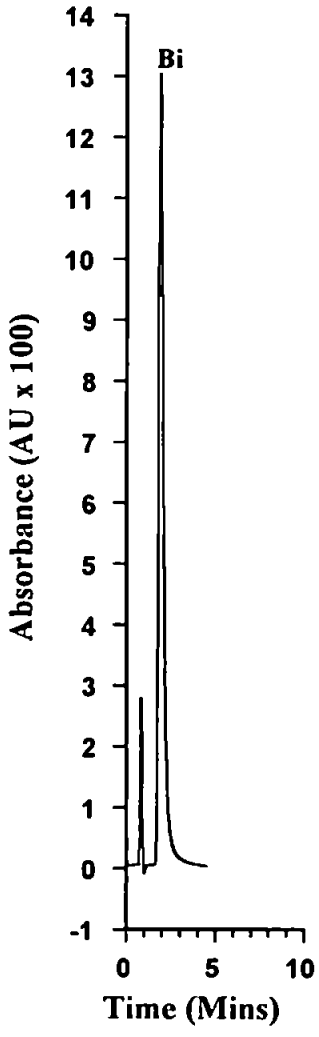

Figure 5.9. A 100 µl injection of 10 mg l^{-1} Bi with the 5 cm MN200 column.

The eluent was 1.8 M HBr with detection at 380 nm.

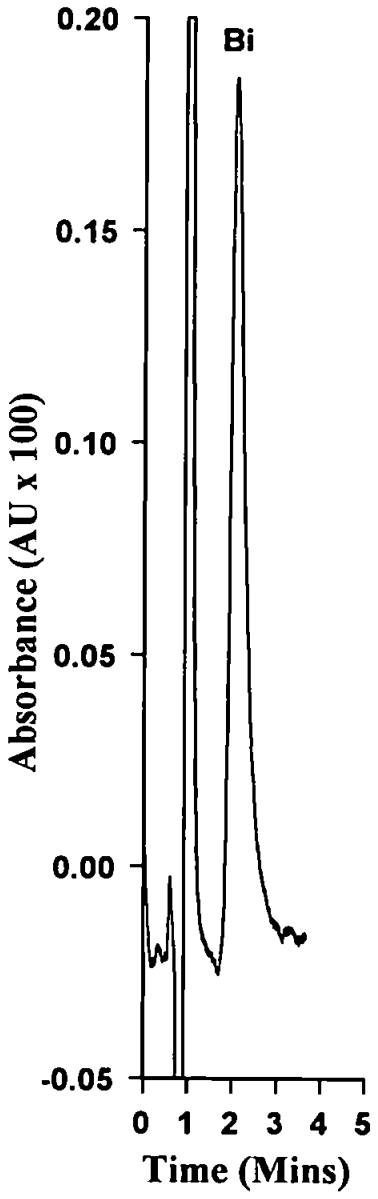

Figure 5.10. A 100µl injection of a 200 µg l^{-1} Bi standard with the 5 cm MN200 column. The eluent was 1.8 M HBr with detection at 370 nm.

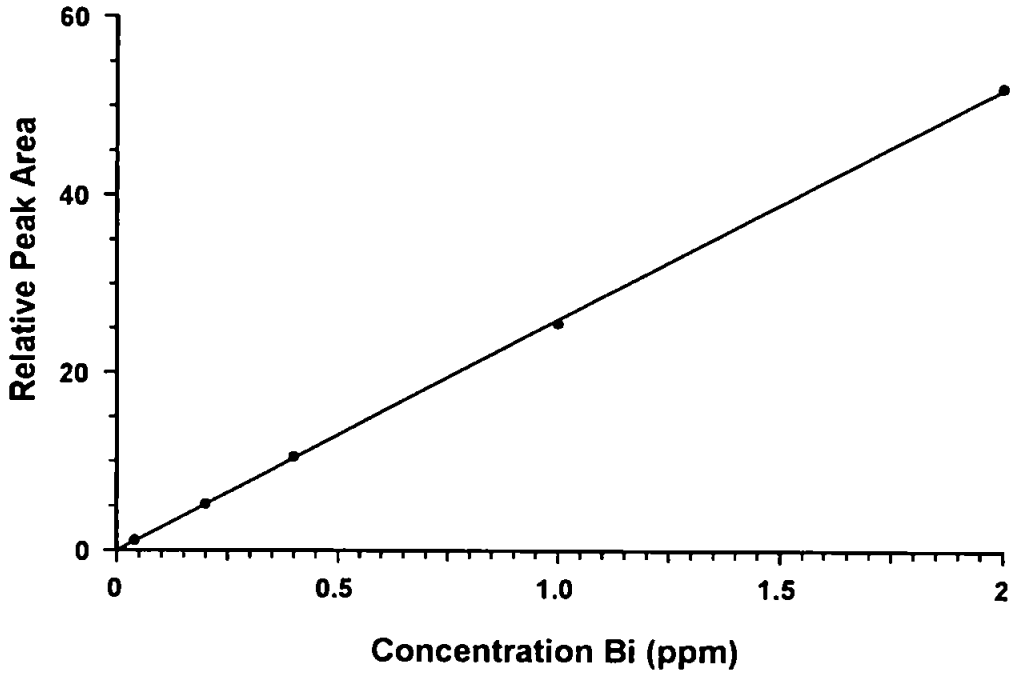

Figure 5.11 Calibration graph for the 100 µl injections of Bi standards

HBr eluent and detection at 370 nm, there was no change in signal at the same retention time for a Bi peak, after a 100 µl injection of 0.1M nitric acid.

5.3.4 Determination of Bismuth in Lead

A certified reference material (CRM 288B, lead pellets) containing Bi was used to evaluate the validity of this method. Standard addition techniques were used throughout this application to account for any matrix interferences which could affect the slope of the calibrations. Approximately 1g of pellets was used for each Bi standard, which was subsequently diluted to 500 ml. Additions of 0.5, 1.0 and 1.5 mg l^{-1} Bi were added to the respective lead samples for each determination and 100 µl injections were made into the system. Figure 5.12 shows a 100 µl injection of one of the samples with a 1 mg l^{-1} Bi addition. A calibration curve for the first sample (A) was constructed from the mean Bi peak areas for replicate injections. A further two calibration curves were constructed after the whole process was repeated for samples B and C. Figure 5.13 illustrates the calibration curve for sample B, which was very similar to the calibration curves for A and C.

5.3.4.1 Bismuth Determinations In Lead Pellet Samples

Table 5.2 displays the information for the three separate analyses. The concentration of Bi determined in the CRM 288B lead pellet samples were all slightly higher when compared to the certified concentration of Bi, which was 215.8 ± 2.4 µg g^{-1} (based on the 95 % confidence interval of the mean of means). This may

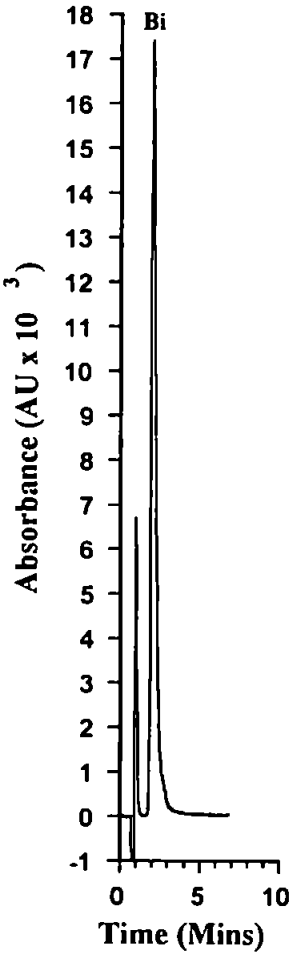

Figure 5.12. A 100 µl injection of lead sample A with 1.0 mg l^{-1} Bi added. The column was 5 cm MN200 and the eluent was 1.8 M HBr with detection at 370 nm.

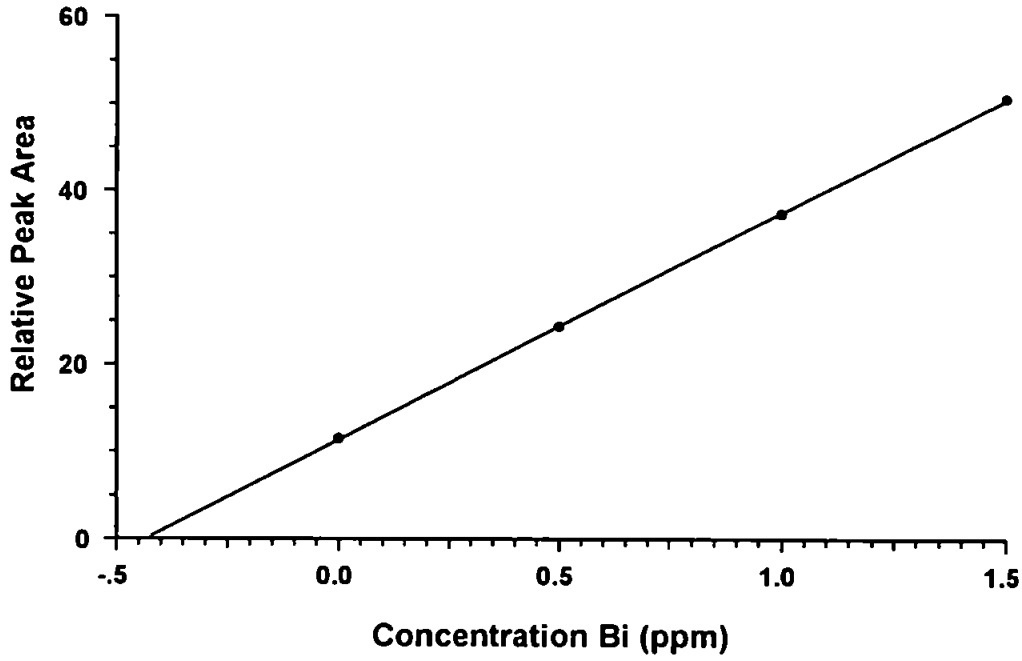

Figure 5.13. Calibration graph for the 100 µl injections of the standard additions for sample B

Lead sample	Amount of Bi determined in the sample, $\mu g\ g^{-1}$	r
A	218.56	0.99927
B	217.26	0.99996
C	219.18	0.99987

Certified result for CRM 288 B = 215.8 $\mu g\ g^{-1}$.

Table 5.2. Results for three separate standard addition determinations for CRM 288B

be attributed to the fact that a standard error was present in the system or because different analytical methods were used. The percentage recoveries, however, were all within 2% of the actual certified value. The mean value, x_m, for the Bi determinations was found to be 218.33 ± 0.98 μg g^{-1}. According to the BCR certificate of analysis accompanying the lead pellet samples, an analytical method is considered to perform well if the mean value, x_m, lies within the limits:

$$(M - 2S) < x_m < (M + 2S)$$

where M is the accepted certified value and S is the standard deviation of the method.

For CRM 288B, M = 215.8 μg g^{-1} and S = 5.3 μg g^{-1}.

Therefore,

$$(215.8 - 10.6) < 218.3 < (215.8 + 10.6)$$

It is clear that the mean value obtained from the new method falls within the set limits and therefore the method is viable as a technique for the analysis of Bi in lead pellet samples. The reproducibility of the system was also investigated, with six repeat 100 μl injections of a 1.0 mg l^{-1} Bi standard yielding a RSD of 1.5 %. The limit of detection of the system (obtained by calculating three times the signal to noise ratio) for a 100 μl injection of Bi was 10 μg l^{-1}, however this may be further improved for the analysis of lead samples with lower concentrations of Bi, by adjusting the sample injection volume, flow rate, HBr concentration and the column length, until the optimum conditions are obtained. Another important feature of the system was the

sample throughput, with each analysis time taking less than five minutes from the time of injection.

5.4 Summary

The bare MN200 column was capable of retaining Bi, yielding improved peak shape quality when compared to dye impregnated columns under the same conditions. The halide detection system was a major improvement compared to the Xylenol Orange post column reaction system and gave much lower limits of detection. It was difficult to explain the actual retention mechanisms of Bi on the bare MN200 column since it does not conform to information obtained from stability constant data. It is very unlikely, however, that simple ion exchange is the retention mechanism for Bi(III) owing to the strong acid conditions employed. There is a case where Fe(III) is retained by ion exchange in 6 M HCl as $FeCl_4^-$[142] and this mechanism may also be true for Bi(III). If N groups were present in the unmodified MN200 then they may become protonated and behave as anion exchange sites for the negatively charged Bi complexes. If this reasoning was true, then an increase in halide concentration would result in an increase in retention time, which was not the case. The system can be more complex, however, as a reversal in retention takes place when the halides compete for the adsorption sites but usually at very high halide concentrations. It is also difficult to explain the lack of retention of the Pb halide complex if the above explanation holds. Results obtained in Chapter 3 indicate that the metal adsorption mechanism of the unmodified MN200 resin was by chelating ion exchange. Davankov

et al. [117], however, postulate complex formation of the metal by interactions of metal ions with the organic moieties from benzene rings in the polystyrene resin.

Chapter 6 - Uranium and Thorium Investigations

6.1 Introduction

6.1.1 Occurrences and General Properties of Uranium and Thorium

Uranium and thorium are members of the actinide series and because of their long lived isotopes, are the only actinides to exist in the natural environment in relatively high concentrations, in spite of all isotopes being radioactive. Protactinium exists as a product of the decay of uranium and thorium, and plutonium is produced by neutron bombardment of uranium. In 1964, Taylor [143] reported the uranium abundance in the continental crust as being 2.5 $\mu g\ g^{-1}$ and thorium being present at 9.6 $\mu g\ g^{-1}$. For a relative comparison, uranium and thorium are almost as abundant as lead, which exists at 12.5 $\mu g\ g^{-1}$ and considerably more abundant than gold, which is present at 0.004 $\mu g\ g^{-1}$.

The most important source of uranium is *pitchblende*, the oxide U_3O_8 (although, it is thought to be more like $UO_{2.25}$ to $UO_{2.67}$) [144]. Pitchblende occurs in south east Germany, the Czech Republic, East Africa, Canada and Colorado. It is also the principle source of radium, which is a decay product of uranium [145]. Other mineral sources of uranium include *autinite*, (a hydrated calcium uranyl phosphate), probably the most common, and *torbenite* (a hydrated copper uranyl phosphate) [144].

The principle source of thorium is from *monazite*, which is a mixed phosphate also containing lanthanum, yttrium and the lanthanides. Monazite occurs widely distributed as an accessory mineral in igneous and metamorphic rocks and in pegmatites. The world's reserves of monazite sand are very large and range from Australia to Brazil and the United States. Thorium may also be found in the thorium silicate form of *thorite* and *thorogummite* (the hydroxyl-containing variant of thorite) [144].

Uranium is thought to consist of two main isotopes, ^{238}U (99.27 % abundance) and ^{235}U (0.72 % abundance). The decay series of ^{238}U ends in a stable isotope of ^{206}Pb whereas the decay series of ^{235}U ends in ^{207}Pb [118]. ^{235}U is of special importance since it is the isotope which undergoes nuclear fission with slow neutrons to yield enormous amounts of energy. Other actinides may be produced by the fission process of ^{235}U, and the neutron capture of $^{238}_{92}U$ in the system can be used to produce ^{239}Pu [144]. Another important use of uranium isotopes is in the geo-dating of rocks and minerals [118].

At least thirteen isotopes of thorium are known, which range in mass from 223 to 235. The isotope of greatest chemical interest is ^{232}Th which is the longest lived of all of the isotopes and the most abundant in nature [144]. The decay series of ^{232}Th ends in the stable isotope ^{208}Pb [118].

The distribution of uranium and thorium radionuclides in the marine environment are displayed in Table 6.1 [146].

Nuclide	Half-life (yr)	Concentration in Oceans $\mu g\ ml^{-1}$	Concentration in Sediments $\mu g\ g^{-1}$
^{228}Th	1.91	1×10^{-15}	-
^{230}Th	75200	1×10^{-12}	$(1\text{-}30) \times 10^{-4}$
^{232}Th	1.41×10^{10}	$(0.36\text{-}4.5) \times 10^{-6}$	2-12
^{234}U	2.48×10^{5}	$(1.6\text{-}2.1) \times 10^{-7}$	$(0.024\text{-}4.9) \times 10^{-3}$
^{235}U	7.13×10^{8}	$(1.9\text{-}2.5) \times 10^{-5}$	0.0028-0.58
^{238}U	4.51×10^{9}	$(2.7\text{-}3.4) \times 10^{-3}$	0.4-80

Table 6.1. Concentration of uranium and thorium isotopes in the marine environment

In aqueous media, thorium is believed to be present as the Th(IV) ion. Uranium may be present as U(IV) or U(VI) but U(IV) is the less stable of the two species, being rapidly oxidised to U(VI) by very strong oxidising agents such as Cr^{6+}, Ce(IV) or Mn^{7+} [147]. The oxidation of U(IV) to U(VI) by air is much slower and is described by de Beer and Coetzée [148] where the behaviour of U(IV) in non-degassed solutions is discussed. The report demonstrates the speciation of U(IV) and U(VI) and a series of chromatograms of the same sample analysed over a period of ten hours, illustrates the slow oxidation of the U(IV) to U(VI).

The reduction chemistry of the uranyl ion at $[H^+] = 1$, with redox potentials given in eV, is as follows [147]:

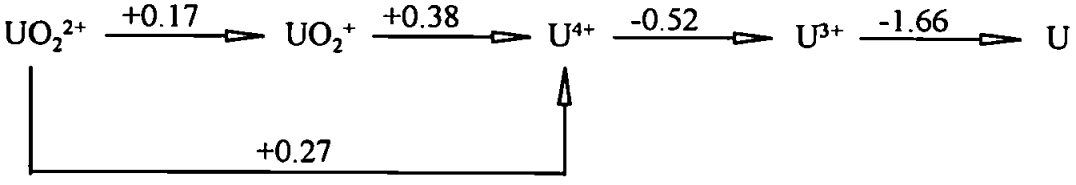

It is evident that in terms of the disproportionation of U(VI) into UO_2^+ and U(IV), U(IV) will predominate. However, in the presence of fluoride, the U(V) may be stabilised by the form $[UF_6]^-$. Thorium only shows an oxidation state of +4.

6.1.2 Preconcentration and Determination Methods for Uranium and Thorium

The separation and determination of uranium and thorium is of interest with respect to environmental samples [60] and in the nuclear industry [149]. A number of separation

methods have been reported, as well as the development of novel sorbents for preconcentration. An example is the development of an amidoxime fibre for use as a large scale preconcentration device for uranium in sea water [150]. In general, however, the preconcentration of these metals is on a much smaller scale and many adsorbents have been developed for analytical purposes. Fischer and Lieser [151] describe a whole series of cellulose exchangers, with tailor-made chelating groups, for the selective separation of uranium from sea water. A cellulose exchanger with chelating amidoxime/hydroxamic acid groups was found to have a uranium loading of almost 0.6 mg per gram. Ghosh and Das [152] studied a macroreticular polystyrene resin containing 1-nitroso,2-naphthol as the functional group. A high exchange capacity for the resin was discovered (0.97 m mol g^{-1}) but poor kinetics of the system made column operations viable only at low flow rates. Investigations into the development of a uranium specific resin have been made by Horwitz *et al* [153]. Amberchrom CG-71ms or Amberlite XAD-7 resins were impregnated with diamyl amylphosphonate (DAAP) and the resultant material was known as U/TEVA-Spec resin (for *u*ranium and *te*travalent *a*ctinide *spec*ific) and is now available commercially from ElChroM (Darien, IL, USA). Uranium and thorium were eluted separately from the column using 6.1 M HCl and 0.0025 M HCl respectively.

The determination of thorium and uranium in environmental and industrial samples has been performed by incorporating some of the special adsorbents into analytical systems. Havel *et al.* [154] have described a flow injection system for the determination of uranium (VI). A silica micro column was used to preconcentrate the uranium before fluorimetric detection. Good sensitivity was achieved and accurate

recoveries of uranium were obtained from natural water samples. Several flow injection systems have also been reported for the determination of thorium and uranium, and uranium in uranium ore leachates, by Moreno Cordero *et al.* [155,156] where no adsorbent was involved. A lead microcolumn was used to reduce U(VI) to U(IV) before detection with Arsenazo III in 3.6 M HCl. Detection was initially achieved without the microcolumn, in order to establish the thorium concentration, and then with the microcolumn to indirectly establish the uranium concentration.

The on-line preconcentration of uranium with ICP-MS detection has also been reported [11]. Preconcentration on silica immobilised 8-hydroxyquinoline was effected, but on-line monitoring was only possible for the preconcentration of a river water sample (SLRS-1). An open ocean water sample (NASS-2) was preconcentrated off-line since the high salt concentrations would have blocked the torch.

The determination of uranium and thorium concentrations in soils by isotope dilution-secondary ion mass spectrometry and isotope dilution-thermal ionisation mass spectrometry have been discussed by Adriaens *et al.* [157]. A pre-analysis clean-up procedure using the U/TEVA SPEC resin described previously was required to separate the uranium and thorium before analysis. Stable isotope dilution spark source mass spectrometry has also been described for this purpose [158]. Chelex-100 was used to preconcentrate uranium and several other metals and the concentrate was evaporated on a graphite or silver electrode. Two spiked sea water samples were used and the uranium recoveries were found to be 100 ± 10 %.

An unusual method for the determination of U(VI) has been reported by Baylor and Buchman [159]. The potential of a reflectance probe for U(VI), using Arsenazo III loaded onto cotton, was documented, but interference effects have not yet been investigated and the system does not appear to be robust.

Direct spectrophotometric and fluorometric methods are also popular for the determination of U(VI). An adsorbent prepared from tri-n-butyl phosphate-plasticized dibenzoylmethane loaded polyurethane foam has been reported for the preconcentration and determination of uranium (VI) in natural waters [160]. Good detection limits were achieved (0.05 $\mu g\ l^{-1}$) but the foam had to be burnt and dissolved in HCl before Arsenazo III could be added for spectrophotometric detection.

Many methods have been developed for the determination of uranium and thorium by liquid chromatography. Cassidy *et al.* [161,149,60] have reported uranium separations from uranium dioxide, thorium-uranium dioxide fuels and uranium ore refining processes. α-Hydroxyisobutyric acid (HIBA) was used as a complexing agent with reversed phase separations and colorimetric detection with Arsenazo III. Similar methods have been demonstrated by Haddad *et al.* [162,62] for the determination of thorium and uranium in mineral sands, Rehkämper [163] for thorium and uranium in geological samples, Barkley *et al.* [164] for uranium and thorium in uranium ores and Kerr *et al.* [165] for the determination of uranium in natural groundwaters. A variation of this method was also developed by Cassidy *et al.* [166] using mandelic acid instead of HIBA.

Another system using reversed phase HPLC has also been developed for the quantification of uranium as a 2,6-diacetylpyridine bis(benzoylhydrazone) complex [167]. The UO_2DIB complex is neutral and was separated from H_2DIB using a LiChrosorb RP2 column with a methanol-water mobile phase and UV detection at 265 nm.

Further investigations using ion chromatography include a cation-exchange system for the determination of thorium and uranium. The system incorporated the use of a chelating column for preconcentration and matrix elimination from the analytes [168]. Low limits of detection were found (typically 1 $\mu g\ l^{-1}$ for uranium and 3 $\mu g\ l^{-1}$ for thorium).

Many systems mentioned have displayed good adsorption, separation and detection qualities for uranium, thorium, or a mixture of both metals. However, in complex matrices, i.e. with large amounts of other metal ions present, some of the systems lose their capacity and often become ineffective. An example of this is the HIBA system with a reversed phase column [60]. In the presence of a high concentration of iron (III) the system loses its ability to separate the uranium from thorium. Some systems require the use of complex matrix elimination steps but these may be time consuming or can increase the complexity of the adsorption or separation system. A system incorporating a single column, which could separate uranium and thorium in the presence of relatively high concentrations of other metal ions, would therefore be of great interest.

This chapter describes the development of a single column IC system for the separation and determination of uranium and thorium from a complex matrix using both modified and unmodified MN200 polystyrene based columns. The HPCIC system used post column reagent spectrophotometric detection based on Arsenazo III. The system was tested for reproducibility and reliability as well as the affects of possible interferences from selected metal ions.

6.2 Experimental

6.2.1 Instrumentation

Investigations using the PAR column were performed in laboratories at the University of Oviedo, Spain, as part of an ERASMUS exchange scheme. The HPCIC system was essentially as described in Section 2.2.1, but a glass column (2 mm i.d. x 100 mm) packed with lead filings was incorporated into the system after the analytical column and before the zero dead volumne T-piece. The eluent pump was a P-500 syringe pump (Pharmacia) and the post column reagent pump was a Minipuls-2 peristaltic pump (Gilson). The HPCIC system used for the other columns was as described in Chapter 3.2.1.

6.2.2 Reagents

The reagents were as for Section 2.2.2 except the post column reagent was 2×10^{-4} M Arsenazo III (Fluka) in 3.6 M HCl, with 1% Triton X- 100 (Merck) or 2×10^{-4} M Arsenazo III in 1% Triton X-100. Dipicolinic acid (2×10^{-2} M) at pH 2 was used to remove strongly held metal ions from the column. Uranium and thorium standards were prepared by serial dilution of 1000 mg l^{-1} commercially available spectroscopic standards (Johnson Matthey, UK).

6.3 Results and Discussion

6.3.1 PAR Column

The first 20 μm MN200 column was prepared using PAR, as described in Chapter 3. A separation of four alkaline earth metals had been previously been achieved using this column. From the k' values, however, it was evident that the column could also be used to separate metal ions in acidic solution. The separation of uranium and thorium appeared to be a good test of the column and was of practical interest. Like bismuth, uranium and thorium are hydrolysed at low pH's, therefore separation of the two metals would necessitate fairly acid conditions. After a series of tests, the PAR column appeared stable in acidic media and was considered suitable for the separation of uranium and thorium.

6.3.2 Detection system

Before work with the PAR column was initiated, a suitable post column detection system for uranium and thorium needed to be developed. The most suitable post column reagent appeared to be Arsenazo III, which has been widely reported for the spectrophotometric detection of uranium and thorium. There was concern that a different source of the Arsenazo III (60% pure) would be too impure for use but, on testing, it was proved to be very sensitive for both uranium and thorium. The same concentration of Arsenazo III was used as reported by Moreno Cordero *et al.* [155] which was prepared in 3.6 M HCl since this concentration was the most sensitive and selective for uranium and thorium. However, U(VI) would not react at such a low pH and a 5 cm lead reduction column was prepared to reduce the U(VI) to U(II), after elution from the PAR separating column and before mixing with the Arsenazo III. The 3.6 M HCl eluent could be a problem when used in a standard HPLC pump with a metal head but, in this case, acid resistant tubing was used with a peristaltic pump and care was taken with waste disposal.

The lead reduction column consisted of a glass column containing fine particles of lead which had been filed from a piece of lead foil. Since the casing of the column was glass, any changes in the column packing could be seen. After passing a nitric acid solution through the column, small bubbles began to appear, but disappeared after a solution of degassed HCl was passed through the column, and the lead packing appeared stable. After a further period of testing, however, the nitric acid was not found to have any serious effect on the column and was used in the eluent.

Initial work with the system provided evidence that the detection system was very sensitive. Uranium and thorium standards (200 $\mu g\ l^{-1}$) were prepared and gave signals significantly above the detection limit when eluting on the solvent front. The eluents used all contained 0.5 M KNO_3, which was present to saturate any ion exchange sites. Oxalic acid (0.05 M) was also added to prevent hydrolysis of the uranium and thorium in the system. An eluent of 0.5 M HCl was initially used, but the acid concentration was lessened to move the analytes away from the solvent front. After a series of trials, the lead column became blocked and the presence of a white powdery substance was noticed in the column. This was assumed to be lead oxalate and the column had to be unpacked and re-packed with more lead powder. It was decided that the oxalic acid was not particularly suitable for use in the system while the lead reduction column was present, unless frequent column repacking was carried out.

The eluent was changed exclusively to nitric acid, however, in case the white precipitate being formed in the lead column was lead chloride. Potassium nitrate was eliminated from the eluent because the high acid concentrations should also suppress the ion-exchange effects. A uranium peak was retained for over ten minutes in 1 M nitric acid and a thorium peak was eluted just after the solvent front at about two minutes. When the acid concentration was subsequently increased to 1.5 M nitric acid, a separation of uranium and thorium was achieved (Figure 6.1). The thorium peak is on the solvent front, which is not ideal, since solvent front disturbances may interfere with the peak shape. The uranium peak is fairly Gaussian in shape and was well above the detection limit at 200 $\mu g\ l^{-1}$.

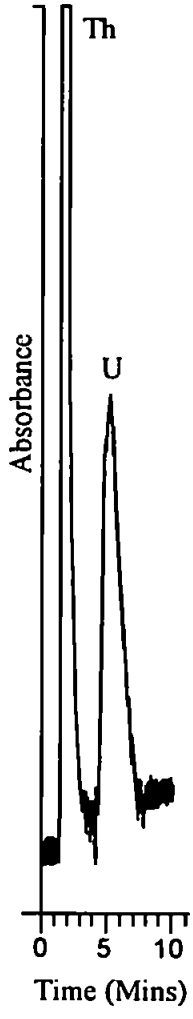

Figure 6.1 A 100 µl injection of 200 µg l^{-1} U(VI) and 200 µg l^{-1} Th(IV) using the 20 µm MN200 PAR column. The eluent was 1.5 M HNO_3 and detection was with Arsenazo III at 665 nm.

In an attempt to improve the shape of the uranium peak, the temperature of the column was increased to 63°C by placing it in a water bath. The uranium and thorium mixture was injected again and the uranium peak became sharper. Unfortunately, a corresponding move closer to the solvent front was apparent which could have been the cause of the improved peak shape. Several other injections of the uranium and thorium mixture were made and it was evident that the uranium peak was gradually moving closer to the solvent front until, finally, the uranium and thorium peaks were unresolved. From this information, it was deduced that the column was degrading. A probable cause of degradation could have been the protonation of the pyridyl nitrogen of the PAR causing an increased solubility of the dye adsorbed on the column. Subsequent bleeding of the dye would decrease the capacity of the column thus reducing the separating power. No bleed from the column was observed, however, but it is possible that a small amount of bleeding from the column could have remained undetected since PAR is pale yellow in colour when dilute in acid conditions. Further work with the PAR column was abandoned for the time being because of this reason.

6.3.3 Calmagite column

Further to the investigations using the PAR column, a Calmagite column which had been prepared by Paull *et al.* [110] was tested for the separation of uranium and thorium. A 10 cm PEEK column which contained a Dionex 8.8 μm high performance reversed phase polystyrene resin had previously been impregnated with the calmagite dye using the same method as for the PAR column.

Initial tests with the column were performed using 0.5 M potassium nitrate eluents to suppress any ion-exchange sites and varying concentrations of nitric acid were used in order to change the retention times of the analytes. An increase in the concentration of nitric acid caused a decrease in retention time. Sample injections of uranium started to show some retention with less than 1.0 M concentrations of nitric acid in the eluent.

6.3.4 Detection system

Oxalic acid was used in the eluent at concentrations of approximately 0.01M. Since oxalic acid is not compatible with the lead reduction column, an Arsenazo III post column reagent was used that could suitably detect U(VI) (the detection of U(VI) was less sensitive as the molar absorption coefficient of U(IV) in 4 M HCl (λ = 670 nm) was 100000, compared to 53000 for U(VI) at pH 2 (λ=665 nm) [148]). Arsenazo III was therefore buffered at pH 2 with potassium chloride and hydrochloric acid. There may have been a slight 'masking' of the uranium signal with the chloride in the post column reagent but it was not important because the system was only being tested for the separation of uranium and thorium and not for the optimisation of the detection limit. Masking of the uranium signal appeared more apparent with the oxalic acid present.

6.3.5 The Separation of Uranium and Thorium

The oxalic acid appeared to have a big effect on the thorium retention times i.e., an increase in the oxalic acid concentration resulted in a decrease in the thorium retention

time. After a series of attempted isocratic separations using different strengths of oxalic acid, it was considered that a step gradient system would provide better results. Uranium could be eluted using a 0.5 M potassium nitrate and 0.1 M nitric acid eluent, and then a stepped eluent of the same composition but with 0.01 M oxalic added, could be used for the elution of thorium. A problem with the proposed system was that a change in baseline occurred after the eluent step which caused the thorium peak to be eluted on a fairly steep slope. The baseline from a blank run was subtracted from the chromatogram which cancelled any major changes in the resulting baseline. A chromatogram representing the separation of 2 mg l^{-1} U(VI) from 2 mg l^{-1} Th(IV) is illustrated in Figure 6.2.

The system was not tested for interferences from other metal ions since it required a different approach in order to be suitable for further investigation. The uranium could not easily be removed from the solvent front without rapid broadening of the peak shape which resulted in interference with the thorium elution. The step gradient system was not considered to be very robust since the blank baseline would have to be subtracted from the main chromatogram after every run, which would double the analysis time. Also, any changes in the system between blank runs could result in a distortion of the uranium and thorium peak shapes.

6.3.6 MN200 column investigations

Although the Calmagite coated column showed potential it would be preferable to use uncoated material wherever possible. From other studies, described in Chapters 3 and

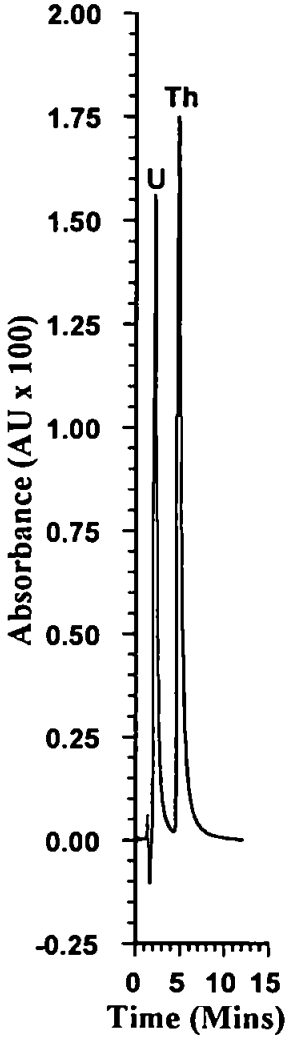

Figure 6.2 A 100 µl injection of 2 mg l^{-1} U(VI) and 2 mg l^{-1} Th(IV) using the 8.8 µm polystyrene Calmagite impregnated column. The eluent was 0.5 M KNO_3 and 0.1 M nitric acid and after 3 minutes, 0.01M oxalic acid was added to the eluent. Detection was with Arsenazo III at pH 2 at 665 nm.

5, the unmodified MN200 was found to have metal retaining properties. The column had shown unusual adsorption properties for bismuth and was stable in strong acid eluents for long periods of time. These factors looked promising and prompted the preparation of a 10 cm 10 μm MN200 column which was used to investigate the adsorption and separation properties of the MN200 for uranium and thorium.

The same system employed in the Calmagite column investigations was to be used, and it was decided that preliminary investigations should be carried out with an eluent of 0.5 M HNO_3. The Arsenazo post column reaction detection system was used as described previously. Several 100 μl injections of 4 mg l^{-1} Th(IV) were made and these eluted on the solvent front. Further injections were made, with reduced acid concentration and the addition of 1.0 M KNO_3, to eliminate any ion exchange effects. Th eluted just after the solvent front when an eluent composition of 0.2 HNO_3 and 1.0 M KNO_3 was used. Injections of uranium, however, produced peaks at a longer retention time for the same eluent composition.

Figure 6.3 illustrates a separation of uranium and thorium, achieved with an eluent of 1.0M KNO_3 and 0.2M HNO_3. The peaks were not fully resolved and the uranium peak was very broad. As with the calmagite column, there was little control in moving the peaks away from the solvent front without rapid broadening of the peaks and further loss of resolution. An investigation into the retention of other metal ions, which could interfere with the system, was performed. A 100 μl injection of 4 mg l^{-1} Fe(III) was made which eluted on the solvent front but was broad enough to cause significant interference with the thorium peak.

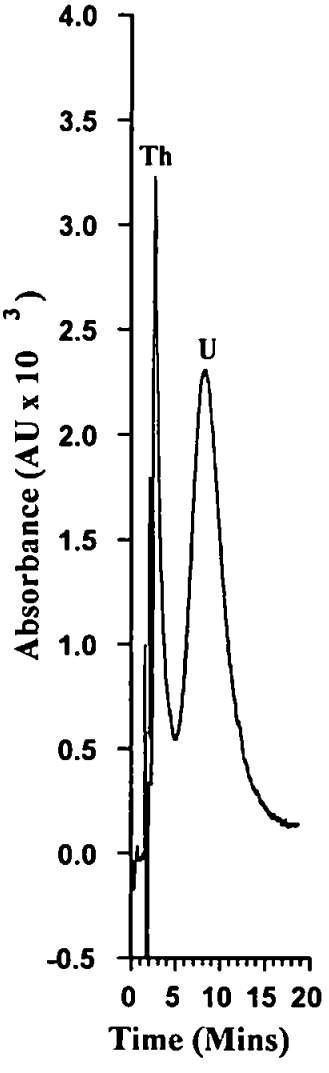

Figure 6.3 A 100 µl injection of 2 mg l^{-1} Th(IV) and 2 mg l^{-1} U(VI) with the 10 cm 10 µm MN200 column. The eluent was 0.2 M HNO_3 and 1.0 M HNO_3. Detection was with Arsenazo III at 654 nm.

It was believed that the nitrate was complexing with the uranium and thorium which, in turn, was reducing the resolution of the system. Although the nitrate complexes of uranium and thorium were relatively weak, they could be significant owing to the high concentration of nitrate in the eluent (for U(VI), log K_1 = -0.62 and for Th(IV), log K_2 = 1.22 at 25°C, in 2.0 M $NaClO_4$ with nitrate,).

As an alternative to the nitric acid and nitrate eluents, it was therefore decided that perchloric acid and perchlorate eluents would improve the system owing to the low complexing ability of the perchlorate ion. Various concentrations of perchloric acid were tested with 1 M sodium perchlorate. Uranium was retained for over thirty minutes with a 0.5 M perchloric acid and 1 M sodium perchlorate eluent, whereas the thorium still eluted close to the solvent front. Figure 6.4 illustrates a separation of 1.3 mg l^{-1} Th(IV) and 1.3 mg l^{-1} U(VI) which was achieved using a 1.0 M perchloric acid and 1.0 M sodium perchlorate eluent. The shape of the uranium peak is quite symmetrical and not too broad considering the retention time, but the thorium peak is asymmetrical with a lot of tailing. The uranium peak should become sharper if the acid concentration is increased and would still be well separated from the thorium. In order to prevent tailing of the thorium peak, it was believed that using a shorter column may prevent dispersion of the thorium inside the column.

6.3.6.1 5 cm 20 µm MN200 column

The acid concentration of the eluent was decreased to 0.5 M instead of 1.0 M since the column was half the length but the sodium perchlorate concentration remained at 1.0 M. Several injections of thorium were made but the column took a short while to

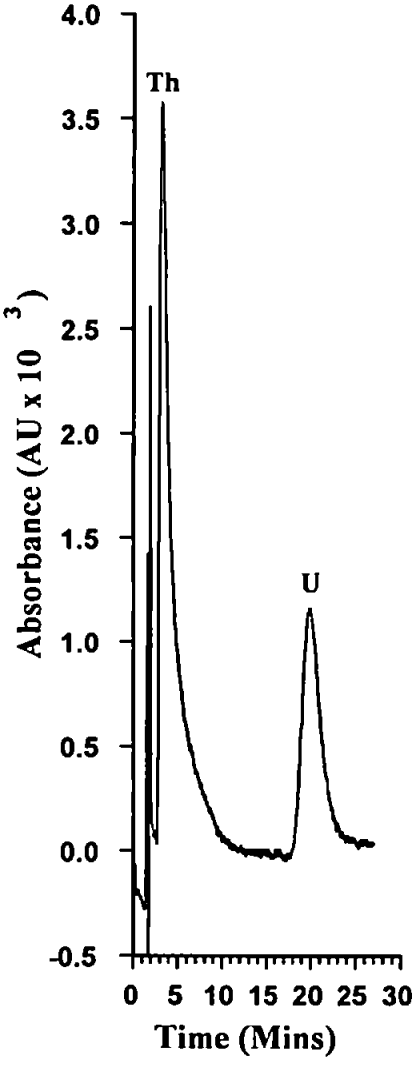

Figure 6.4 A 100 µl injection of 1.3 mg l^{-1} Th(IV) and 1.3 mg l^{-1} U(VI) using the 10 cm 10 µm MN200 column. The eluent was 1.0 M perchloric acid and 1.0 M sodium perchlorate. Detection was with Arsenazo III at 654 nm.

equilibrate with the new eluent and chromatograms were poor. After a period of adjustment, the 100 µl injections of thorium resulted in peaks further away from the solvent front but still with a fair amount of tailing. Figure 6.5 illustrates a 100 µl injection of 2 mg l^{-1} Th(IV) and 2 mg l^{-1} U(VI) with an eluent of 0.5 M perchloric acid and 1.0 M sodium perchlorate. The peak shapes were slightly better than those of the 10 cm MN200 column and the run time was considerably shorter. One problem that was present for both columns, however, was a significant baseline change with an increase in acid concentration of the eluent. The possibility of investigations with an eluent gradient program were therefore temporarily ruled out.

6.3.6.2 Linearity of Detector Response

The 5 cm MN200 was utilised to test the linearity of the post column reaction detection system. The 0.5 M perchloric acid and 1.0 M sodium perchlorate eluent was used and a series of U(VI) standards from 50 µg l^{-1} to 5 mg l^{-1} were prepared in nitric acid. The standards were injected twice and Figure 6.6 shows a calibration graph which was constructed from the peak areas. The retention time for the uranium peaks remained fairly constant throughout the experiment but it was noted that it was much less than had previously been found with the same eluent concentration. The correlation coefficient, r = 0.99999 for the calibration indicated that there was excellent linearity up to 5 mg l^{-1} although the determinations made at 50 µg l^{-1} were approaching the determination limit (Figure 6.7). The system was also tested for any interference from the standard blanks. Since nitric acid was used to prepare the

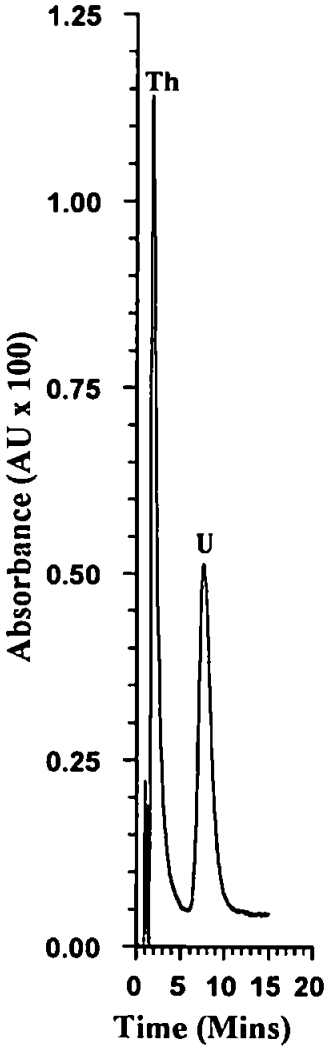

Figure 6.5 A 100 µl injection of 2 mg l^{-1} Th(IV) and 2 mg l^{-1} U(VI) using the 5 cm 20 µm MN200 column. The eluent was 0.5 M perchloric acid and 1.0 M sodium perchlorate. Detection was with Arsenazo III at 654 nm.

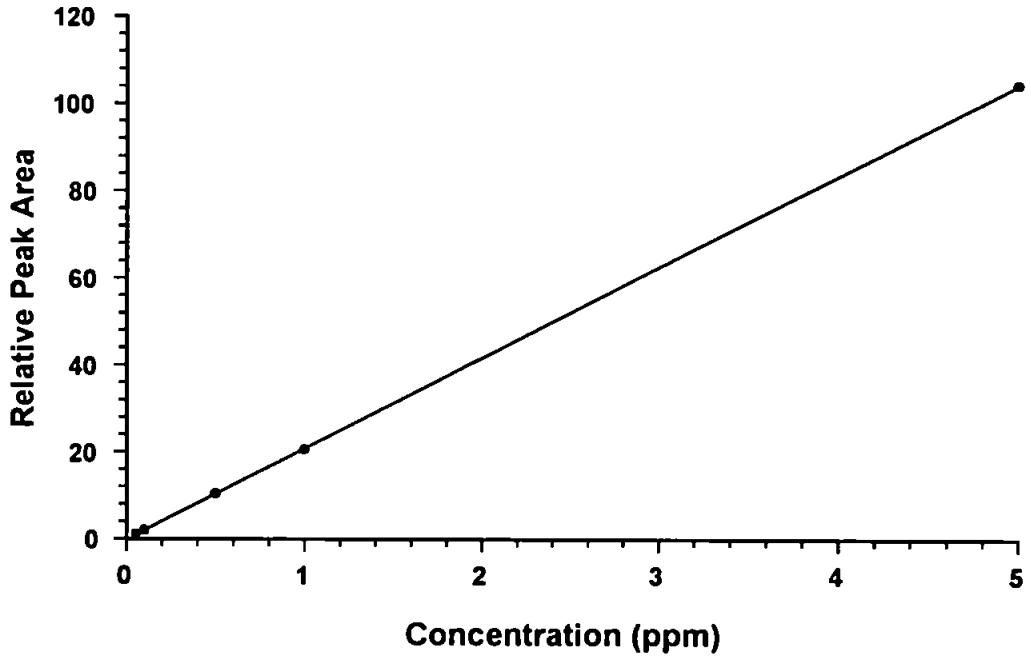

Figure 6.6 Calibration graph for 100 µl injections of U(VI) standards

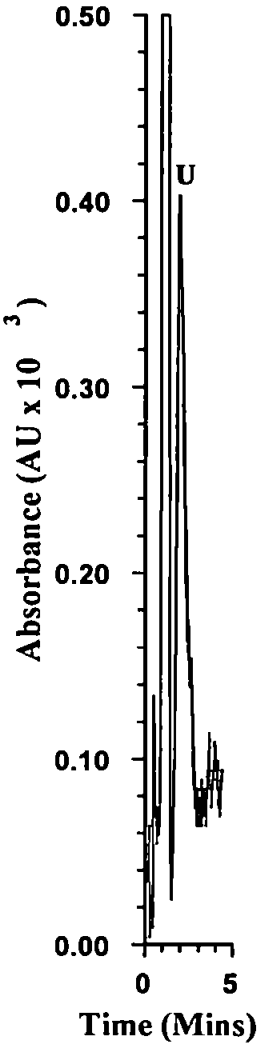

Figure 6.7 A 100 µl injection of 50 µg l^{-1} U(VI). The eluent was 0.5 M perchloric acid and 1.0 M sodium perchlorate. Detection was with Arsenazo III at 654 nm.

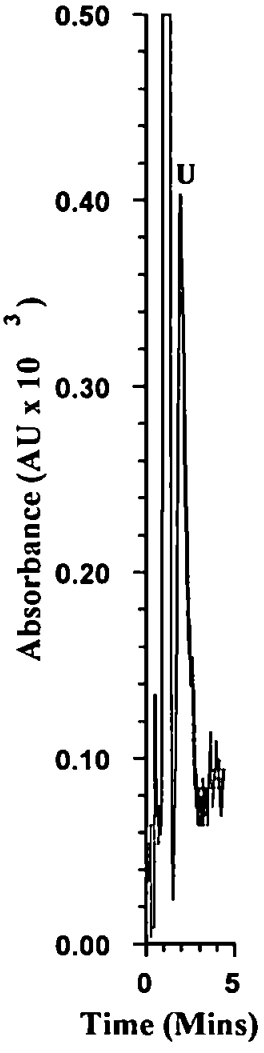

Figure 6.7 A 100 µl injection of 50 µg l^{-1} U(VI). The eluent was 0.5 M perchloric acid and 1.0 M sodium perchlorate. Detection was with Arsenazo III at 654 nm.

standards, 100 µl injections of 0.1 M HNO_3 were made into the system but no significant changes in signal were observed.

6.3.7 Lanthanide Interference

The lanthanide series of metals were believed to be a source of possible interferences for the uranium and thorium separation system since they form strong complexes with many ligands, although not as strong as thorium and uranium. For EDTA complexes with La (III), log K_1 = 15.3 and for Th (IV), log K_1 = 25.3 at 20°C in 0.10 M $NaClO_4$. La (III) was chosen as a representative of that series for investigation since it forms the strongest complexes of the lanthanide series. At low acidities, lanthanum (III) did not react with the Arsenazo III reagent used for the previous determinations, and a Xylenol Orange post column reagent, buffered at pH 6 with 0.5 M hexamine and nitric acid, was used. Figure 6.8 displays a 100 µl injection of 5 mg l^{-1} La (III). The eluent was 0.1 M perchloric acid and 1.0 M sodium perchlorate. The post column reagent was sensitive with regards to the lanthanum and a large response was recorded close to the solvent front. It was therefore assumed that lanthanum would not cause an interference at the higher concentrations of perchloric acid and other lanthanide metals should behave accordingly.

6.3.8 Iron (III) interference

Iron (III) was a problem since it may be present in factors of one hundred times the concentrations of uranium and thorium in some types of environmental samples. It

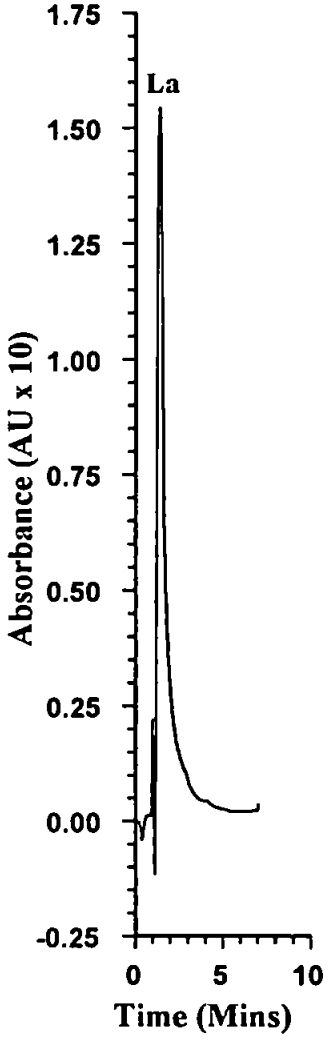

Figure 6.8. A 100 µl injection of 5 mg l^{-1} La using the 5 cm MN200 column. The eluent was 0.1 M perchloric acid and 1.0 M sodium perchlorate. Detection was with Xylenol Orange (buffered at pH 6 with hexamine) at 575 nm.

also forms strong complexes with many ligands and investigations were required to check that Fe(III) did not co-elute with either U(VI) or Th(IV). Fe (III) was found to react with Arsenazo (III) at pH's between 1 and 3, and tailed very badly from the solvent front. A method, to eliminate this problem, was to selectively reduce the iron (III) to iron (II). Ascorbic acid was suitable for this purpose and was not found to interfere with the uranium and thorium separations.

Experiments were performed to determine the amount of ascorbic acid required to reduce a known concentration of iron (III) to iron (II). The ascorbic acid did not affect the oxidation states of the uranium and thorium and a decision to test the 5 cm column for a separation in a relatively high iron concentration was made. Ascorbic acid was added to a mixture of 1 mg l^{-1} uranium (VI), 1 mg l^{-1} thorium (IV) and 10 mg l^{-1} lanthanum (III) with 100 mg l^{-1} iron (III). A 100 µl injection of the mixture yielded a poor separation of uranium and thorium with approximately 10 % resolution between the peaks. Further injections of the mixture gave similar results and it was suspected that the selectivity ratio of the column was reduced. The ascorbic acid was not thought to be a problem since previous injections with uranium in the presence of ascorbic acid gave stable retention times and iron (II) should not have any affinity for the column in high acid concentrations. It was therefore decided to return to using the 10 cm column for the separation of uranium and thorium in the presence of a high concentration of iron.

6.3.9 Further investigations with the 10 cm 10 µm MN200 column

The same mixture of ascorbic acid, iron, lanthanum, uranium and thorium, described previously, was tested on the 10 cm 10 µm MN200 column. Figure 6.9 illustrates a 100 µl injection of the mixture and a separation of thorium and uranium was achieved. The shape of the thorium peak was not very good and appeared to be affected by the solvent front. The uranium peak shape, on the other hand, was very symmetrical and the uranium was well retained on the column, indicating that the column was very selective for uranium.

Further investigations led to a similar 100 µl sample being injected but with 500 mg l^{-1} iron (III) present, and a higher concentration of ascorbic acid (0.08 M). After several injections, the retention time of the uranium and thorium peaks gradually decreased and it appeared evident that the column was losing capacity. Figure 6.10 illustrates a 100 µl injection of 0.08 M ascorbic acid, 500 mg l^{-1} iron (III), 10 mg l^{-1} lanthanum (III), 2 mg l^{-1} thorium (IV) and 0.5 mg l^{-1} uranium (VI). The eluent was 0.5 M perchloric acid and 1.0 M sodium perchlorate with Arsenazo III detection at 654 nm. The retention time of the uranium was considerably decreased in comparison with the first series of investigations and there was bad fronting of the peak shape. If there was a problem with the degradation of the chelating functional groups of the column, then a new MN200 column should have been able to reproduce the results obtained from the preliminary results. None of the 10 µm MN200, which had been used for the previous 10 cm column remained, but a new 10 cm column, containing 15 µm MN200, was prepared for the purpose of reproducing the uranium and thorium separations.

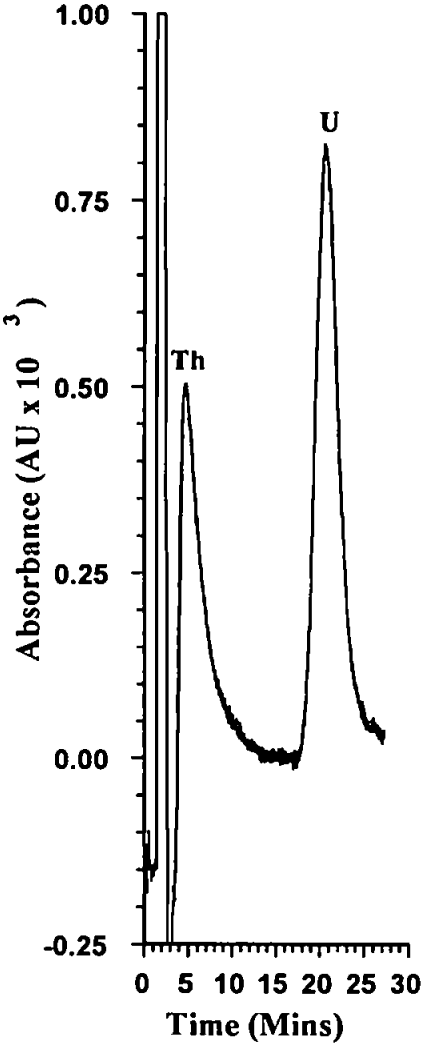

Figure 6.9 A 100 µl injection of 1.5 x 10^{-2} M ascorbic acid, 100 mg l^{-1} Fe(III), 10 mg l^{-1} La(III), 1 mg l^{-1} Th(IV) and 1 mg l^{-1} U(VI) using the 10 µm MN200 column. The eluent was 0.5 M perchloric acid and 1.0 M sodium perchlorate and detection was with Arsenazo III at 654 nm.

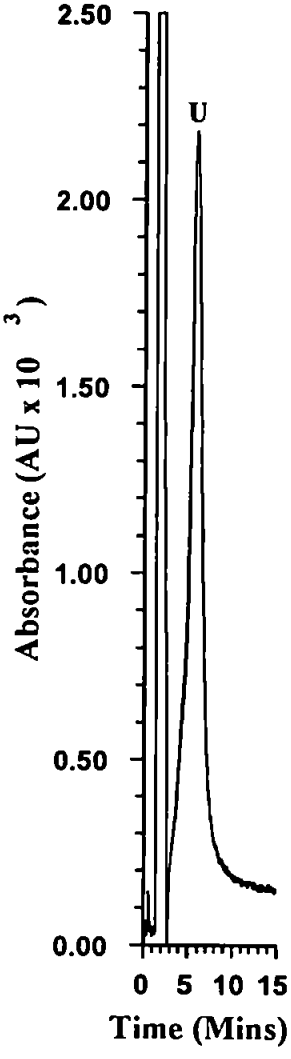

Figure 6.10 A 100 µl injection of 0.08 M ascorbic acid, 500 mg l^{-1} Fe(III), 2 mg l^{-1} Th(IV) and 0.5 mg l^{-1} U(VI) using the 10 cm 10 µm column. The eluent was 0.5 M perchloric acid and 1.0 M sodium perchlorate. Detection was with Arsenazo III at 654 nm.

6.3.10 Investigations with a new 10 cm 15µm MN200 column

It was believed that using similar conditions, a separation of uranium and thorium could be achieved using the new MN200 column. An eluent of 0.2 M perchloric acid and 1.0 M sodium perchlorate was used. A series of 100 µl injections of 4 mg l^{-1} uranium (VI) were injected until the retention time of the uranium peak was stable. The peak was much broader than before and the retention time was much less for the same eluent composition. 100 µl injections of similar concentrations of thorium, with the same eluent, gave peaks which were very broad with bad tailing and retention times greater than for uranium, i.e. the order of elution had changed. This implies that the previous separations on the 5 cm and 10 cm MN200 columns were not by interactions solely with the column and that other factors were involved.

The column histories of the 5 cm and 10 cm MN200 columns were checked and three main reagents could have been possible for the modification of the columns, Triton X-100 (which had been measured in a vessel prior to the column preparation), methanol (which had been pumped through the columns) and dipicolinic acid (used for 'scavenging' metals from the column when attempting separations of the alkaline earth metals). A series of experiments had previously been made to test for dipicolinic acid adsorption on the column. The results indicated that there was no affect on the separation of transition metals after using an eluent of dipicolinic acid. However, dipicolinic acid still seemed the most likely cause of the problem and a further series of experiments confirmed that after using dipicolinic acid, the retention time of uranium was greatly increased. It was therefore assumed that dipicolinic acid was forming an

unstable coating on the column which was degrading in the strong acid eluents. If the dipicolinic acid was unstable in the strong eluents, it was believed that a dipicolinic acid presence in the eluent could equilibrate with the column and form a stable system suitable for the required separations. It could only be assumed that any dynamic coating of dipicolinic acid present during transition metal investigations was not detected because interactions with the metal ions was very weak. This indicates that dipicolinic acid interactions with U(VI) were unusually strong, even at low pH.

6.3.11 Dipicolinic acid dynamic coating of the 10µm MN200 column

Experiments were necessary to identify the optimum concentration of dipicolinic acid in the eluent to achieve a separation of uranium from thorium in the presence of lanthanum and iron. The stable constituent of the eluent was the sodium perchlorate concentration, which was always 1.0 M, but the concentrations of perchloric acid and dipicolinic acid were initially varied. After a period of investigation, a perchloric acid concentration of 1.0 M was chosen and the dipicolinic acid concentration was adjusted to 4×10^{-4} M. The retention time of the uranium was very long at first, since the dipicolinic acid concentration had previously been much higher, but when the system had reached equilibrium (after several 100 µl injections of uranium) the retention time of the uranium peaks remained essentially stable. Figure 6.11 displays two consecutive 100 µl injections of 4 mg l^{-1} uranium superimposed on each other to illustrate the stability of the system. Although the system was capable of separating uranium and thorium, it was regarded to be quantitative only for uranium since the thorium peaks

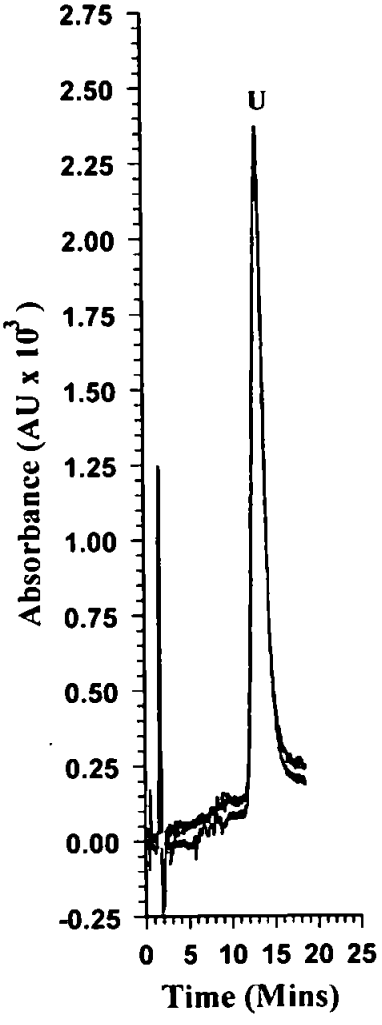

Figure 6.11. Two consecutive 100 µl injections of 4 mg l^{-1} U(VI) using the 10 µm MN200 column. The eluent was 1.0 M perchloric acid with 1.0 M sodium perchlorate with 4 x 10^{-4} M dipicolinic acid. Detection was with Arsenazo III at 654 nm.

were largely affected by the solvent front disturbances and the peak shapes were not very symmetrical.

6.3.12 Uranium spiked synthetic sample

Since a stable system had been developed for the determination and possible isolation of uranium from thorium and other metals, it was decided to investigate a synthetic sample of 500 mg l^{-1} Fe(III), 10 mg l^{-1} La (III) and 2 mg l^{-1} Th(IV), spiked with 2 mg l^{-1} U(VI). Ascorbic acid (0.08 M) was added to the mixture to reduce Fe(III) to Fe(II). Three additions of 1.92 mg l^{-1}, 3.76 mg l^{-1} and 5.54 mg l^{-1} uranium (additions were to be in increments of 2 mg l^{-1}, but adjustments were made for changes in volume) were made to the spiked sample mixture respectively. 100 µl injections of the sample mixture and the three samples with uranium additions were made. The eluent was 1.0 M perchloric acid and 1.0 M sodium perchlorate with 4×10^{-4} M dipicolinic acid. Detection was with Arsenazo III at 654 nm. Figure 6.12 displays a calibration curve constructed from the peak areas.

6.3.13 Uranium recovery from the spiked synthetic sample

The correlation coefficient was r = 0.99999 which indicates that the curve was linear over the chosen range. The amount of uranium in the spiked synthetic sample was 2.00 mg l^{-1} and the amount determined by the standard addition method was 1.9207 mg l^{-1}. Therefore:

$$\% \text{ Recovery} = (1.9207 / 2.00) \times 100\ \%$$

$$= 96.04\%$$

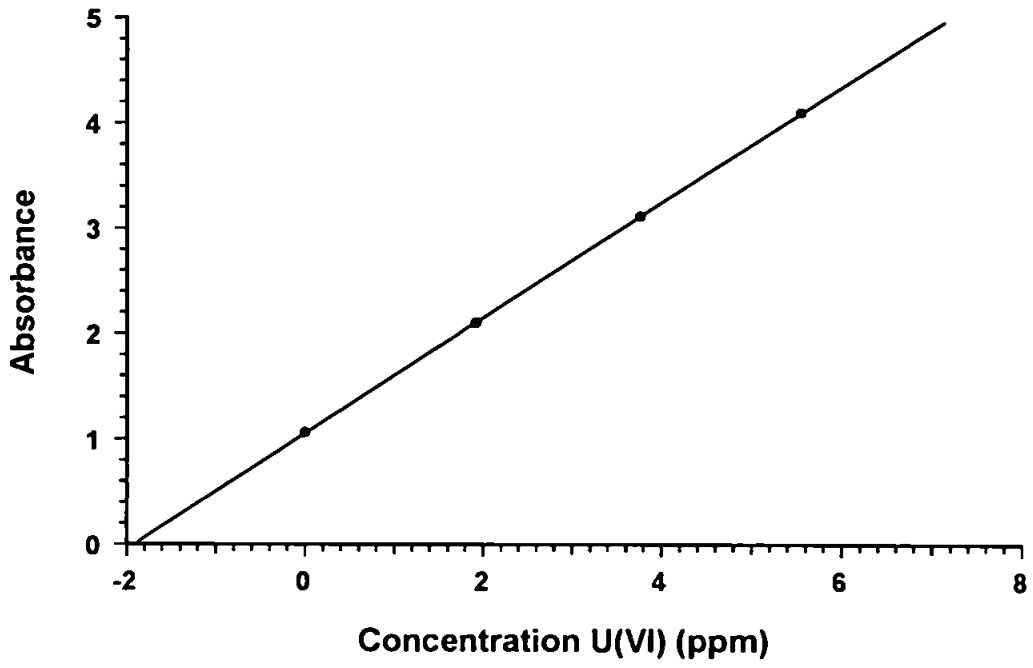

Figure 6.12. Calibration graph for the 100 µl injections of the standard additions.

The percentage recovery of 96.04% of the original uranium spike was acceptable and illustrated that the system was suitable for the determination of uranium in the presence of high levels of iron. The retention times of the uranium peaks remained fairly stable throughout the standard addition investigations. Figure 6.13 illustrates sample chromatograms of 100 µl injections of all of the samples used. The thorium peaks did not vary much in shape but, as mentioned previously, due to interactions with the solvent front disturbances, thorium was not viable for quantitative measurement. The reproducibility of the system was also investigated with seven repeat 100 µl injections of the uranium spiked sample with 1.92 mg l^{-1} uranium added. The eluent was also 1.0 M perchloric acid and 1.0 M sodium perchlorate with 4 x 10^{-4} M dipicolinic acid. Detection was with Arsenazo III at 654 nm.

Figure 6.14 illustrates a bar chart constructed from the relative peak areas from the reproducibility experiment. The mean area was 21.274 ± 0.519 with a relative standard deviation of 1.9 %.

6.4 Summary

The PAR column was not stable enough in the strong acid conditions to give reproducible results owing to a possible degradation of the column. PAR coated columns could still be useful as long as the acidity was not too low and the system is used at room temperature. The Calmagite column was able to produce a good separation of uranium and thorium but the system required data manipulation after the chromatograms were obtained, to remove baseline changes caused by eluent

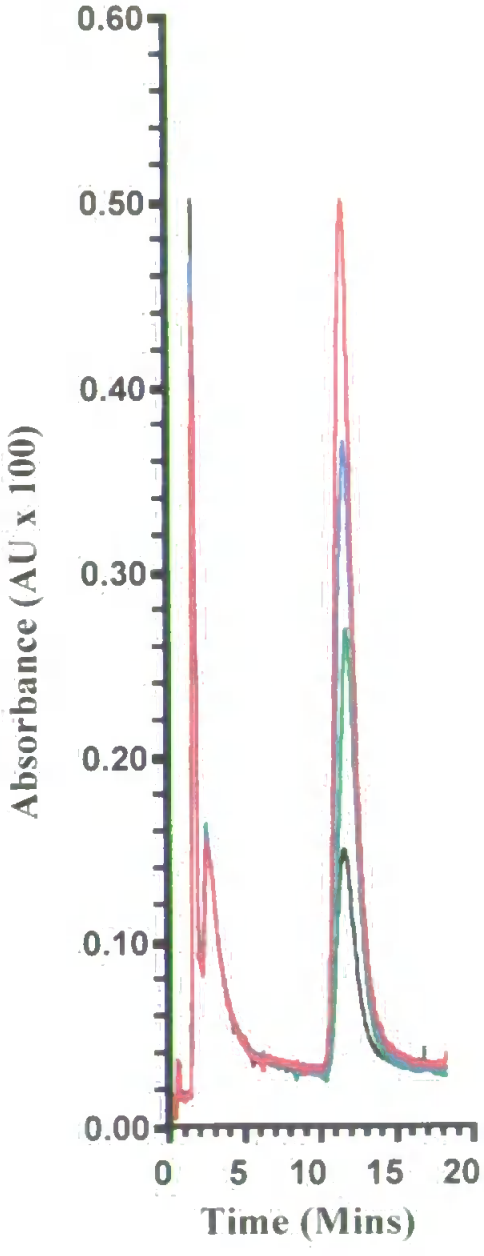

Figure 6.13. Sample chromatograms of 100 µl injections of all of the samples used for the standard additions using the 10 µm MN200 column. The eluent was 1.0 M perchloric acid and 1.0 M sodium perchlorate with 4 x 10^{-4} M dipicolinic acid. Detection was with Arsenazo III at 654 nm.

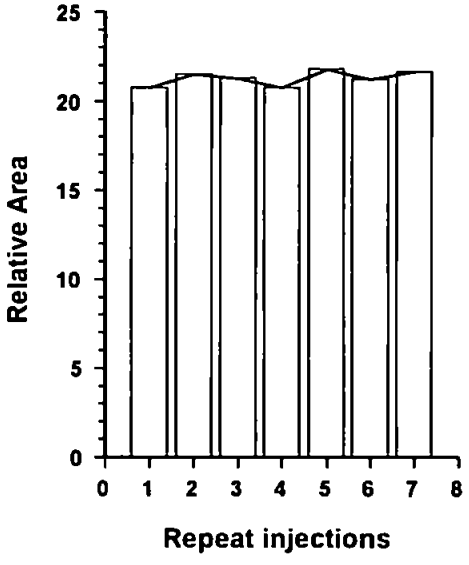

Figure 6.14 A bar chart showing the reproducibility of the uranium recoveries from the spiked synthetic sample

modifications. Any contamination in the system would also disrupt the separation. The peak shapes obtained from the Calmagite column, however, indicated that a separation of thorium and uranium was possible, but re-evaluation of the eluent system was required.

A system was developed that enabled the separation of uranium and thorium in a high concentration of iron (II) and the direct quantification of uranium from the system. A stable system was obtained using a dynamically coated (with dipicolinic acid) MN200 column which was suitable for both the isolation and determination of uranium from thorium and lanthanum in a relatively high concentration of iron. The system was not able to determine thorium quantitatively, but it was detected close to the solvent front. Further modifications of the system could be made in order to increase the detection limits of U(VI) for the analysis of real samples. Although there was a problem with bad peak 'tailing' and disturbance of high levels of other metals with thorium, the investigations undertaken could be a significant breakthrough in the HPLC of uranium.

Chapter 7 - Conclusions and Suggestions for Further Work

7.1 Conclusions

The work presented in this thesis has described the preparation and characterisation of novel, high efficiency chelating sorbents prepared from both hydrophilic and hydrophobic substrates which were suitable for the preconcentration, separation and determination of trace metals from complex matrices using single columns. Cellulose based materials were used as hydrophilic substrates and polystyrene resins were used as hydrophobic substrates. Modification of the substrates was achieved using chelating dyes, either covalently bound, in the case of the cellulose, or physically adsorbed (impregnated) onto the surface, in the case of the polystyrene resins.

Investigation of the polystyrene resins was essentially composed of three main areas of research. The first studies involved the batch dyeing of a range of large particle size resins which were characterised by their dye loadings and metal retaining capacity. Further investigations involved the dye impregnation of a range of polystyrene resins which had been crushed to an intermediate particle size. The resins were then suitable for packing into a column, enabling the capacity factors (k' values) for each column with a range of metal ions to be determined. From the results obtained, a resin was selected for small particle size evaluation in an HPCIC system. A study of analytical separations and selectivities was possible and the suitability for analytical and preparative applications of the resin was determined.

After characterisation of the dye coated substrates, a selection of the novel chelating sorbents were chosen for specific preparative and analytical applications which would exploit their particular metal separating capabilities. The first of these studies was applied to the isolation of strontium from calcium, rubidium and barium in gypsum samples. The second involved the separation and determination of trace bismuth in lead and the third described the separation and determination of thorium and uranium from a complex metal containing matrix.

A number of reactive dyes with chelating properties were chemically bonded to a range of different cellulose type materials (cellulose, cotton wool and calico). It was found that there was not much difference in performance between the different materials, although cellulose fibres were in a form which facilitated column packing and required less preparation than the cotton wool and calico dyed substrates. The determination of the capacity factors for the dyed cellulose revealed that there was a high affinity for copper with all of the dyed substrates, which could assist in isolation and removal of copper from fairly acid solutions. The overall capacity of the column was quite low so the substrate may only be suitable for "polishing" of solutions such as fine chemicals or drinking water. Although much time was spent in an attempt to obtain the highest possible dye loadings on the cellulose based substrates, the maximum loading achieved was still less than 5 % W/W, which was probably a result of the relatively large size of the dye molecules. Large molecules cannot penetrate the cellulose structure as effectively as small molecules and it is likely that a higher dye loading could have been achieved using smaller dye molecules. A high performance separation was achieved using a Procion Violet dyed cellulose fibre column, but the peak shape of the longer

retained peak was poor. The separation could probably have been improved by significantly reducing and normalising the size of the dyed cellulose fibres used in the column since the cellulose dyed substrates appeared to have good kinetics of exchange. It was considered that low capacity and poor efficiency of the dyed cellulose was not consistent with the aims of this work and a decision was made to pursue investigations with polystyrene based substrates.

Preliminary investigations with polystyrene resins showed that a new 'hypercrosslinked' resin compared favourably with a number of standard crosslinked resins in terms of dye adsorption and metal retaining capacities. The dye impregnated hypercrosslinked resins were consequently chosen for further investigations after crushing to an intermediate particle size. Capacity factor and metal retaining capacity determinations of the dye impregnated resins indicated that the dye impregnated hypercrosslinked polystyrene resins were suitable for further investigations using an even smaller particle size to obtain high efficiency columns suitable for analytical separations. The neutral hypercrosslinked 'macronet' resin, MN200, was chosen for this study and was crushed to a mean particle size of approximately 20 μm.

The first investigation with 20 μm MN200 was the preparation of a column impregnated with PAR. A good separation of alkaline earth metals was achieved with the column under isocratic conditions. The determination of capacity factors (k' values) for three 20 μm MN200 columns, impregnated with Phthalein Purple, Aluminon and Sudan Orange G gave the expected order of relative chelating strengths, i.e. Phthalein Purple > Aluminon > Sudan Orange G. Complexing groups present in

the eluents (used for buffering) during k' value determinations were found to cause a decrease in k' values. Aluminon gave the best separation of Cd, Zn and Pb from the three columns and an unusual chromatogram obtained for the Sudan Orange G column led to the investigations of the metal adsorbing properties of the MN200 resin.

The results of the k' values indicated that the bare MN200 column had a relatively lower chelating strength when compared to the dyed columns for peaks eluting close to the solvent front. A separation of Cd, Zn and Pb was achieved with a 15 cm unmodified MN200 column and the peak shapes and elution order of the metal ions were characteristic of a chelating ion exchange mechanism.

The MN200 was further crushed to a mean particle size of about 10 μm and a column was prepared by impregnation of the resin with Phthalein Purple. A separation of Cd, Zn and Pb was achieved using the column and the efficiency was found to be greater than for a similar Phthalein Purple column prepared from 20 μm MN200. It was considered that the efficiency of the MN200 could be further increased by reducing the particle size range of the resin.

Phthalein Purple impregnated 20 μm columns were used for the isolation of strontium from calcium, rubidium and barium in gypsum samples. Strontium was successfully separated from the calcium matrix along with barium and rubidium, which were present in the gypsum samples. An ammonium nitrate eluent developed for the system was easily removed from the strontium fractions by evaporation and then sublimation processes. Two runs through the HPCIC system were required for each of the

strontium fractions collected, but this would probably not have been the case if high purity reagents were used for the first run. High resolution thermal ionisation-mass spectrometry (TI-MS) for determination of strontium isotope ratios was successfully performed on collected strontium fractions by a collaborating group in Munich. Results were similar to those found from a more laborious classical method of strontium extraction.

The determination of trace bismuth in lead was achieved using an unmodified 5 cm 20 µm MN200 column. Several dye impregnated columns (Aluminon and Phthalein Purple) were investigated, but the unmodifed resin appeared to show improved peak shapes with bismuth. A Xylenol Orange post column reaction system was used in preliminary investigations. The combined elution and detection of bismuth was found to simplify the system and an increase in sensitivity was obtained. A certified reference material (CRM 288B) for lead was used to validate the method, and the bismuth determinations using the developed HPCIC system were found to fall well within the acceptable limits. The method was therefore considered viable for analytical determinations. A relative standard deviation of 1.5% (from six repeat injections) also indicated that the system was reproducible.

The 20 µm column impregnated with PAR was also used for the separation of thorium and uranium. A separation was achieved with the column, but could not be reproduced, owing to a degradation of the column caused by strong acid conditions and slightly elevated temperature. PAR impregnated columns are still considered

suitable for use providing that the acid concentrations are not too high and separations are performed at room temperature.

A separation of uranium and thorium was also achieved using an 8.8 μm Calmagite column. A step gradient was required to elute the thorium which resulted in a baseline change (which was removed by subtracting the signal from a blank run). Although the system appeared to have good separating potential, it was decided that investigations with the unmodified MN200 column should be pursued.

Increased retention time and good peak shapes for uranium were achieved using a 10 μm 10 cm unmodified MN200 column. The peak shape of thorium was poor in comparison to uranium, and investigations of uranium detection with the Arsenazo III post column reaction system gave a good linear range between 0.05 - 5 mg l^{-1}. Lanthanide (III) and iron (III) (which was reduced to iron (II) using ascorbic acid) interferences in the system were investigated. Responses with the system were determined and were found to interfere with the elution of the thorium peak. It was discovered that the increased retention of uranium was a result of a small amount of dipicolinic acid retained on the column. The dipicolinic acid did not form a stable coating which caused the retention time of uranium to decrease between subsequent runs. An MN200 column, dynamically coated with dipicolinic acid, was found to give a stable retention time for uranium. The recovery of uranium from a complex matrix was performed and was found to be 96.04% for a 2 μg l^{-1} sample. A relative standard deviation of 1.9% was also found for seven repeat injections for uranium. It is possible the investigations could be a significant breakthrough in the HPLC of uranium.

Suggestions for Further work

The cellulose substrates impregnated with reactive dyes were found to have relatively low chelating dye loadings, and thus low capacities for retaining metal ions. Collaboration with the Department of Colour Chemistry at the University of Leeds is proposed which involves the use of enhanced dyeing methods. The utilisation of these methods, could improve the capacity of the dyed cellulose sorbents making them suitable for a wide range of preconcentration applications. The particle size of the cellulose could also be improved to increase the efficiency of prepared columns enabling the columns to be utilised for analytical determinations. Short columns could be used with the high efficiency cellulose columns (to decrease column pressure which would cause the column to collapse) since the sorbents showed enhanced kinetics over dye impregnated polystyrene columns.

Crushing of the MN200 hypercrosslinked resins to smaller particle sizes increased the efficiency of the columns, but it is considered that the efficiency of the columns could be further improved by a reduction of the particle size range. Further preparations of the crushed resins are required and it is suggested that an automated system is used for crushing the resin particles, such as using a ball mill, in order that the desired mean particle size and range can be obtained more effectively and in a shorter period of time.

The preparation of dye impregnation of the polystyrene columns requires further investigations with respect to the production of reproducible columns. A method of producing stable dye loadings after equilibration is required in order that columns

prepared from the same dyes and substrates have similar separation properties. Further dye types, such as N,N and N,S should also be considered in future studies as these could give different selectivities and capacities to the N,O and O,O, type chelators investigated in this work.

A wider diameter column with a higher capacity than previously used could be prepared for the strontium isolation from calcium, rubidium and barium in gypsum samples. The higher capacity column would enable a higher concentration or larger volume samples to be used which would reduce the number of fractions collected. This would save time and also reduce the effects of background contamination by reducing the amount of eluent in the collections. Further collaboration with the group in Munich using a wider variation of samples, such as fossils and wines, is proposed.

Optimisation of the bismuth system is suggested in order that lower concentrations of bismuth in lead may be determined. Parameters such as the column length and hydrobromic acid concentrations can be altered until the optimum conditions are formed. MN200 columns with increased efficiency (after reducing the particle size range) can also be used to improve the system.

Optimisation of the uranium and thorium system is required in order that determinations of both uranium and thorium in complex metal containing matrices may be made. Again, smaller particle size MN200 would increase efficiency and thus improve peak shapes. The eluent system may also be optimised to increase the retention time and sharpen the peak shape for thorium. The sensitivity of the detection

system could be improved by using a lead reduction column in the system and highly acidic Arsenazo III for determination of the U(IV) species.

REFERENCES

[1] N. P. Vela and J. A. Caruso, *J. Anal. At. Spectrom.*, **8**, (1993), 787.

[2] H. Small, T. S. Stevens and W. C. Bauman, *Anal. Chem.*, **47**, (1975), 1801.

[3] H. Small, *J. Chromatogr.*, **546**, (1991), 3.

[4] J. Lehto and R. Harjula, RSC Publication, Ion Exchange Developments and Applications, 1996, 234.

[5] Ion Exchange Resins, BDH, Poole, England, Fifth Edition, 1968.

[6] I. M. Kolthoff and P. J. Elving, Treatise on Analytical Chemistry, Second Edition, Wiley, Chichester, 1979, 605.

[7] A. Ringbom, Chemical Analysis, Volume XI, Clarendon Press, Oxford, 1977, 52.

[8] G. V. Myasoedova and S. B. Savvin, *CRC Critical Reviews in Analytical Chemistry*, **17**, (1986), 1.

[9] J. M. Hill, *J. Chromatogr.*, **76**, (1973), 455.

[10] R. E. Sturgeon, S. S. Berman, S. N. Willie and J. A. H. Desaulniers, *Anal. Chem.*, **53**, (1981), 2337.

[11] D. Beauchemin and S. S. Berman, *Anal. Chem.*, **61**, (1989), 1857.

[12] B. Mohammad, A. M. Ure and D. Littlejohn, *J. Anal. At. Spectrom.*, 7, (1992), 695.

[13] D. Chambaz and W. Haerdi, *J. Chromatogr.*, **482**, (1989), 335.

[14] R. Kocjan, *Analyst*, **117**, (1992), 741.

[15] D. E. Leyden and G. H. Luttrell, *Anal. Chem.*, **47**, (1975), 1612.

[16] M. Gimpel and K. Unger, *Chromatographia*, **16**, (1982), 117.

[17] D. Chambaz, P. Edder and W. Haerdi, *J Chromatogr.*, **541**, (1991), 443.

[18] K. Terada, K. Matsumoto and H. Kimura, *Anal. Chim. Acta*, **153**, (1983), 237.

[19] J. D. Glennon and S. Srijaranai, *Analyst*, **115**, (1990), 627.

[20] N. Ryan and J. D. Glennon, *Anal. Proc.*, **29**, (1992), 21.

[21] N. Ryan, J. D. Glennon and D. Muller, *Anal. Chim. Acta*, **283**, (1993), 344.

[22] L. Ebdon, A. S. Fisher, S. J. Hill and P. J. Worsfold, *J. Autom. Chem.*, **13**, (1991), 281.

[23] R. A. Nickson, S. J. Hill and P. J. Worsfold, *Anal. Proc.*, **32**, (1995), 387.

[24] R. Christell, S. Forberg and T. Westermark, *J. Inorg. and Nuclear Chem.*, **19**, (1961), 187.

[25] J. H. H. G. Van Willigen and R. C. Schonebaum, *Talanta*, **85**, (1966), 35.

[26] G. H. Luttrell Jr., C. More and C. T. Kenner, *Anal. Chem.*, **43**, (1971), 1370.

[27] J. P. Riley and D. Taylor, *Anal. Chim. Acta*, **40**, (1968), 479.

[28] S-C. Pai, *Anal. Chim. Acta*, **211**, (1988), 271.

[29] P. Murugaiyan, H. Parasuramiyer and Ch. Venkateswarlu, *Indian J. Technol.*, **26**, (1988), 194.

[30] M. Pesavento, R. Biesuz, M. Gallorini and A. Profumo, *Anal. Chem.*, **65**, (1993), 2522.

[31] D. Strachan, S. Tymochowicz, P. Schubert and H. M. Kingston, *Anal. Chim. Acta*, **220**, (1989), 243.

[32] A. Siiriraks and H. M. Kingston, *Anal. Chem.*, **62**, (1990), 1185.

[33] S. Blain, P. Appriou and H. Handel, *Anal. Chim. Acta*, **272**, (1993), 91.

[34] M. Groschner and P. Appriou, *Anal. Chim. Acta*, **297**, (1994), 369.

[35] W. Szczepaniak and K. Kuczynski, *React. Polym.*, **3**, (1985), 101.

[36] J. Das and M. Pobi, *Anal. Chim. Acta*, **242**, (1991), 107.

[37] A. G. Howard and R. Danilona-Mirzaians, *Anal. Lett.*, **22**, (1989), 257.

[38] E. Antico, A. Masana, V. Salvado, M. Hidalgo and M. Valiente, *Anal. Chim. Acta*, **296**, (1994), 325.

[39] M. L. Marina, V. Gonzalez and A. R. Rodriguez, *Microchem. J.*, **33**, (1986), 275.

[40] J. L. Lundgren and A. A. Schilt, *Anal. Chem.*, **49**, (1977), 974.

[41] A. G. Howard and M. H. Arbab-Zavar, *Talanta*, **26**, (1979), 895.

[42] K. Brajter and E. Olbrych-Sleszynska, *Talanta*, **30**, (1983), 355.

[43] J. Chwastowska and E. Mozer, *Talanta*, **32**, (1985), 574.

[44] J. Chwastowska and D. Przygoda, *Chemia Analityczna*, **31**, (1986), 545.

[45] M. L. Marina, V. Gonzalez and A. R. Rodriguez, *Microchem. J.*, **36**, (1987), 103.

[46] K. Isshiki, F. Tsuji and T. Kuwamoto, *Anal. Chem.*, **59**, (1987), 2491.

[47] K. Brajter, E. Olbrych-Sleszynska and M. Staskiewicz, *Talanta*, **35**, (1988), 65.

[48] A. K. Singh and T. G. S. Kumar, *Microchem. J.*, **40**, (1989), 197.

[49] O. Abollino, E. Mentasti, V. Porta and C. Sarzanni, *Anal. Chem.*, **62**, (1990), 21.

[50] L. Ebdon, H. W. Handley, P. Jones and N. W. Barnett, *Mikrochim. Acta*, **2**, (1991), 39.

[51] H. W. Handley, P. Jones and L. Ebdon, *Anal. Proc.*, **28**, (1991), 37.

[52] V. Porta, C. Sarzanini, O. Abollino, E. Mentasti and E. Carlini, *J. Anal. At. Spectrom.*, 7, (1992), 19.

[53] A. M. Naghmush, M. Trojanowicz and E. Olbrych-Sieszynska, *J. Anal. At. Spectrom.*, 7, (1992), 323.

[54] R. D. Rocklin, *J. Chromatogr.*, **546**, (1991), 175.

[55] J. I. Toei, *Chromatographia*, **23**, (1987), 355.

[56] J. I. Toei and N. Baba, *J. Chromatogr.*, **361**, (1986), 368.

[57] R. M. Cassidy and B. D. Karcher, Reaction Detection In Liquid Chromatography, Marcel Dekker, NewYork, 1986, 129.

[58] K. Kawazu and J. S. Fritz, *J. Chromatogr.*, 77, (1973), 397.

[59] J. R. Jezoreck and H. Freiser, *Anal. Chem.*, **51**, (1979), 373.

[60] D. J. Barkley, M. Blanchette, R. M. Cassidy and S. Elchuk, *Anal. Chem.*, **58**, (1986), 2222.

[61] R. M. Cassidy, *Chem. Geol.*, **67**, (1988), 185.

[62] P. E. Jackson, J. Carnevale, H. Fuping and P. R. Haddad, *J. Chromatogr. A*, **671**, (1994), 181.

[63] P. Jones, P. J. Hobbs and L. Ebdon, *Analyst*, **109**, (1984), 703.

[64] C. J. Bowles, L. W. Bader and K. W. Jackson, *Talanta*, **37**, (1990), 835.

[65] P. M. Collins, Ed., Carbohydrates, Chapman and Hall, London and New York, 1987, 14.

[66] R. L. Allen, Colour Chemistry, Appleton, New York, 1971.

[67] P. R. Austin, C. J. Brine, J. E. Castle and J. P. Zikakis, *Science*, **212**, (1981), 749.

[68] E. Maranon Amd H. Sastre, *Bioresource Technology*, **40**, (1992), 73.

[69] W. M. Hosny, A. K. Abdel Hadi, H. El-Saied and A. H. Basta, *Polymer International*, **37**, (1995), 93.

[70] T. Heinze, K. Helbig and D. Klemm, *Acta Polymerica*, **44**, (1993), 108.

[71] A. M. Naghmush, K. Pyrzynska and M. Trojanowicz, *Talanta*, **42**, (1995), 851.

[72] J. R. Deans and B. G. Dixon, *Water Res.*, **26**, (1992), 469.

[73] P. Schramel, L. Xu, G. Knapp and M. Michaelis Fres., *J. Anal. Chem.*, **345**, (1993), 600.

[74] G. I. Tysin, I. V. Mikhura, A. A. Formanovsky and Y. A. Zolotov, *Mikrochim. Acta*, **3**, (1991), 53.

[75] S. Imai, M. Muroi and A. Hamaguchi, *Anal. Chim. Acta*, **113**, (1980), 139.

[76] R. S. Shreedhara Murthy and D. E. Ryan, *Anal. Chim. Acta*, **140**, (1982), 163.

[77] A. H. Basta, W. M. Hosny, H. El-Saied and A. K. Abdel Hadi, *Cellulose*, **3**, (1996), 1.

[78] H. Kubota and Y. Shigehisa, *J. Appl. Polym Sci.*, **56**, (1995), 147.

[79] R. A. A. Muzzarelli, Chitin, 1977.

[80] R. A. A. Muzzarelli and O. Tubertini, *Talanta*, **16**, (1969), 1571.

[81] F. J. Millero, D. J. Hawke and L. K. Bell, *Abstracts Of Papers Of The American Chemical Society*, **201**, (1991), 43.

[82] R. A. A. Muzzarelli, F. Tanfani, S. Mariotti and M. Emanuelli, *Carbohydrate Research*, **104**, (1982), 235.

[83] A. Hase, T. Kawabata and K. Terada, *Anal. Sci.*, **6**, (1990), 747.

[84] S. Hoshi, Y. Kamada, S. Inoue and M. Matsubara, *Anal. Sci.*, **4**, (1988), 227.

[85] S. Hoshi, S. Kanagami, M. Uto and M. Matsubara, *Anal. Sci.*, **8**, (1992), 103.

[86] R. Golombek and G. Schwedt, *J. Chromatogr.*, **452**, (1988), 283.

[87] T. A. Walker, *J. Chromatogr.*, **546**, (1991), 199.

[88] T. A. Walker, *J. Chromatogr.*, **602**, (1992), 97.

[89] T. A. Walker, *J. Liq. Chromatogr.*, **16**, (1993), 1573.

[90] M. L. Marina, J. C. Diez-Masa and M. V. Dabrio, *J. Liq. Chromatogr.*, **12**, (1989), 1973.

[91] C. H. Risner and J. R. Jezorek, *Anal. Chim. Acta*, **186**, (1986), 233.

[92] K. H. Faltynski and J. R. Jezorek, *Chromatographia*, **22**, (1986), 5.

[93] M. Lauth and P. Gramain, *J. Chromatogr.*, **395**, (1987), 153.

[94] N. Simonzadeh and A. A. Schilt, *Talanta*, **35**, (1988), 187.

[95] G. Bonn and S. Reiffenstuhl, *J. Chromatogr.*, **499**, (1990), 669.

[96] P. N. Nesterenko, I. P. Smirnov, J. D. Brykina and T. A. Bol'shova, *Moscow Univ. Chem. Bull.*, **46**, (1991), 49.

[97] Jezorek and Thompson, *Anal. Chem.*, **63**, (1991), 75.

[98] J. D. Glennon, E. Horne, K. Hall, D. Cocker, A. Kuhn, S. J. Harris and M. A. McKervey, *J. Chromatogr. A*, **731**, (1996), 47.

[99] P. Nesterenko and P. Jones, *J. Liq. Chrom. & Rel. Technol.*, **19**, (1996), 1033.

[100] J. Morris and J. S. Fritz, *J. Chromatogr.*, **602**, (1992), 111.

[101] P. Jones and G. Schwedt, *J. Chromatogr.*, **482**, (1989), 325.

[102] M. Torre and M. L. Marina, *CRC Critical Rev. Anal. Chem.*, **24**, (1994), 327.

[103] O. J. Challenger, S. J. Hill and P. Jones, *Anal. Proc.*, **29**, (1992), 91.

[104] P. Jones, O. J. Challenger and S. J. Hill, Ion Exchange Process: Advances and Applications, 1993, 279.

[105] O. J. Challenger, S. J. Hill and P. Jones, *J. Chromatogr.*, **639**, (1993), 197.

[106] B. Paull, M. Foulkes and P. Jones, *Analyst*, **119**, (1994), 937.

[107] B. Paull, M. Foulkes and P. Jones, *Anal. Proc.*, **31**, (1994), 209.

[108] B. Paull, M. Foulkes and P. Jones, *J. Chromatogr.*, **673**, (1994), 173.

[109] B. Paull and P. Jones, *Chromatographia*, **42**, (1996), 528.

[110] L. Svoboda, P. Jandera and J. Churacek, *Collect. Czech. Chem. Commun.*, **56**, (1991), 317.

[111] V. A. Davankov and M. P. Tsyurupa, *Angew. Makromol. Chem.*, **91**, (1980), 127.

[112] V. A. Davankov and M. P. Tsyurupa, *Pure Appl. Chem.*, **61**, (1989), 1881.

[113] M. P. Tsyurupa, T. A. Mrachkovskaya, L. A. Maslova, G. I. Timofeeva and V. A. Davankov, *React. Polym.*, **19**, (1993), 55.

[114] V. A. Davankov and M. P. Tsyurupa, *React. Polym.*, **13**, (1990), 27.

[115] M. Beth, K. K. Unger, M. P. Tsyurupa and V. A. Davankov, *Chromatographia*, **36**, (1993), 351.

[116] M. P. Tsyurupa, M. M. Ilyin, A. I. Andreeva and V. A. Davankov, *Fres. J. Anal. Chem.*, **352**, (1995), 672.

[117] V.A. Davankov, M.P. Tsyurupa, O. G. Tarabaeva and A.S. Shabaeva, RSC Publication, Ion Exchange Developments and Applications, 1996, 209.

[118] P. Henderson, Pergamon Press Ltd., Oxford, UK First Edition, Inorg., Geochem., 1982 .

[119] Isotopes In The Earth Sciences, R. Bowen, Elsevier, 1988, 163.

[120] D. W. Muller and P. A. Mueller, *Earth Planet. Sci. Lett.*, **107**, (1991), 1.

[121] Encylclopedia of Geochem. and Environ. Sci., River Geochemistry, Van Nostrand Reinhold, New York, 1972, 1054.

[122] P. Horn *et al*, *Z. Lebensm Unters Forsch*, **196**, (1993), 407.

[123] P. Horn, St. Holzl and D. Storzer, *Naturwissenschaften*, **81**, (1994), 360.

[124] P.R. Haddad, P. W. Alexander and M. Trojanowicz, *J. Chromatogr.*, **294**, (1984), 397.

[125] E. A. Gautier, R. T. Gettar and R. E. Servant, *Anal. Chim. Acta*, **283**, (1993), 350.

[126] R. Aruga, *Inorg. Chem.*, **19**, (1980), 2895.

[127] R. P. Singh, E. R. Pambid, P. Debayle and N. M. Abbas, *Analyst*, **116**, (1991), 409.

[128] Darien, *Spec. News*, Eichrom, **2**, (1993), 1.

[129] E. P. Horwitz, R. Chiarizia and M. L. Dietz, *Solvent Extracion and Ion Exchange*, **10**, (1992), 313.

[130] D. Tait and A. Wiechen, *J. Radioanal. Nucl. Chem.*, **159**, (1992), 239.

[131] S. R. Radel and M. H. Navidi, (Second Edition) West Publishing Company, St. Paul, U.S.A. "Chemistry", 1994, 1043.

[132] Encyclopedia of Geochem. and Environ. Sci., Biogeochemistry, Van Nostrand Reinhold, New York, 1972, 82.

[133] M. N. Hill, Ed, The Sea, Volume 2, Interscience Publishers, New York, 1963.

[134] F. A. Cotton and G. Wilkinson, Fifth Edition, John Wiley and Sons, New York., 1988, 380.

[135] Materials For The Engineering Technician, Higgins, 2nd Edition, Edward Arnold, 1987.

[136] Angus Macmillan, Woodhead Publishing Ltd., Cambridge, England Base Metals Handbook, 1, 1993, 1.

[137] S. G. Higgins, B. Closset and M. Bray, *Journal Of Power Sources*, **53**, (1995), 75.

[138] P. Judex, S. Heissler and C. Adelhelm, *Fres. J. Anal. Chem.*, **347**, (1993), 413.

[139] Y. Suzuki and Y. Marumo, *Anal. Sci.*, **12**, (1996), 129.

[140] G. H. Jeffery, Fifth Edition, Longman Scientific and Technical, U.K., 1989, 685.

[141] Stability Constants Database, SCQUERY, IUPAC and Academic Software, 1993.

[142] E. B. Sandell and H. Onishi, Fourth Edition, J. Wiley and Sons, Chichester, 1978.

[143] S. R. Taylor, *Geochim. Cosmochim. Acta*, **28**, (1964), 1273.

[144] T. Yoshino, H. Imada, S. Murakami and M. Kagawa, *Talanta*, **21**, (1974), 211.

[145] E. B. Uvarov and A. Isaacs, Penguin Books Ltd., London, UK, Sixth Edition Dictionary Of, Science 1986, 310.

[146] Encyclopedia Of Oceanography, R. W. Fairbridge, Van Nostrand Reinhold, New York, 1996, 732.

[147] A. G. Sharpe, Longman Group Ltd., Essex, UK, Third Edition Inorg., Chem., 672.

[148] H. De Beer and P. P. Coetzee, *Radiochim. Acta*, (1988), 113.

[149] C. H. Knight, R. M. Casssidy, B. M. Recoskie and L. W. Green, *Anal. Chem.*, **56**, (1984), 474.

[150] A. Goto, K. Kusakabe, S. Morooka and T. Kago, *Separ. Sci. Technol.*, **28**, (1993), 1273.

[151] H. J. Fischer and K. H. Leiser, *Fres. J. Anal. Chem.*, **346**, (1993), 934.

[152] J. P. Ghosh and H. R. Das, *Talanta*, **28**, (1981), 274.

[153] E. P. Horwitz, M. L. Dietz, R. Chiarizia and H. Diamond, *Anal. Chim. Acta*, **266**, (1992), 25.

[154] J. Havel, M. Vrchlabsky and Z. Kohn, *Talanta*, **39**, (1992), 795.

[155] J. L. Pavon, C. G. Pinto, E. R. Garcia and B. M. Cordero, *Anal. Chim. Acta*, **264**, (1992), 291.

[156] J. L. Perez Pavon, B. Moreno Cordero, E. Rodriguez Garcia and J. Hernandez Mendez, *Anal. Chim. Acta*, **230**, (1990), 217.

[157] A. G. Adriaens, J. D. Fassett, W. R. Kelly, D. S. Simons and F. C. Addams, *Anal. Chem.*, **64**, (1992), 2945.

[158] A. P. Mykytiuk, D. S. Russell and R. E. Sturgeon, *Anal. Chem.*, **52**, (1980), 1281.

[159] L. C. Baylor and B. R. Buchanan, *Appl. Spectrosc.*, **49**, (1995), 679.

[160] M. Aziz, S. G. Beheir and K. Shakir, *J. Radioanal. Nucl. Chem.*, **172**, (1993), 319.

[161] R. M. Cassidy, S. Elchuk, N. L. Elliot, L. W. Green and B. M. Recoskie, *Anal. Chem.*, **58**, (1986), 1181.

[162] H. Fuping, P. Haddad, P. E. Jackson and Joe Carnevale, *J. Chromatogr.*, **640**, (1993), 187.

[163] M. Rehkamper, *Chem. Geol.*, **119**, (1995), 1.

[164] D. J. Barkley, L. A. Bennet, J. R. Charbonneau and L. A. Pokrajac, *J. Chromatogr.*, **606**, (1992), 195.

[165] A. Kerr, W. Kupferschmidt and M. Attas, *Anal. Chem.*, **60**, (1988), 2729.

[166] S. Elchuk, K. I. Burns, R. M. Cassidy and C. A. Lucy, *J. Chromatogr.*, **558**, (1991), 197.

[167] A. Casoli, A. Mangia and G. Predieri, *Anal. Chem.*, **57**, (1985), 563.

[168] M. P. Harrold, A. Siriraks and J. Riviello, *J. Chromatogr.*, **602**, (1992), 119.

APPENDIX 1 - Sample Preparation Scheme for 'Stag's Mandible'

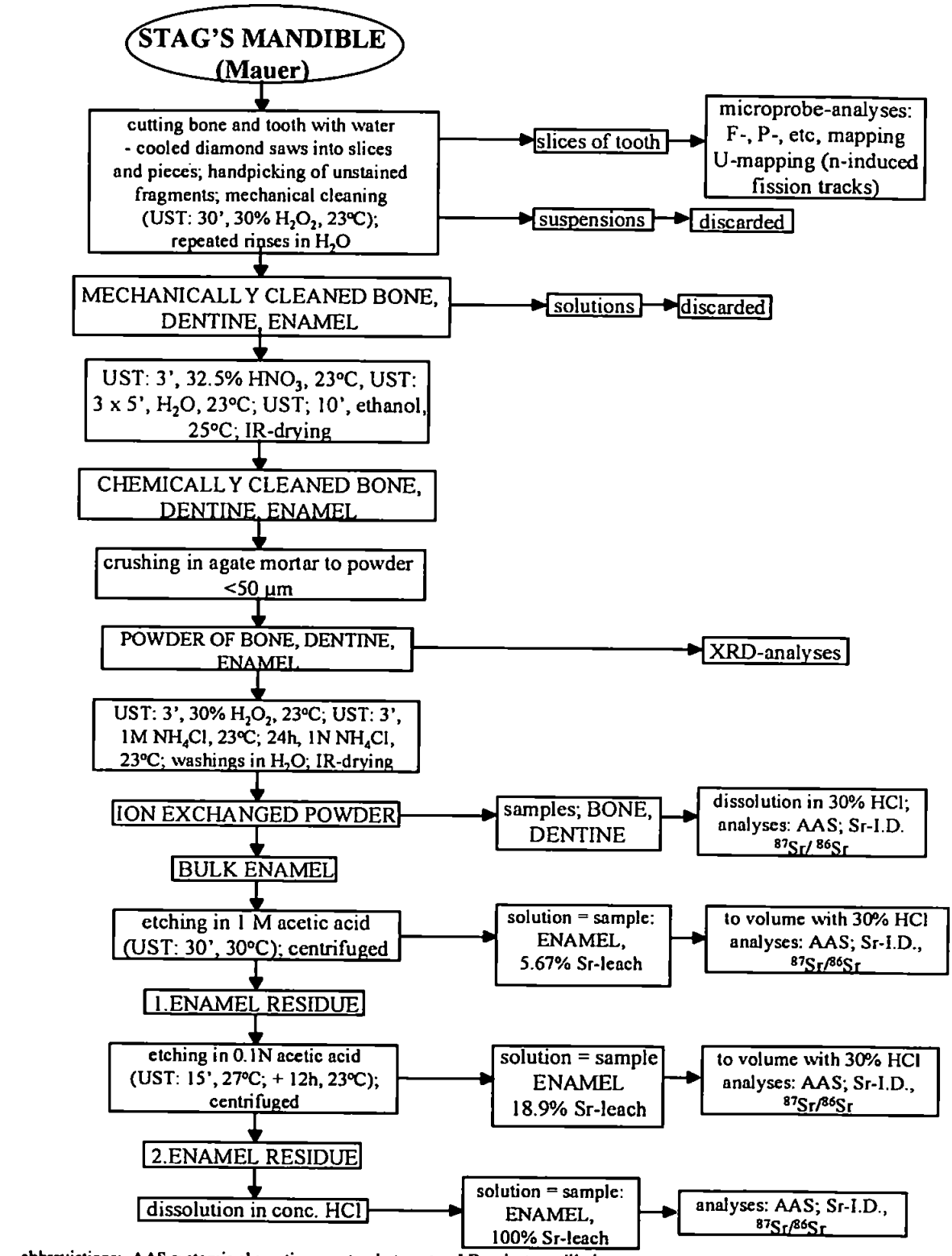

abbreviations: AAS = atomic absorption spectrophotometry, I.D. = isotope dilution mass spectrometry, I. R. = infrared light, UST = ultrasonic treatment